A Morphological Study Comparing Heart Size Measurement on Chest Radiograph with Echocardiography in Local Population

DR. AHMED ALI KHAN
06-113192-001

BAHRIA UNIVERSITY ISLAMABAD
PAKISTAN

A Morphological Study Comparing Heart Size Measurement on Chest Radiograph with Echocardiography in Local Population

DR. AHMED ALI KHAN
06-113192-001

A thesis submitted in fulfilment of the
requirements for the award of the degree of
Master of Philosophy (Anatomy)

Department of Anatomy

BAHRIA UNIVERSITY MEDICAL & DENTAL COLLEGE

SEPTEMBER 2021

APPROVAL SHEET

SUBMISSION OF HIGHER RESEARCH OF DEGREE THESIS

Candidate's Name: Dr. Ahmed Ali Khan

Discipline: Anatomy

Faculty/Department: Department of Anatomy

I hereby certify that the above candidate's work including the thesis has been completed to my satisfaction and that the thesis is in a format of editorial standard recognized by faculty/department as appropriate for examination.

Signature: _____

Principal Supervisor: Prof. Dr. Aisha Qamar

Date: 30th September, 2021

The undersigned signifies as:

1. The candidate presented at a pre-completion seminar, an overview and synthesis of major findings of thesis, and that research is of a standard and extent appropriate for submission as a thesis.
2. I have checked the candidate's thesis and its scope, format and editorial standards are recognized by the faculty/department as appropriate.

Signature: _____

Head of Department: Prof. Dr. Ambreen Usmani

Date: 30th September, 2021

APPROVAL FOR EXAMINATION

Student's Name: Dr. Ahmed Ali Khan Registration No. 66216

Program of Study: MPhil (Anatomy)

Thesis Title: "A Morphological Study Comparing Heart Size Measurement on Chest Radiograph with Echocardiography in Local Population"

It is to certify that the above student's thesis has been completed to my satisfaction and, to my belief. Its standard is appropriate for submission and evaluation. I have also conducted plagiarism test of this thesis using HEC prescribed software and found similarity index at 11% that is within the permissible limit set by the HEC for the MPhil degree thesis. I have also found the thesis in a format recognized by the BU for the MPhil thesis.

Principal Supervisor's Seal & Signature: _____

Date: 30th September, 2021

Name: Prof. Dr. Aisha Qamar

AUTHOR'S DECLARATION

I, Dr. Ahmed Ali Khan hereby state that my MPhil thesis titled "A Morphological Study Comparing Heart Size Measurement on Chest Radiograph with Echocardiography in Local Population" is my own work and has not been submitted previously by me for taking any degree from this university, the Bahria University Medical and Dental College, Karachi or anywhere else in the country/world.

At any time if my statement is found to be incorrect even after my graduation, the University has the right to withdraw/cancel my MPhil degree.

Name of student: Dr. Ahmed Ali Khan
Date: 30th September, 2021

THESIS COMPLETION CERTIFICATE

Student's Name: Dr. Ahmed Ali Khan Registration No. 66216

Program of Study: MPhil (Anatomy)

Thesis Title: "A Morphological Study Comparing Heart Size Measurement on Chest Radiograph with Echocardiography in Local Population"

It is to certify that the above student's thesis has been completed to my satisfaction and, to my belief. Its standard is appropriate for submission and evaluation. I have also conducted plagiarism test of this thesis using HEC prescribed software and found similarity index at 11% that is within the permissible limit set by the HEC for the MPhil degree thesis. I have also found the thesis in a format recognized by the BU for the MPhil thesis.

Principal Supervisor's Seal & Signature: _____

Date: 30th September, 2021

Name: Prof. Dr. Aisha Qamar

THESIS COMPLETION CERTIFICATE

Student's Name: Dr. Ahmed Ali Khan Registration No. 66216

Program of Study: MPhil (Anatomy)

Thesis Title: "A Morphological Study Comparing Heart Size Measurement on Chest Radiograph with Echocardiography in Local Population"

It is to certify that the above student's thesis has been completed to my satisfaction and, to my belief. Its standard is appropriate for submission and evaluation. I have also conducted plagiarism test of this thesis using HEC prescribed software and found similarity index at 11 % that is within the permissible limit set by the HEC for the MPhil degree thesis. I have also found the thesis in a format recognized by the BU for the MPhil thesis.

Principal Co-Supervisor's Seal & Signature: _____

Date: 30th September, 2021

Name: Surgeon Commodore Muhammad Nadir Khan

PLAGIARISM UNDERTAKING

I, solemnly declare that research work presented in the thesis titled "A Morphological Study Comparing Heart Size Measurement on Chest Radiograph with Echocardiography in Local Population" is solely my research work with no significant contribution from any other person. Small contribution / help wherever taken has been duly acknowledged and that complete thesis has been written by me.

I understand the zero tolerance policy of the HEC and Bahria University towards plagiarism. Therefore I as an Author of the above titled thesis declare that no portion of my thesis has been plagiarized and any material used as reference is properly referred / cited.

I undertake that if I am found guilty of any formal plagiarism in the above titled thesis even after award of MPhil degree, the university reserves the right to withdraw / revoke my MPhil degree and that HEC and the University has the right to publish my name on the HEC / University website on which names of scholars are placed who submitted plagiarized thesis.

Scholar / Author's Sign: _____

Name of the Scholar: Dr. Ahmed Ali Khan

Dedicated to all those who inspire me and give me hope

ACKNOWLEDGEMENT

I am grateful for this day. And grateful for this accomplishment. It would not have been possible without the patience of many. Those who showed me the way, stood by me all along, and gave a part of their lives and time to help me achieve this milestone, I acknowledge your sincere help. I don't have to mention your names, you know who you are. A guiding light, and a ray of hope when there was none. I am grateful for this journey, it could not have been planned better than this. I am indebted to all who have taught me since I was a little child, at home and school. I thank BUMDC, Karachi for this wonderful opportunity, and all those who welcomed me on my first day. You treated me as one of your own, I acknowledge it and feel honored.

Thank you,
Dr. Ahmed Ali Khan

ABSTRACT

***Background**:* Heart size is an important index for identifying an enlarged heart early in the course due to physiological or underlying pathological reasons. The gold standard for estimation of heart size is a 2D transthoracic echocardiography, but it is not performed merely for the assessment of heart size, as it not only estimates the size of individual chambers, but also permits a detailed structural and functional inspection of the heart which forms the basis of therapeutic decisions. In contrast, chest X-ray (PA view) is a humble imaging modality, which allows the measurement of the heart size using a simple ratio between the transverse cardiac diameter of the heart and the transverse thoracic diameter of the thoracic cavity. The cardiothoracic ratio (CTR), as it is known, is a frequently reported parameter on chest radiographs that foretells about the heart size. The CTR has been at the center of debate among many researchers, who question if it is still a valid convention used today or should it be altogether rendered obsolete. Early identification of heart enlargement permits time to further investigate the possible causes and initiate appropriate treatment. Most studies agree upon the screening potential of chest X-rays (PA view), and thus CTR, for determining the normality of heart size, especially in a poor resource setting. It also raises concern, if radiographic CTR can be employed as a preliminary investigation to streamline patients for echocardiography or a judicious referral to a tertiary care center from a secondary or lower-level healthcare facility. It poses a challenge, to choose between a simpler tool for investigation when more advanced techniques are available, and the costs that come with such advancements.

***Objectives**:*

1. To determine heart size measurements on chest X-ray (PA view) in a local population
2. To correlate these measurements with echocardiographic measurements for the same person
3. To determine the specificity and sensitivity of the measurement of cardiothoracic ratio (CTR) on a chest X-ray (PA view) in determining heart enlargement

***Subjects, Materials and Methods**:* The current comparative cross-sectional study was conducted in a local population of Karachi. It was carried on 79 participants (44 males and 35 females) with a mean age of 52.71 ± 14.54, and an age range of 19 to 75 years. A Toshiba DS-TA-5A was used to obtain chest X-rays (PA view), and Canon Aplio i600CV was used to perform transthoracic echocardiography. The radiological parameters used were transverse thoracic diameter (TTD), transverse right cardiac diameter (TRD), transverse left cardiac diameter (TLD), transverse cardiac diameter (TCD) and cardiothoracic ratio (CTR). The echocardiographic parameters used were the end-diastolic and end-systolic left ventricular (LV) internal diameters (LVIDd and LVIDs, respectively), end-diastolic interventricular septum thickness (IVSd), end-diastolic posterior wall thickness (PWd), LV ejection fraction (EF), right atrial diameter (RAD), left atrial diameter (LAD), right ventricular diameter (RVD), Tricuspid Annular Plane Systolic Excursion (TAPSE), aortic annulus diameter and pulmonary artery systolic pressure (PASP). Based on the findings obtained from comparing chest X-ray (PA view) to echocardiography, the study participants were categorized into four groups. Group A had an enlarged heart size on both imaging modalities, Group B had an enlarged heart size only on chest X-ray (PA view), Group C had an enlarged heart size only on echocardiography, and Group D had a normal heart size on both the imaging modalities.

***Results**:* The total number of enlarged hearts identified in the study were 28 (35.44%) on chest X-ray (PA view) and 46 (58.22%) on echocardiography. The prevalence of enlarged hearts in the study population was 58.23%. The findings of chest X-ray (PA view), i.e. a normal or enlarged heart size, were compared to the findings of echocardiography for the same. Participants in each of the four groups were assessed for the differences which led to their categorization into their respective groups. The study determined that chest X-ray (PA view) had a sensitivity of 54.35%, a specificity of 90.90%, a positive predictive value of 89.29%, a negative predictive value of 58.82%, a positive likelihood ratio of 5.98, a negative likelihood ratio of 0.50, a false negative rate of 45.65%, a false positive rate of 9.09%, a probability of positive tests of 35.44%, a probability of negative tests of 64.56%, and an accuracy of 69.62%.

***Conclusion**:* The current study demonstrated the prevalence of an enlarged heart in participants with heart-related complaints or disorders. A chest X-ray can precisely measure the heart size, and with the help of a single measurement (CTR), it can identify an enlarged heart with high specificity and reasonable accuracy. In contrast, echocardiography measures multiple chambers for this purpose. The role of a chest X-ray is limited when it comes to appraising the function of the heart. But given that other radiological signs are present on a chest X-ray (PA view), e.g. pulmonary congestion, the clinical presentation and subsequent evaluation of the patient can help a clinician infer useful information in a less resourceful setting. It can serve as a baseline investigation for future comparisons. For a normal CTR on chest X-ray (PA view), the mean values of echocardiographic parameters ranged between the mean values of Group C and D (i.e. false negative and true negative). Similarly, for an increased CTR on chest X-ray (PA view), the mean values of echocardiographic parameters ranged between the mean values of Group A and B (i.e. true positive and false positive).

***Keywords**:* Heart Size, Enlarged Heart, Cardiothoracic Ratio, Transverse Cardiac Diameter, Chest X-ray (PA view), Echocardiography

TABLE OF CONTENTS

LIST OF TABLES

LIST OF FIGURES

LIST OF ABBREVIATIONS

ABBREVIATION	FULL FORM
2D	Two Dimensional
A4C	Apical 4 Chamber View
Aorta*	Aortic Annular Diameter
AP (View)	Anterior-posterior View
ASE	American Society of Echocardiography
CTR	Cardiothoracic Ratio
EACVI	European Association of Cardiovascular Imaging
EF*	Ejection Fraction
IVSd*	End-diastolic Interventricular Septum Thickness
LA	Left Atrium
LAD*	Left Atrial Diameter
LV	Left Ventricle
LVEDV	Left Ventricular End-diastolic Volume
LVESV	Left Ventricular End-systolic Volume
LVIDd*	End-diastolic Left Ventricular Internal Diameter
LVIDs*	End-systolic Left Ventricular Internal Diameter
LVM*	Left Ventricular Mass
PA (View)	Posterior-anterior View
PASP	Pulmonary Artery Systolic Pressure
PLAX	Parasternal Long Axis View
PWd*	End-diastolic Posterior Wall thickness
RA	Right Atrium
RAD*	Right Atrial Diameter
RV	Right Ventricle
RVD*	Right Ventricular Diameter
RWT*	Relative Wall Thickness
SIVC	Subcostal Inferior Vena Cava View
TAPSE*	Tricuspid Annular Plane Systolic Excursion,
TCD	Transverse Cardiac Diameter
TLD	Transverse Left (Cardiac) Diameter
TRD	Transverse Right (Cardiac) Diameter
TTD	Transverse Thoracic Diameter

*When these parameter were indexed to Body Surface Area (BSA), their abbreviations were represented by a preceding or a succeeding small letter ‘i’

LIST OF APPENDICES

CHAPTER 1

INTRODUCTION

1.1 The Heart Size

Heart size is an important index in clinical medicine and forensic science. For an anatomist, it remains a subject of research despite the extensive knowledge that exists about it, as there is still little agreement on a standard value for the normal heart size. This is mainly due to the huge amount of variability that results from a range of factors affecting the size of the heart, including height, weight, sex and age (Pfaffenberger et al., 2013). In addition, the parameters measured or the imaging modality used also contribute to this gamut of variations. An enlarged heart shadow on a posterior-anterior (PA) view chest X-ray is usually pathognomonic of heart disease with very few exceptions. In contrast, a small heart shadow is seen in a condition called Small heart syndrome, often associated with Chronic fatigue syndrome (CFS) and other conditions, such as asthmatic paroxysm with emphysema or adrenal insufficiency (Miwa & Fujita, 2008).

A review of earlier studies related to heart size shows that the average normal heart size varies widely and is dependent on the population studied (Molina & DiMaio, 2012). While these values may vary in a close range, the difference will never be known unless studied for a given population. For instance, heart size stated in Gray's anatomy is 12 cm in length, 8.5 cm in width and 6 cm in thickness (Gray, 2015), and the values for the same in a cadaveric study are 11.25 cm, 8.78 cm, 3.97 cm respectively for males, and 10.60 cm, 8.31 cm, 3.63 cm for females (Gupta et al., 2014). In another cadaveric study, the respective values for the same were 10.5 cm, 8.51 cm and 5.86 cm in males, and 9.2 cm, 7.67 cm and 5.47 cm in females (Mannan et al., 2009). Thus local reference values of various cardiac measurements must be known for accurate estimation and diagnosis of cardiomegaly (Elmissiri et al., 2016). The convenient tools at disposal for measuring heart size are chest radiography and echocardiography, the latter being the gold standard. Chest radiography uses ionizing radiation in the form of high-energy electromagnetic radiation, which limits its use. The dimensions of heart size are usually measured using a radiographic index called the cardiothoracic ratio (CTR) which compares the largest diameter of heart shadow with the

largest internal diameter of the thoracic cavity in the posterior-anterior (PA) view. The anterior-posterior (AP) view is not used for these measurements due to an artificially enlarged and widened appearance of the heart and mediastinum, respectively (Chana et al., 2015).

On the other hand, echocardiography uses high-pitched sound waves to produce an image of the heart, allowing structural and functional assessment. The sound waves are directed at the heart through a handheld device called the transducer or probe (Figure 1.1). A gel is applied to the area of the patient's skin to be contacted by the probe to get better conduction for transmitting sound waves and receiving the echoes reflected off the various tissue structures of the heart (Figure 1.2). The echoes are received as signals and displayed as a black and white moving image of the heart on a video monitor. Color can be added via 'Doppler' to show blood moving in and out of the chambers. The dimensions of heart size are measured by quantifying the heart chambers via a set of measurements. The standard reference values used for these measurements are taken from reputed professional standard-setting organizations, such as the American Society of Echocardiography (ASE) and the European Association of Cardiovascular Imaging (EACVI) (Marsan et al., 2020; Lang et al., 2015).

An enlarged heart, whether it be from physiologic or pathological causes, is an important sign that foretells a probable heart-related problem that requires exclusion of pathology. Its significance can be understood from the fact that it is a component of different scores and criteria used for different diseases, including heart failure. The Framingham Criteria for Heart Failure, for example, has radiological evidence of cardiomegaly enlisted as a major criterion. Similarly, Jones Criteria for acute rheumatic fever includes carditis affecting any of the layers of heart as a major and minor component (Gewitz et al., 2015), given that the carditis is moderate to severe, because when mild it may not appear on a radiograph (Blauwet & Cooper, 2010).

1.2 The Embryology of Heart

1.2.1 General Origin of thoracic structures

Most structures of the thoracic cavity develop from mesoderm, including the thoracic wall itself. The mesoderm is a germ layer that develops in the third week by the process of gastrulation. Another structure that also forms during this period from progenitor cells in the

primitive node and pit is the notochord, which induces the formation of the neural plate that develops into a neural tube.

As the notochord expands along the anterior-posterior axis, closer to the dorsal than the ventral surface of the developing embryo, the mesoderm which lies alongside the notochord divides along the mediolateral axis into the paraxial, intermediate and lateral plate mesoderm. These mesodermal subtypes give rise to specific structures:

1. The paraxial mesoderm undergoes presomitic mesoderm specification and somitogenesis to give rise to somites. Mature somites contain two major populations: the sclerotome and dermomyotome. The sclerotome gives rise to the vertebrae and associated ribs, tendons, and other tissues, such as vascular cells of the dorsal aorta, intervertebral blood vessels, and meninges. The dermomyotome produces two components: the myotome and the dermatome. The myotome gives rise to the musculature of the back, rib cage, ventral body wall, and limbs. The dermatome gives rise to the dermis of the back. The notochord gives rise to the nucleus pulposus, which later forms the vertebral discs (Tam & Trainor, 1994).
2. The lateral plate mesoderm (by the 18^{th} day), forms the splanchnic (splanchnopleuric) mesoderm adherent to the endoderm externally, the somatic (somatopleuric) mesoderm adherent to the inner surface of the ectoderm, and the extraembryonic membranes. The splanchnic mesoderm gives rise to components of the circulatory system, such as the heart, blood vessels and blood cells. The somatic mesoderm gives rise to the pelvic skeleton and mesodermal components of the limbs, except for the muscles, which are derived from the dermomyotome (Prummel et al., 2020).
3. The intermediate mesoderm forms the urogenital system, including the kidneys and gonads (Dressler, 2009).

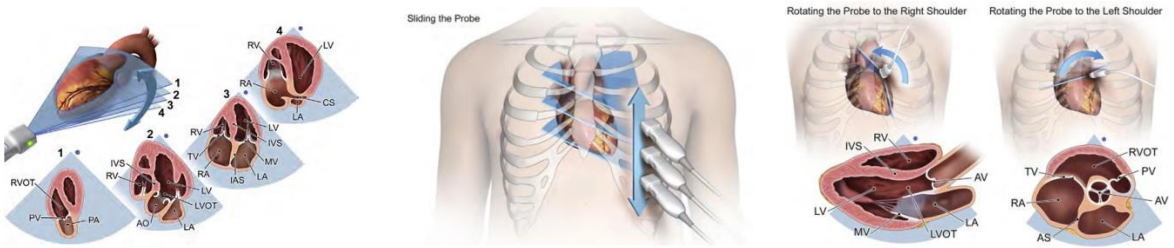

(A) (B) (C)

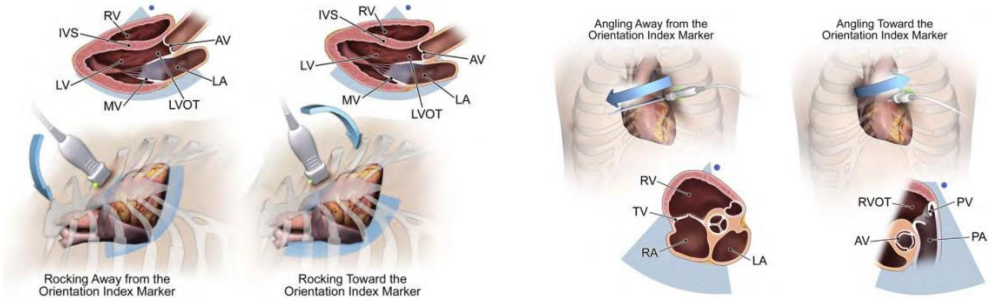

(C) (D)

Figure 1.1 Transducer scanning maneuvers: (A) tilting; (B) sliding; (C) rotating (towards the right or left shoulder); (D) rocking (away or towards the orientation index marker); (E) angling (away or towards the orientation index marker) (Mitchell et al., 2019)

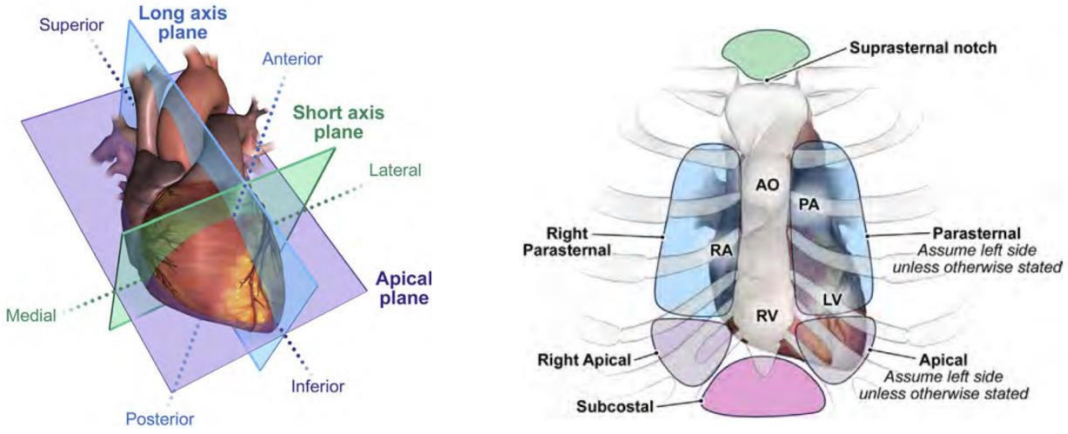

(A) (B)

Figure 1.2 (A) The scanning planes of the heart; (B) The echocardiographic windows to obtain images (Mitchell et al., 2019)

1.2.2 Formation of the pericardial and pleural cavities:

The spaces within the lateral plate mesoderm coalesce during the fourth week to form the intraembryonic coelom which will later divide to form the pericardial, pleural and peritoneal cavities. The early form of these cavities come to be as a result of lateral folding that occurs during the fourth week, as the two lateral folds fuse in the mid-line to close the ventral body wall (thus eliminating the connection between the intraembryonic and extraembryonic coelom) (Figures 1.3 A, B and D).

In the fifth week, the intraembryonic coelom consists of thoracic and abdominal parts separated partially by septum transversum, and the two parts communicate via a canal found on each side of the foregut, called the pericardioperitoneal canals (Figure 1.3 C). Two sets of membranes partition the intraembryonic coelom, the paired pleuroperitoneal membranes separate the pleural and peritoneal cavities, and the paired pleuropericardial membranes separate the mediastinum from the pleural cavities. The free edges of the pleuroperitoneal membranes project into the caudal end of pericardioperitoneal canal, growing medially and ventrally from the dorsolateral body wall to fuse with the dorsal mesentery of the esophagus and septum transversum by the end of the sixth week (Sant, 2008). The pleuropericardial membranes appear as small folds of mesenchyme projecting into the primitive undivided thoracic cavity, and fuse with the mesoderm ventral to the esophagus or primitive mediastinum by the seventh week, dividing the thoracic cavity into a pericardial and two pleural cavities (Figures 1.3 E and F). The pleuropericardial folds contain the common cardinal veins that drain the primitive venous system of the body of the embryo into the sinus venosus of the primitive heart (Figure 1.3 D). With the growth of lung buds into the medial wall of the primitive pleural cavities (i.e. the pericardiopleural canals), the pleural cavities expand around the heart into the body wall, and split the mesenchyme into an outer layer that becomes the chest wall and an inner layer that forms the fibrous pericardium (Figures 1.3 E and F) (Lee & Olak, 1994).

1.2.3 Formation of the heart

1.2.3.1 The Heart Fields

The primitive heart and vascular system first appear in the middle of the third week. Cells of mesodermal origin migrate from the primitive streak to form bilaterally paired strands of primary or first heart field, also referred to as the 'cardiac crescent' at the cranial border of the embryonic disc (Figure 1.5). Two more areas have been defined with progenitor cells that come from the pharyngeal mesoderm, and the studies that confirm these heart fields refer to them separately although they define overlapping areas of mesoderm, called the anterior heart field and the second or secondary heart field (Abu-Issa et al., 2004). The dorsal cardiac mesoderm positioned between the primary heart tube and the primitive gut is described as the second heart field, it encompasses the pre-pharyngeal mesoderm caudal to the outflow tract. In contrast, the anterior field is much broader than the second heart field, and not only encompasses the pre-pharyngeal mesenchyme, but also involves the lateral and more anterior splanchnic mesoderm that extends into the middle of cranial pharyngeal arches (Tzahor & Evans, 2011).

The initial two solid strands of the primary heart field approach each other ventrally and acquire a lumen lined by endothelial cells, giving rise to the initial tubular heart which serves as the precursor of the left ventricle and atrial chambers. The second heart field contributes to the distal myocardium of the outflow tract and smooth muscle in tunica media at the base of the aorta and pulmonary trunk. It also contributes cells to both the arterial and venous ends of the heart tube, the semilunar valves and the walls of great arteries. The branchiomeric muscles of the head which are involved in operating the jaw, facial expression, feeding and breathing also arise from the second heart field (Tzahor & Evans, 2011). The anterior heart field contributes to the entire ascending limb of the looped heart, i.e. the myocardium of the right ventricle, conus and truncus. While some researchers insist it only contributes to the distal conus and truncus (Kelly et al., 2014). The cells of the second heart field remain in an undifferentiated, proliferative state longer than the cells in the primary heart field. After migration into the heart, cells of the second heart field also differentiate and express contractile proteins, and become indistinguishable from cells derived from the first heart field (Dyer & Kirby, 2009).

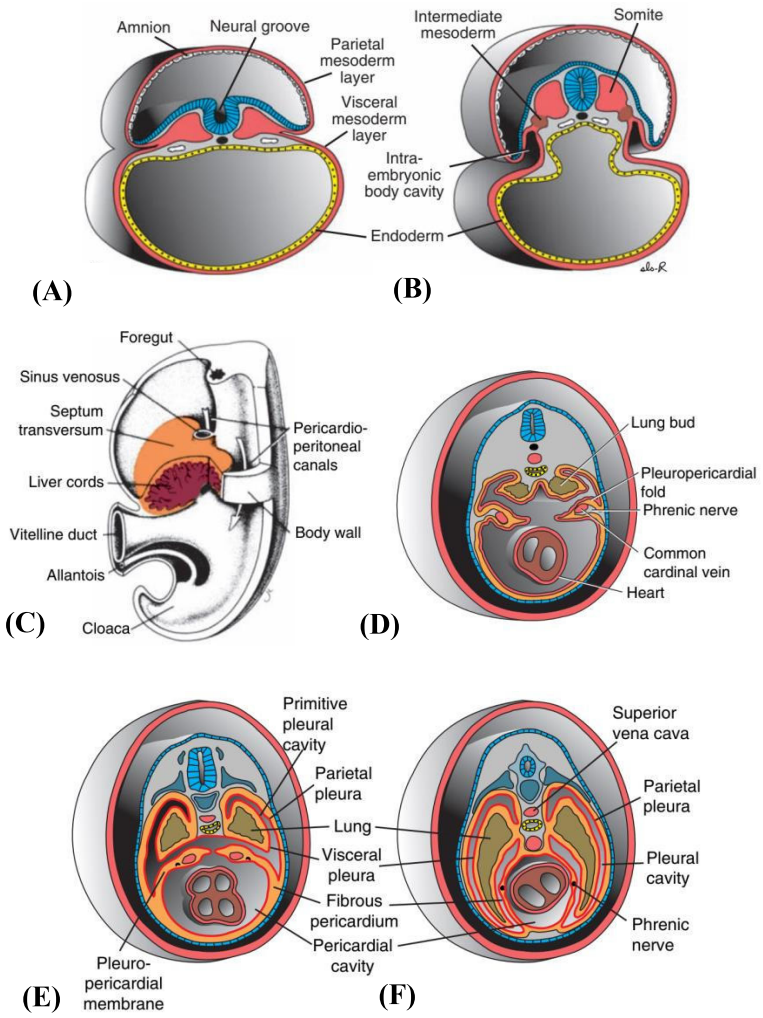

Figure 1.3 (A) and (B) shows the transverse section of an embryo at day 17 and 19, respectively. The mesodermal sheet gives rise to paraxial, intermediate and lateral plate mesoderms. (C) The human embryo at approximately 5 weeks, illustrating the pericardioperitoneal canal. The primitive pleuropericardial cavity is partially separated from the abdominal cavity by septum transversum; the two primitive cavities communicate with each other (shown by the arrows). (D) The growth of lung buds into the pericardioperitoneal canals. The pleuropericardial folds are also visible. (E) The transformation of the pericardioperitnoeal canals into the pleural cavities and formation of the pleuropericardial membranes. The mesenchyme of the body wall splits into the pleuropericardial membranes and the definitive body wall. (F) The thorax after the fusion of the pleuropericardial folds with each other and with the root of the lungs (Sadler, 2019)

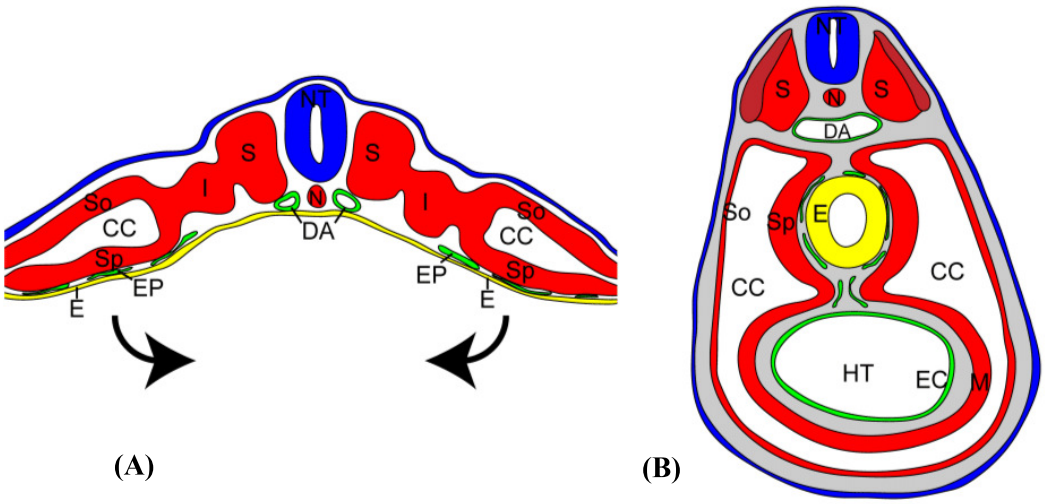

Figure 1.4 Heart tube formation in an HH14 (22 somite, or 50 to 53 hours) chick embryo. (A) Schematic of a transverse section through the posterior region, demonstrating the relationship of the splanchnic mesoderm and endoderm prior to lateral folding. The lateral plate mesoderm divides to form the somatic (So) and splanchnic mesoderm (Sp) with an intervening coelomic cavity (CC). An endothelial plexus (EP, green) resides between the splanchnic mesoderm and endoderm (E, yellow). Lateral folding (arrows) will unite the somatopleure and splanchnopleure ventrally. (B) The anterior region of the embryo (still in HH14 stage) after lateral folding. The endoderm has been excluded from the heart tube (HT) and cells of the endothelial plexus have formed the endocardial (EC) lining of the heart tube lumen. Dorsal to the heart tube, the endoderm of the gut tube remains invested by the endothelial plexus and splanchnic mesoderm (Winters & Bader, 2013)

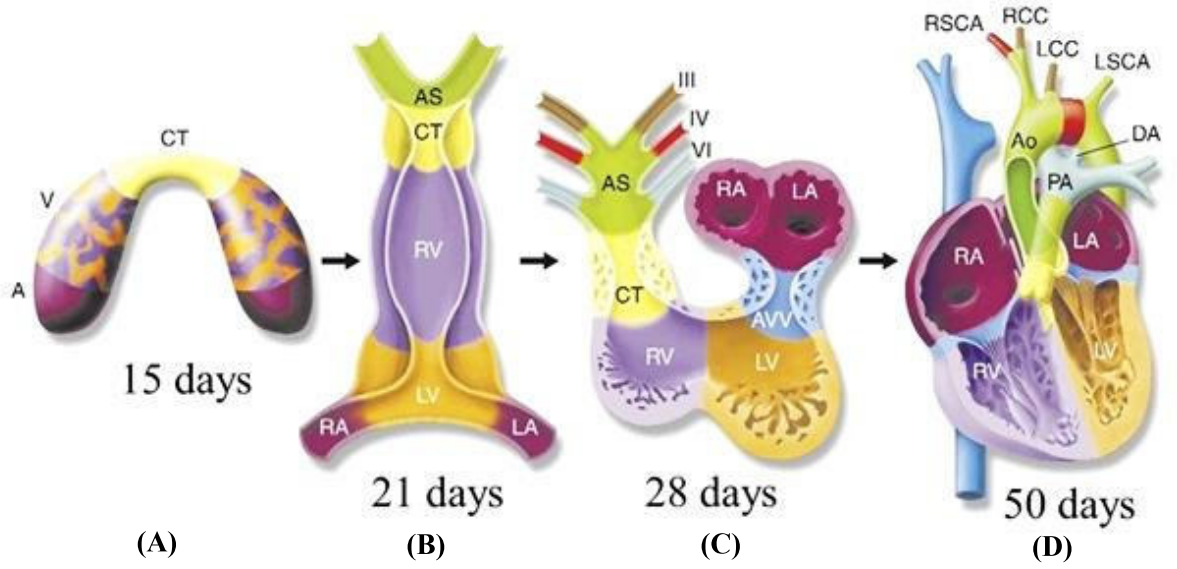

Figure 1.5 A schematic representation of the stages of human heart development, with the morphologically related regions color-coded, as observed from ventral veiw. The cardiogenic precursors form a crescent (shown in A), which is specified to form specific segments of the linear heart tube (shown in B) patterned along the anterior-posterior axis, forming the various regions and chambers of the looped and mature heart (shown in C and D, respectively). Each cardiac chamber balloons out from the outer curvature of the looped heart tube in a segmental manner. Abbreviations: AS, aortic sac; CT, conotruncal segment; AVV, atrioventricular valve segment; A, aortic sac; V, ventricle; RV, right ventricle; LV, left ventricle; RA, right atrium; LA, left atrium; PA, pulmonary artery; Ao, aorta; DA, ductus arteriosus; RSCA, right subclavian artery; LSCA, left subclavian artery; RCC, right common carotid; LCC, left common carotid (Lindsey et al., 2014; Srivastava & Olson, 2000)

1.2.3.2 Primary Heart Tube

Studies suggest that the mesoderm of the primary heart field gives rise to the primary heart tube consisting of an atrium connected to sinus venosus, an atrioventricular canal, a ventricular inflow tract, the bulboventricular fold and an outflow tract connected to the aortic sac. The layers of the heart wall are derived from different sources, the endocardium is a regionally specialized endothelium that arises through a process of de novo vasculogenesis from a distinct population of mesodermal cardiogenic precursors in the cardiac crescent (Harris & Black, 2010), the myocardium is derived from the splanchnic mesoderm surrounding the pericardial cavity or more specifically from the pharyngeal mesoderm anterior to the early heart tube (anterior heart field) (Zaffran et al., 2004), and the epicardium or visceral pericardium is derived from mesothelial cells on the outer surface of sinus venosus.

Most of the epicardial cells derive from the somatopleural investment of the septum transversum, from where they migrate to the dorsal aspect of the ventricles and atria. These cells then migrate over the lateral surfaces and the atrioventricular sulcus to the ventral aspect of the heart. The ventral migrating epicardial tissue ensheaths the truncus arteriosus, while the sinus venosus is coated with epicardium from the beginning, where the epicardial cells derive in part from the cuboidal cells of the pleuroperitoneal canal and in part from somatopleural cells (Viragh & Challice, 1981).

During the folding of the embryo, there is concurrent development of alternate constrictions and dilations of the tubular heart as it elongates. The parts of the heart at this stage, from the cranial to the caudal end, are called the bulbus cordis, primitive ventricle, primitive atrium and sinus venosus. Bulbus cordis has three parts, the cranial part continuous with the aortic sac (and thus the pharyngeal arch arteries) is called truncus arteriosus, caudal to which lies the conus arteriosus and conus cordis that are continuous with the primitive ventricle. The sinus venosus develops a right and left horn giving the primary heart tube an inverted ‘Y’ shape. The two arms of the ‘Y’ are positioned inferiorly, being continuous with the developing venous tributaries of the embryo, yolk sac and placenta. These vessels are named the common cardinal, the vitelline and the umbilical veins respectively (Moorman et al., 2003).

The concurrent growth of the head and tail regions result in cephalocaudal folding which re-positions the primordial heart and pericardial cavity anterior to the foregut and caudal to the head fold and oropharyngeal membrane. With further development, the heart tube sinks into the pericardial cavity and is attached to the dorsal wall by a fold of tissue called the dorsal mesocardium. Eventually, the dorsal mesocardium breaks down entirely, leaving the heart tube freely suspended in the pericardial cavity. The ends of the heart tube are held in position by the septum transversum caudally and the pharyngeal arches cranially. The caudal pole or the venous end of the heart tube receives three major veins of fetal circulation. The oxygen-rich blood is supplied in the umbilical vein coming from the chorionic sac, and oxygen-poor blood is supplied in the vitelline and cardinal veins coming from the umbilical vesicle and body of the embryo, respectively. The blood that reaches the heart tube is pumped through the arterial end into the aortic sac, and thereby via bilateral pharyngeal arches, it reaches the dorsal aortae (Kau et al., 2007).

The primary heart tube is genetically primed to undergo a dextral looping, approximately at 23rd to 28th day. The looping results in the formation of the bulboventricular loop due to which the apex of the heart points toward the left. At first, the primary heart tube is centrally placed within the embryo until bending of the loop occurs. As a result, the primitive atrium and sinus venosus with its two horns come to lie posterior to the truncus arteriosus, bulbus cordis and primitive ventricle. As the looping is taking place, the partitioning of primary heart tube also starts during the middle of the fourth week and is completed by the end of the eighth week (Moore et al., 2020).

1.2.3.3 The Atrioventricular Canal

The atrioventricular canal is partitioned in the fifth week when mesenchymal cells invade the atrioventricular endocardial cushions that develop from cardiac jelly and neural crest cells at the end of the fourth week. These cushions form on the dorsal and ventral walls of the atrioventricular canal, and as they fuse they divide the canal into a right and left canal. The formation of the canals separates the primitive atrium from the primitive ventricle, and the endocardial cushions are transformed to play role in the development of the valves and membranous septa. The septal leaflets of these valves are derived from the fused endocardial

cushions, and the mural leaflets are derived from the surrounding mesenchyme (Moore et al., 2020).

1.2.3.4 The Atria

The primitive atrium is divided into a right and left atrium by the end of the fourth week via the development and transformation of two septa. The first septum is a thin crescentic membrane called septum primum that grows from the roof of the primitive atrium towards the endocardial cushions. The division of the primitive atrium brought about by this septum is incomplete, leaving a large opening between the crescentic free margin of the septum and the fusing endocardial cushions. This opening is called foramen primum which serves as a shunt for the oxygenated blood from the right to the left atrium. During the course of further development of the septum, this foramen progressively diminishes until it disappears as the septum fuses to the left side of the endocardial cushions. Before the foramen primum disappears, there appear perforations in the central part of the septum primum via the process of apoptosis. These perforations coalesce to form another opening within the septum primum called foramen secundum that keeps shunting oxygenated blood from the right atrium to the left (Anderson et al., 2002).

The second septum is a thick crescentic muscular fold called septum secundum that grows in the fifth to sixth weeks from the anteriocranial wall of the right atrium, adjacent to the septum primum. It forms an incomplete partition between the two atria, resulting in a foramen ovale. During intrauterine life, this foramen not only maintains shunting of blood from the right atrium to the left but also prevents the reverse flow of blood by virtue of septum primum which acts as a valve flap. It closes after birth as the left atrial pressure becomes higher than that of the right atrium. Fossa ovalis forms by the fusion of the valve of foramen ovale with the septum secundum, forming a complete partition between the two atria called the interatrial septum (Naqvi et al., 2018).

Initially, the primitive atrium has an opening at the center of its dorsal wall for the sinus venosus which has two horns of equal size. Due to shunting of blood from the left to right as a result of modifications to vitelline and umbilical veins, and from anastomoses between anterior cardinal veins which form the left brachiocephalic vein, the right horn becomes proportionately larger than the left horn as it receives more blood. The disproportion between

the right and left horns of sinus venosus is noticeable by the end of fourth week. The superior vena cava brings blood from the head and neck, while the inferior vena cava brings blood from the placenta and lower body. Due to these developments, the sinoatrial orifice moves more towards the right and opens in the part of the primitive atrium that is destined to become the right atrium. The right horn is eventually incorporated into the right atrium forming the smooth part of its wall called sinus venarum, and the left horn becomes the coronary sinus. The remaining walls of the right atrium with a rough trabeculated appearance, i.e. the anterior wall and the right auricle, are derived from the primitive atrium. The smooth part of the right atrium is delineated from its rough parts from within by a vertical ridge called crista terminalis and on the outside by a shallow groove called sulcus terminalis. The crista terminalis forms from remnants of the cranial part of right sinoatrial valve. The remnants of the caudal part of the sinoatrial valve form the valves of the inferior vena cava and coronary sinus. Similarly, most of the left atrial wall is smooth because the primordial pulmonary vein and its main branches are incorporated within the wall of the left atrium as it expands. The primordial pulmonary vein arises just to the left of septum primum as an outgrowth of the dorsal atrial wall. The rough trabeculated part of the left auricle is derived from the primitive atrium. The left sinoatrial valve is incorporated into the interatrial septum after fusion with the septum secundum (Moore et al., 2020).

1.2.3.5 The Ventricles

The ventricles are partitioned by the growth of a median ridge in the floor of the primitive ventricle near the apex. This ridge, with a concave free edge, is called the muscular interventricular septum. It grows both as a result of ventricular dilatation and active proliferation of the septum myocytes. The crescentic interventricular foramen which persists till the end of the seventh week, is present between the free edges of the interventricular septum and the endocardial cushions. This foramen is sealed off by tissue from three sources, i.e. the right bulbar ridge, the left bulbar ridge and the fused endocardial cushions. The membranous interventricular septum is derived from the right side of endocardial cushions, and grows toward the muscular septum with contributions from neural crest cells. As these changes occur (i.e. the closure of the foramen, and complete formation of the interventricular septum), the right and left ventricles emerge as separate chambers with the pulmonary trunk communicating with the right ventricle, and the aorta communicating with the left ventricle.

The trabeculae carneae which are a spongy mass of muscular bundles within the cavity of ventricular walls, form papillary muscles and chordae tendinae attached to the atrioventricular valves (Lin et al., 2012).

1.2.3.6 The Outflow Tract

The walls of bulbus cordis and truncus arteriosus have mesenchymal cells that undergo active proliferation to form bulbar and truncal ridges which are continuous with each other. These ridges are largely derived from neural crest cells that migrate from across the primordial pharynx and pharyngeal arches. The ridges are spirally orientated due to the blood flow from the ventricles, thus the aorticopulmonary septum formed by the fusion of these ridges is spiral as well. When the fusion is complete, two separate channels are formed namely the ascending aorta and the pulmonary trunk. Part of the bulbus cordis that gets incorporated into the ventricular walls forms the infundibulum of the right ventricle, and the aortic vestibule in the left ventricle (Webb et al., 2003).

1.2.3.7 The Valves of the Heart

The semilunar valves start to develop via three swellings from the subendocardial tissue around the orifices of the newly formed arterial channels that undergo transformation to form three cusps of the valves. The atrioventricular valves develop from the proliferation of tissue around the atrioventricular canals, with the septal leaflets derived from the fused endocardial cushions, and the mural leaflets derived from adjacent mesenchyme (Lange et al., 2004).

1.2.3.8 The Conducting System of Heart

The heart contractions initially originate in the muscle layers of sinus venosus, occurring in peristaltic waves across the continuous muscle layers of the primitive atrium and ventricle. During the fourth week, contractions of the heart become coordinated and the blood flow becomes unidirectional, the circulation being ebb-and-flow type before that (Moore et al., 2020). It is not until the fifth week that the sinuatrial node develops in the right wall of the sinus venosus. As the sinus gets incorporated into the wall of the right atrium, the sinoatrial node is relocated in the right atrium, near the opening of the superior vena cava. Cells from the left wall of the sinus venosus and the atrioventricular region together form the atrioventricular node and bundle, located in the base of the interatrial septum or just above

the endocardial cushions. The atrioventricular bundle gives rise to fibers that cross into the ventricles to be divided into right and left bundle branches, and distributed in the ventricular myocardium (Moorman & Christoffels, 2003). The sinoatrial node, atrioventricular node, atrioventricular bundle and the right and left bundle branches are the only electrical pathway that exists between the atria and the ventricles as they become electrically isolated by the development of fibrous tissue from the epicardium, also called the fibroskeleton of the heart. These structures together are referred to as the conducting system of the heart, which is well developed before being supplied with nerves that enter the heart. Neural crest cells play an important role in the formation of the conducting system and the parasympathetic supply of the heart (Buijtendijk et al., 2020).

1.2.4 Formation of the Vascular System

The primordial blood vessels are indistinguishable as arteries or veins structurally, however they are named according to their future fates and association with the heart. During the early development of the heart, the three paired veins draining into the primordial heart's venous end or sinus venosus undergo a series of transformations so that the configuration of blood vessels at birth is compatible with life. These changes are accompanied by concurrent growth of the embryo, development of viscera and changes that occur in the horns of the sinus venosus. Of the paired blood vessels, the left vitelline vein regresses and the right vitelline vein forms most of the hepatic portal circulation and the hepatic segment of the inferior vena cava. The left umbilical vein persists except for its cranial part which degenerates, and supplies oxygen from the placenta to the embryo, while the right umbilical vein degenerates entirely. The left umbilical vein forms a shunt called ductus venosus with the inferior vena cava within the liver. The caudal part of the left anterior cardinal vein degenerates, and the proximal part along with the shunt between the anterior cardinal veins form the left brachiocephalic vein. The right anterior cardinal and the right common cardinal veins form the superior vena cava. The posterior cardinal veins largely disappear along with the interim kidney with which they had started to develop. They are subsequently replaced by the subcardinal and supracardinal veins. What remains of the posterior cardinal veins form the root of azygus vein and the common iliac veins. The derivatives of the subcardinal vein and the subcardinal anastomosis are the stem of the left renal vein, the suprarenal and gonadal veins, and the pre-renal segment of the inferior vena cava. The remnants of the anastomoses

between the subcardinal veins cranial to the kidneys form the azygos and hemiazygos veins. There is an anastomosis between the subcardinal and the supracardinal veins which persists on the right side to form the renal segment of the inferior vena cava. The left supracardinal vein degenerates distal to the kidneys, while the right supracardinal vein forms the postrenal segment of the inferior vena cava (Yagel et al., 2010).

The pharyngeal arch arteries arise from the aortic sac, with contribution from neural crest cells, to supply the pharyngeal arches which form during the fourth and fifth weeks. These arteries terminate in the dorsal aortae that are initially paired and run through the entire length of the embryo. The caudal parts of these aortae fuse to form a common lower thoracic or abdominal aorta. Of the cranial parts that remain, the right dorsal aorta degenerates and the left one forms the primordial aorta. The dorsal aorta has about thirty intersegmental branches that pass in between and deliver blood to somites and their derivatives. These branches lose most of their original connections with the dorsal aorta, except the vertebral arteries in the neck, intercostal arteries in the thorax, lumbar and common iliac arteries in the abdomen, and the lateral sacral arteries in the sacral region (Rana et al., 2014). The vitelline and umbilical arteries are also branches of the dorsal aorta. The vitelline arteries pass to the primitive gut through the umbilical vesicle and give rise to the celiac arterial trunk, and the superior and inferior mesenteric arteries. The umbilical arteries pass into the connecting stalk to become continuous with chorionic vessels carrying deoxygenated blood to the placenta. The proximal parts of umbilical arteries contribute to the formation of internal iliac and superior vesicle arteries, while the distal parts form the medial umbilical ligaments (Hikspoors et al., 2017).

1.3 The Structure of Heart

The thoracic cavity is divided into a median compartment called the mediastinum, and two lateral compartments called the pleural cavities. The mediastinum is further divided into a superior and inferior segment by an imaginary line passing through the sternal angle anteriorly and the intervertebral disc between the fourth and fifth thoracic vertebrae posteriorly. The superior segment acts as a passageway for structures passing from the neck through the thorax on their way to the abdomen. The inferior segment has three divisions, the anterior division lies between the sternum anteriorly and the pericardium posteriorly, the posterior division lies between the pericardium anteriorly and the fifth to twelfth thoracic

vertebrae posteriorly, and the middle division occupied by the pericardium lies between the anterior and posterior divisions (Roberts & Weinhaus, 2005). The two lateral pleural cavities are potential spaces between the two pleurae surrounding the lungs. The pleurae are a serous membrane that folds back onto itself to form a two-layered structure, being continuous at the hila of the lungs. The outer or parietal pleura is adherent to the inner aspect of the chest wall and the inner or visceral pleura closely surrounds the lungs and associated structures (e.g. blood vessels, nerves and bronchi). The parietal pleura is very sensitive to noxious stimuli, whereas the visceral pleura is not. The upper part of the pleural cavities and the underlying lung apices occupy the thoracic inlet, the lower part of the cavity follows the convexity of the diaphragm, flatter in the central part and sloping down becoming narrow towards the attachment of the diaphragm to the chest wall, also known as costophrenic angle (Charalampidis et al., 2015).

Within the inferior middle mediastinum and between the lungs, the heart is separated from the surrounding structures by the pericardium and the pericardial cavity which provides protection and a friction-free surface for heart movements. The heart is oriented obliquely such that the apex points downward, forward and toward the left. This orientation of the heart is referred to as the anatomical cardiac axis, which is not the same as the electrical cardiac axis. The latter represents the mean direction of the electrical depolarization of the ventricles. Studies show that the in-vivo anatomical axis (normal anatomical position of the heart) and the electrical cardiac axis determined by electrocardiogram do not correlate, although unexplained how but changes in the anatomical axis will show up as changes in the electrical axis (Sathananthan et al., 2015). The apex of the heart lies between the junction of the fourth and fifth ribs near their articulation with their costal cartilages (just left to the sternum). The base of the heart lies at the level of the third costal cartilage, and the great vessels are attached here. The surfaces of the heart include the posterior surface, formed mostly by the left atrium and partly by the right atrium, the anterior or sternocostal surface formed mostly by the right ventricle inferiorly and the atria superiorly, the inferior or diaphragmatic surface formed by the ventricles, the right pulmonary surface formed by the right atrium and right ventricle, and the left pulmonary surface formed mostly by the left ventricle and part of the left atrium. Due to the oblique orientation of the heart, the posterior surface is directed upward, backward and to the right. The sternocostal surface is directed forward, upward and to the left. The

diaphragmatic surface is directed downward and backward. The right and left pulmonary surfaces are directed laterally and accommodated within the cardiac impressions of their respective lungs. The cardiac impression is deeper and larger on the left lung due to the projection of the heart more towards the left side across the median plane. These surfaces of the heart are separated from each other by borders. They include the right border which is formed by the right atrium, and the left border which is formed by the left ventricle and a small part contributed by the left atrium. The right and left borders of the heart are deflected anteriorly and posteriorly, respectively. The superior border of the heart is formed by the atria and great vessels, and the inferior border is formed by the ventricles (mostly the right ventricle). It is noteworthy that the right border of the heart silhouette on a radiograph is formed by the right atrium, the terminal part of the superior vena cava above and the terminal part of the inferior cava below. Similarly, the lower part of the left border on a radiograph is formed by the left ventricle and a small part by the left atrium, and the upper part is formed by the pulmonary artery, aorticopulmonary window and the aortic notch. The anatomic description of the right and left borders of the heart is thus different from their radiological description (Proschek & Vogl, 2015).

The pericardium is a membrane that surrounds the heart and the roots of the great vessels, which has two layers, an outer tough fibrous layer (fibrous pericardium) that provides protection and holds the heart in position, and an inner thinner layer (serous pericardium) that has an outer layer (parietal pericardium) fused to the fibrous pericardium and an inner layer (visceral pericardium or epicardium) fused to the heart, forming the outermost layer of the heart wall. The pericardial cavity lies between the two layers of the serous pericardium, i.e. between the parietal and the visceral layers. The transverse sinus of the pericardial cavity lies between the ascending aorta and the pulmonary trunk anteriorly, and the venae cavae and the atria posteriorly. It serves as a communication between the right and left sides of the pericardial cavity, and is used in coronary artery bypass grafting. The oblique sinus is a blind pericardial pouch that lies behind the left atrium and is bounded on the right by the right pulmonary veins and inferior vena cave, on the left by the pulmonary veins and superiorly by a reflection of serous pericardium extending transversely between the right and left superior pulmonary veins. The heart wall has a thicker middle layer called the myocardium, which consists of a complex swirling pattern of cardiac muscle, forming a figure of eight

around the atria and the roots of great vessels, and then again in the deeper layers around the ventricles towards the apex, making the heart a more effective pump. The more superficial layers of ventricular myocardial muscle wrap around both ventricles. The innermost layer of the heart wall is called the endocardium which resembles the endothelium of a blood vessel, and it lines the surfaces of the chambers and valves of the heart (Akhter, 2011).

The four chambers of the heart are separated by three septa, the interatrial septum separating the two atria, the interventricular septum separating the two ventricles, and the atrioventricular septum separating the atria from the ventricles. The atrioventricular septum is marked by the presence of four openings guarded by valves that allow blood flow in one direction from the atria to the ventricles (the atrioventricular valves), and from ventricles to the pulmonary artery and aorta (the semilunar valves). These valves are surrounded by dense fibrous rings called annuli (singular: annulus) that are part of the fibrous cardiac skeleton which strengthens the atrioventricular septum and provides insulation for the electrical conduction system of the heart, part of which lies within the interventricular septum (Saremi et al., 2017; van Gils, 1981).

The atrioventricular valve on the right side has three leaflets (anterior or superior, posterior or inferior and septal), hence called the tricuspid valve, and that on the left side has two leaflets (anterior and posterior), resembling a mitre or a bishop's hat, hence the name mitral. The leaflets of each of these valves are inserted into their respective annuli that surround the valve and constitute the anatomical junction between the ventricles and their corresponding atria. Based on the insertion site of the leaflet, the annulus is segmentally divided as anterior, posterior or septal. The mitral annulus has a saddle shape, with two commissural areas i.e. anterolateral and posterolateral commissures. Commissural areas are regions where the edges of valve leaflets lean against each other, acting as support to the base structure of the cusps. The tricuspid annulus is also saddle-shaped, with three commissural areas i.e. the anteroseptal, anteroposterior and posteroseptal commissures. During systole, the commissural areas are displaced apically, while the contraction of the annulus narrows its circumference and the valve cusps close. The mitral annulus is surrounded by structures such as the aortic valve, coronary sinus and circumflex artery. The tricuspid annulus is surrounded by the AV node (superior to the septal leaflet) and coronary sinus.

The right semilunar (pulmonic) and left semilunar (aortic) valves both have three flaps. The annuli of these valves are similar in that both have three arches surrounding the valve orifice and the apices of the arches merge along the line of valve commissures. Unlike the atrioventricular valve annuli, the semilunar valve annuli do not lie in the same plane. The pulmonary valve annulus is roughly perpendicular to the aortic valve annulus. These annuli also serve as a transition point between the right ventricle and the root of pulmonary trunk, and between the left ventricle and the aortic root, respectively (Misfeld & Sievers, 2007).

Between the pulmonary valve cusps and the dilated proximal part of the pulmonary trunk are spaces called pulmonary sinuses. These sinuses prevent the cusps from flattening against the wall of the proximal pulmonary trunk during systole as they open, which may restrict valve closure during diastole. The aortic sinuses are located just above the aortic valve, bounded by the leaflets of the aortic valve internally and the bulges of aortic walls externally. They are three in number, one anterior (right coronary) and two posterior (left posterior or coronary and right posterior) (Figure 1.6). While the anterior and left posterior sinuses give rise to the right and left coronary arteries respectively, the right posterior aortic sinus does not contribute to any vessel and is thus called the non-coronary sinus.

The external surface of the heart has three main sulci (singular: sulcus). These sulci carry important blood vessels. The coronary sulcus runs transversely around the heart, demarcating the boundaries of the atria and the ventricles. The anterior and posterior interventricular sulci run vertically on their respective surfaces demarcating the boundary between the right and left ventricles. The coronary sulcus contains the right and left coronary arteries on their respective sides and the coronary sinus posteriorly on the left side. The anterior interventricular sulcus contains the left anterior descending or anterior interventricular artery (a branch of the left coronary artery) and the great cardiac vein. The posterior interventricular sulcus contains the posterior descending or posterior interventricular artery (a branch of right coronary artery or sometimes it branches off the circumflex coronary artery) and the middle cardiac vein. Other branches of the left coronary artery include the left marginal and left circumflex arteries. The right coronary artery also gives off a branch called the right marginal artery that supplies most of the right ventricular myocardium.

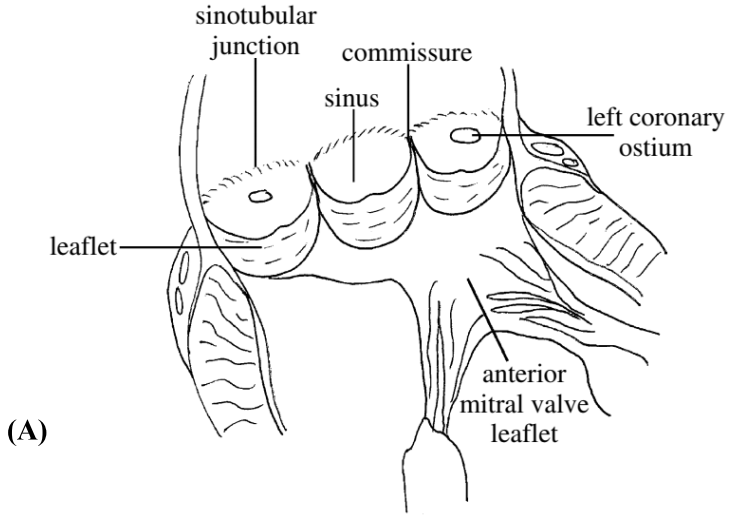

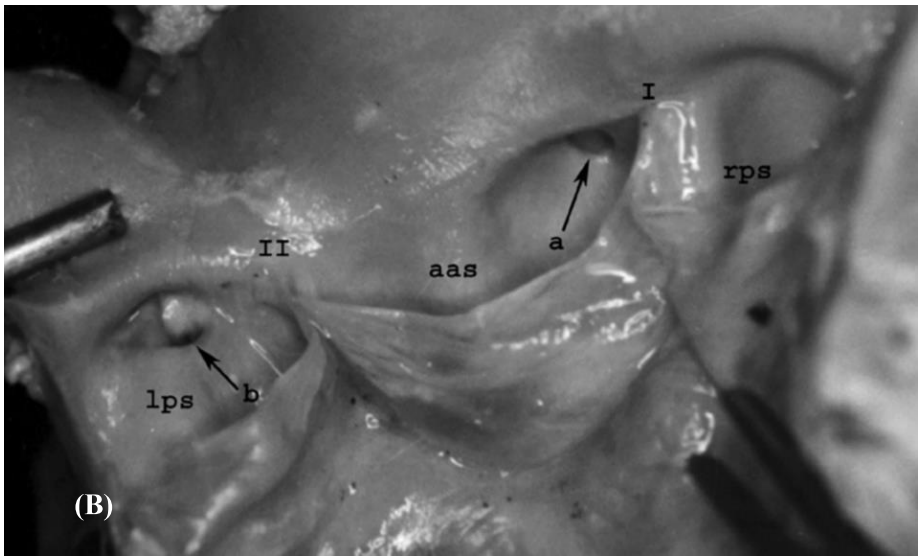

Figure 1.6 (A) shows a schematic drawing of aortic root structures after longitudinal opening of the root (Misfeld & Sievers, 2007). (B) shows the circumferential deviation of the right coronary ostium (arrow 'a') towards the commissure 'I'. The left coronary ostium is similar to a horizontal slit. The margin of the slit has been lifted and the lower margin is at arrow 'b'. Abbreviations: Aas – anterior aortic sinus (right coronary); lps – left posterior sinus (left coronary) (Joshi et al., 2010)

The coronary sinus is the main vein of the heart and it drains into the right atrium. Its opening is located between the right atrioventricular orifice and the inferior vena cava. The tributaries that drain into the coronary sinus are the great cardiac vein, small cardiac vein (located on the anterior surface of the heart), left marginal vein (located alongside the lateral margin of the left ventricle), left posterior ventricular vein (courses over the inferior wall of the left ventricle) and the middle cardiac vein. The right marginal vein which travels along the inferior margin of the heart does not drain into the coronary sinus (Joshi et al., 2010).

Based on function, the heart can be divided into a right and left side, each with its own receiving chamber or atrium, a pumping chamber or ventricle, and an outflow tract. With the heart at its center, there are two circulatory circuits, the low-pressure pulmonary and the high-pressure systemic circuits. They are both distinct but linked to each other. The right side chambers have smaller pressure and size as they are associated with pulmonary circulation compared to the chambers of the left side that are associated with the systemic circulation. The functional capacity of each ventricle is reflected in its shape. The left ventricle has a prolate ellipsoid or conical shape, appearing circular on cross-section. While the right ventricle has a more complex shape that appears triangular in lateral view and crescentic when viewed in cross-section (Hudsmith et al., 2005). The shape of the ventricles is influenced by the habitus of an individual, chest shape and several other factors, especially disease states of the heart that result in a typical shape, e.g. the left ventricle becomes more spherical in dilated cardiomyopathy or spade-shaped in apical hypertrophic cardiomyopathy. Even the right ventricle overload, e.g. in pulmonary hypertension, is manifested as a D-shaped left ventricle due to the flattening of the interventricular septum (Cativo Calderon et al., 2017).

1.4 An Enlarged Heart (Cardiomegaly) and Its Clinical Significance

1.4.1 Cardiomegaly

Cardiomegaly is the medical term for an enlarged heart which is a common finding in pathological conditions related to the heart, e.g. primary or acquired cardiomyopathies, or secondary to a disease process of some other organ system, e.g. chronic renal disease (Amin & Siddiqui, 2020). It may also be observed associated with physiological processes, e.g. in pregnancy and athletes (Chung & Leinwand, 2014; Utomi et al., 2013). Hence, it is not a

disease itself but a manifestation or a consequence of some other condition or underlying pathology (Arts et al., 2012). It is noteworthy that not all diseased hearts are associated with cardiomegaly, in fact a person may be going through a medical emergency related to heart function, yet the heart size will be normal. By definition, it is present when the transverse cardiac diameter of the cardiac silhouette is greater than 50% of the transverse diameter of the thorax on a posterior-anterior (PA) view of chest X-ray, magnetic resonance imaging (MRI) or computed tomography (CT).

In forensic medicine, the heart is frequently weighed and evaluated for the presence of pathology, as are other organs. First stated in 1670, the weight of a human heart was found to weigh 283 g. Later researchers used more thorough methods to arrive at the normal value of heart weight, recording measurements for the gross weight of the heart, i.e. with the epicardial fat included, and for the net weight as well, i.e. after the removal of fat. Today researchers recommend there be an establishment of a normal range for heart weight, much like the ranges used for hemoglobin, hematocrit, albumin, electrolytes and other laboratory tests. From a review of previous studies, it can be recognized that the average normal heart weight varies widely and is dependent on the population studied. For example, a normal human heart weight stated in one study was 233 to 383 g for adult males (Molina & DiMaio, 2012), and 148 to 296 g for adult females (Molina & DiMaio, 2015); weights stated in Gray's anatomy are, 280 to 340 g in men and 230 to 280 g in women (Gray, 2015); while in Robin's textbook, heart weight ranges from 300 to 360 g for men and 250 to 320 g for women (Kumar et al., 2015). Most studies related to postmortem heart weight still use methods and normal values introduced more than ninety years ago, including those defined by Smith (Smith, 1928).

There is no standard classification of cardiomegaly. Instead, it is described according to enlargement of the involved chamber(s), e.g. the ventricles, or the pathology of the heart muscle involved in the enlargement, e.g. dilated cardiomyopathy is characterized by a thin and stretched heart muscle, and hypertrophic cardiomyopathy is characterized by hypertrophy of the heart muscle. The differentials of cardiomegaly include conditions that may cause an enlarged cardiomediastinal silhouette on a chest X-ray e.g. anterior mediastinal mass, pericardial effusion, prominence of epicardial fat, and mediastinal widening (e.g. secondary to pulmonary or aortic pathology). Cardiomegaly frequently involves the

ventricles (either single or both), and when enlarged the atria are also reflected in the overall increase in transverse cardiac diameter on a PA view radiograph. Based on the part of the heart affected and the degree of dysfunction, cardiomegaly may be a sign of a serious underlying condition. In the form of dilatation or hypertrophy, it leads to a range of symptoms depending on the severity and the underlying cause (Amin & Siddiqui, 2020).

1.4.1.1 Pathological Processes Involved

The processes involved in the development of cardiomegaly include cardiac remodeling and hypertrophy of the muscle, eventual fibrosis and contractile malfunction. There is both genetic and non-genetic component to this process. The list of influencing stimuli includes mechanical stretching, neuro-hormones and oxidative stress. These stimuli signal inflammatory cytokines and mitogen-activated protein (MAP) kinase transduction in cardiomyocytes which lead to alterations in structural and regulatory proteins (that regulate excitation and contraction) (Ruwhof & van der Laarse, 2000). In dilated cardiomyopathy, there is a reduced force of contraction and reduced content of the sarcomere. In contrast, hypertrophic cardiomyopathy and its variants result in hyperdynamic contraction, poor relaxation and increased energy consumption (Tsiviltidou et al., 2017).

In dilated cardiomyopathy, there is an increase in the size of the myocardial fibers due to decreased overlapping of actin and myosin filaments as a result of heart tissue becoming enlarged and stretched, a consequence of the heart working harder than it normally should. As there is decreased overlapping of these filaments within the sarcomeres, they are not able to pull on one another effectively to shorten the muscle fibers. The sliding filament mechanism of the heart is affected, resulting in its failure to shorten properly and a failure of the heart to contract. The blood is not pumped into pulmonary circulation for oxygenation and thus into the systemic circulation for delivery of oxygenated blood to the tissues of the body. In ventricular hypertrophy, myocyte architectural changes are the culprit, the ensuing fibrosis and extensive myocardial scarring result from the development of fibroblasts between myocytes (Fujiu & Nagai, 2014). Myocytes in a healthy myocardium are arranged in a typical parallel alignment, however in hypertrophic cardiomyopathy, they become enlarged, hypertrophied and distorted. This leads to the disorientation of adjacent cells and their arrangement in a random pattern (myocyte disarray), which may be localized and

surrounded by normal myocardium, or it can occupy most of the ventricular surface. There is premature cellular death and continuous myocardial tissue remodeling due to pathological myocyte morphology, with the participation of cardiac fibroblasts. Thickening and narrowing of intramural coronary artery walls result from collagen accumulation between the smooth muscle cells (Stroumpoulis et al., 2010).

1.4.1.2 Symptoms and Physical Examination

Most patients are asymptomatic, and whether or not there is an accompanying symptom is not diagnostically specific or sensitive. Because it is not uncommon for patients to be asymptomatic at rest and only become symptomatic on exertion. When there are symptoms, they are usually related to the underlying cause and its severity, e.g. if the cardiomegaly is severe enough that the heart's ability to pump blood effectively is compromised, then symptoms of congestive heart failure may be present. Based on the severity of dysfunction, the symptoms can be classified or risk-stratified according to any standard classification system, e.g. New York Heart Association (NYHA) classification of severity of heart failure (HF). The NYHA classification groups a subject being asymptomatic with ordinary physical activity as class I, and those with symptoms at rest as class IV. Although NYHA classification has served as a fundamental tool for risk stratification of HF, recent studies have pointed out that it poorly discriminates HF patients across the spectrum of functional impairment (Caraballo et al., 2019).

Investigative imaging for cardiomegaly is often aided by taking history to explain the symptoms which may be associated, e.g. shortness of breath on exertion or rest, orthopnea, or paroxysmal nocturnal dyspnea, and the findings of physical examination. Findings on examination may include sinus tachycardia (due to increased sympathetic stimulation), diminished pulse pressure (due to reduced stroke volume), S3 or ventricular gallop in early diastole (due to volume overload and systolic dysfunction), S4 or atrial gallop in late diastole (due to diastolic dysfunction), jugular venous distension or positive abdominojugular reflex (due to elevated right-sided filling pressures), pulmonary crackles (due to elevated left-sided filling pressures), respiratory distress according to the severity of the condition, hepatomegaly, ascites and peripheral edema (due to increased pressure in hepatic and systemic veins) (Malik et al., 2021).

1.4.1.3 Investigations

Cardiomegaly is best diagnosed through imaging techniques, and the imaging options available today allow not only assessment of the heart's size but also its function, identifying any structural abnormality or dysfunction that may be present. Other techniques employed to investigate cardiomegaly besides radiological imaging, include electrocardiogram (ECG), transthoracic echocardiography (two-dimensional, 2D; or three-dimensional, 3D), cardiac computerized tomography (CT) scanning and cardiac magnetic resonance (CMR) imaging. Most of the later imaging modalities investigate the cause of cardiomegaly rather than cardiomegaly itself. Newer studies are using CMR for structural and functional assessment of the heart, and it is emerging as the new gold standard for ventricular volume quantification (La Gerche et al., 2013), and for evaluating myocardial function and scarring (Salerno et al., 2017). CMR has an emerging role in diagnosing heart failure by measuring left ventricular ejection fraction, identifying structural heart disease and diastolic dysfunction (Webb et al., 2018). CMR has an advantage over CT in that it uses a magnetic field and radio waves to produce signals that create images of the heart, while CT utilizes an X-ray tube that rotates around the body and collects images of the heart and chest.

In the setting of a heart failure (HF), the routine investigations include blood tests e.g. serum pro-BNP levels and serum troponin I and T levels (Nadar & Shaikh, 2019), and stress tests e.g. stress electrocardiography or stress echocardiography, and coronary angiography (Steeds et al., 2019). Stress tests evaluate how well the heart works during physical activity. It usually involves walking on a treadmill or riding a stationary bike while the heart rhythm and function, blood pressure, and breathing are monitored. To measure heart size and establish cardiomegaly, chest X-ray remains the basic tool available but the gold standard for this purpose is 2D echocardiography. There have been studies making use of 3D echocardiography, but it has been proposed by researchers that further studies are needed to support the introduction of 3D echocardiography into common cardiac practice (Ruddox et al., 2013). Time and again it has been observed that despite standard workup, the etiology of cardiomegaly may not be clear, necessitating further and more advanced investigations. Often a diagnosis by exclusion is obtained to initiate treatment, delaying of which may result in loss of crucial time and compromise patient wellbeing. Most of the emergency conditions will require a referral from a less equipped facility to a well-equipped one. Besides the

question of identifying whether or not a patient needs a referral, precious time is lost even when the patient is being transported to a tertiary care center (Cervantes et al., 2003).

1.4.2 Clinical Significance

There are several known causes of an enlarged heart and in most cases, the presentation can give a clue towards identifying the underlying pathology e.g. congenital or congestive heart disease. An enlarged heart identified on a chest X-ray diminishes the possibility of normal heart function and requires further investigation (Siddiqui et al., 2013). With relevant physical examination and simple investigative tools for exclusion, a physician working in a remote health facility can make better decisions related to treatment or judge the urgent nature of a condition. Clinicians do not have to delay initiating treatment awaiting diagnostic certainty (Kassirer & Kopelman, 1989). Frequent referrals with insufficient information lead to unnecessary investigations, waste of crucial time and resources (Morales et al., 2012).

Cardiomegaly is considered a nonspecific finding that occurs in most patients with chronic HF, with notable exceptions including HF from acute MI, constrictive pericarditis, restrictive cardiomyopathy, valve or chordae tendineae rupture, or HF due to tachyarrhythmias or bradyarrhythmias. The fact that it excludes most of the acute conditions that cause HF, explains the need to determine how specific and sensitive it practically is. Some studies support the usefulness of chest X-ray (PA view) as a screening tool in identifying cardiomegaly. In contrast, some authors insist that a chest X-ray (PA view) even when used together with electrocardiography (ECG), is not sufficient to allow a reliable prediction of HF (Fonseca et al., 2004). It must be taken into account, that cardiomegaly is almost always not the only finding in any heart condition, there will be associated symptoms and the findings on physical examination will reveal more. Before adopting any strategy, the first step is always a careful history, which is crucial to determining the cause of a patient's problems. Kassirer and Kopelman (1989) highlighted that the purpose of diagnostic process is to sufficiently diminish any ambiguity for making ideal decisions for the ensuing care. Investigations help clarify and narrow the differential diagnosis, and as the list becomes narrowed to one or two possibilities, the lead diagnosis is checked for its ability in explaining the patient's signs and symptoms (Kassirer, 2010). Besides, an increasing emphasis on diagnostic testing has the concern of researchers that clinical examination skills have been

underrated in contemporary professional health care education and training (Kassirer, 2014; Kugler & Verghese, 2010). Disorders or conditions that cause pseudo-cardiomegaly on a chest X-ray (PA view), e.g. epicardial fat pad, mediastinal mass, thymus tumor, chest wall or vertebral column deformities and a chest X-ray obtained in expiration, can usually be distinguished from true cardiomegaly based on the presentation of the patient and physical examination, or if any uncertainty remains it can be further investigated (Walker et al., 1990).

Heart failure (HF) (or congestive HF) is an eventual outcome of most heart conditions that start off as separate entities. In fact, most heart conditions, e.g. cardiomyopathies or coronary artery disease (CAD), are managed for the underlying cause and to prevent the development of HF. The heart's function to pump blood to the lungs or systemic circulation is compromised in HF. It may be chronic and considered stable when the compensatory mechanisms (e.g. Frank Sterling mechanism, activation of neurohumoral systems and myocardial adaptation) are not saturated, but as these processes become overwhelmed with disease progression, it becomes decompensated chronic HF. The decompensation is manifested as orthopnea and paroxysmal nocturnal dyspnea (Joseph et al., 2009). The term acute HF describes the nature of the clinical presentation, which may not necessarily be severe but recent in onset. It is characterized by worsening of signs and symptoms reflecting the inability of the heart to function. Most patients may have a previous decompensating chronic heart failure. Based on left ventricular ejection fraction (EF), HF can be categorized into systolic and diastolic heart failures. When the symptoms of HF are present with a left ventricular EF of less than 45%, it signifies systolic HF due to abnormal function of the systolic pump. Systolic HF is also referred to as HF with reduced systolic function or reduced EF (HFrEF). When the symptoms are present with EF of more than 50%, the symptoms are attributed to diastolic HF in which there is an impaired relaxation of the heart during diastole (Aziz et al., 2013). The diastolic HF is also called HF with preserved systolic function or preserved EF (HFpEF). Frequently, patients have both diastolic and systolic heart failures simultaneously, but such a condition will still be referred to as systolic heart failure (Hajouli & Ludhwani, 2021).

Cardiomyopathies are a heterogeneous group of diseases involving the myocardium. They manifest as a failure of myocardial performance, which can be a mechanical (i.e. diastolic or systolic) dysfunction leading to congestive HF, or an electrical dysfunction leading to life-

threatening arrhythmias. They present as inappropriate ventricular hypertrophy or dilatation, and are due to a variety of causes. Primary cardiomyopathies are frequently due to genetic causes, and secondary cardiomyopathies are due to myocardial involvement as a component of a systemic or multi-organ disorder. Cardiomyopathies are classified according to the anatomic abnormalities that result from the underlying cause, and include three main pathologic patterns: dilated cardiomyopathy (90% of all cases), hypertrophic cardiomyopathy and restrictive cardiomyopathy (least frequent). Within each of these patterns, there is a spectrum of clinical severity and sometimes the clinical features overlap (Wexler et al., 2009).

Coronary artery disease (CAD) or coronary heart disease, develops over time due to atherosclerotic plaque buildup inside the arteries supplying blood to the heart muscle, resulting in narrowing and stiffening of these vessels and thus reduction of blood flow to the heart muscle. The patients frequently present with chest pain, located centrally and often radiating to the left shoulder or angle of the jaw, associated with sweating and nausea. Atypical symptoms may be present particularly in women, older patients, and patients with diabetes mellitus. When the symptoms occur at predictable times e.g. with physical or emotional exertion, and relieved at rest it is considered stable angina. As these symptoms change character, frequency or intensity, it is called unstable angina which may be followed by an acute MI. In contrast to stable angina, unstable angina is characterized by chest pain that starts suddenly at rest or with minimal exertion (Shahjehan & Bhutta, 2021).

Acute coronary syndrome (ACS) is a medical emergency and is usually diagnosed in the emergency department with the help of ECG and cardiac markers (troponin I and T, and H-FABP or the Heart-type Fatty Acid Binding Protein) (Nadar & Shaikh, 2019). It is called a syndrome due to the set of signs and symptoms that are frequently associated with it, all of which result from decreased blood flow in the coronary arteries supplying the heart. It is further subdivided into three types which include unstable angina, ST-Elevation MI (STEMI) and Non-ST Elevation MI (NSTEMI). When the symptoms are prolonged beyond 20 to 30 minutes, the ACS is termed acute MI, which is considered a type of ACS. In summary, an ACS where there is no cell death is called unstable angina, and when there is cell death it is called an acute myocardial infarction (MI), which is further classified as a STEMI and NSTEMI based on ECG results. The diagnosis is straightforward, if the ECG shows an

absence of ST-segment elevation, there are two possibilities. First, the cardiac markers are elevated in blood indicating heart damage and the chest pain is attributed to NSTEMI. Second, the cardiac markers are within normal limits indicating there is no evidence of heart damage and the chest pain is due to unstable angina. In contrast, when the ST segment is elevated it is strongly indicative of STEMI. Depending on whether it is a STEMI or NSTEMI, there are distinct guidelines for each with a general aim to comfort the patient's pain (by using nitroglycerin or morphine), unblock the involved blood vessels (via PCI or Percutaneous Coronary Intervention, fibrinolysis, and CABG or Coronary Artery Bypass Graft), reduce blood clot formation or prevent its enlargement and reduce ischemia (through antithrombotics, that lyse thrombus and achieves reperfusion), and modify risk factors to prevent future MIs (Kumar & Cannon, 2009).

1.5 Body Surface Area & Indexed Echocardiographic Values

Body surface area (BSA) is a measure of the surface area of a human body. In physiology and medicine, different formulae have been developed that calculate BSA without a direct measurement (Alhaji Saganuwan, 2015). These formulae have been published previously based on studies that applied different methods. The results were used to yield a formula and construct a normogram from that formula. Direct measurement of BSA is a very inconvenient task that takes time; instead, an estimate is obtained from height and weight by applying the different formulae that serve well for prediction purpose. For example, the Du Bois formula was derived from the measurements of nine North American subjects, the entire bodies of whom were separately coated with a mold that was later cut away and spread out so that its area could be measured. A formula was derived from the results which has been widely used in scientific literature. The metric formulae used for calculating BSA are expressed in m^2, the weight is measured in kilograms (kg) and the height in centimeters (cm). It is considered a better indicator of metabolic mass compared bodyweight because it is less affected by abnormal adipose mass. The average BSA values for different age groups and gender can be estimated using statistical survey data and a BSA formula. There are now several other formulae available in publications for the calculation of BSA, the Schlich formula being the only one that takes gender into account (Flint & Hall, 2021). BSA has been accepted as the most appropriate biometric unit for normalizing physiological indices related to body metabolism in individuals of different body sizes. These indices include renal clearance,

cardiac index or output, basal metabolic rate, blood volume and ventilation. It is widely used in clinical medicine for determining dosages of drugs e.g. anesthetics, fluid rehydration therapy or parenteral fluids and electrolytes in critical care medicine, estimation of the correct volume of plasma expanders for use in the prophylaxis of shock from burn injuries, and chemotherapy. Several studies have analyzed the use of BSA in detail to determine the dosage of medications with a narrow therapeutic index, e.g. chemotherapy. There are studies that propose environmental and ethnic differences bear influence on BSA and the variables that determine BSA, i.e. height and weight (Nwoye & Al-Shehri, 2003).

Most echocardiographic parameters vary according to gender, weight, height, ethnicity, physical fitness and age. It is impossible to factor or incorporate all these variables into every single measurement, which will result in prolonged reporting times and reference tables that will be too cumbersome to use. To remedy this problem, echocardiographic parameters are often indexed according to BSA. There is abundant evidence that this approach is reasonable for certain parameters, e.g. left atrial (LA) volume, and for others it may not be useful, e.g. LA internal dimensions and left ventricular (LV) internal diameter.

Caution is advised when interpreting indexed echocardiographic values for obese patients, i.e. those with a BMI of more than 30 kg/m^2, because obesity is likely to cause changes in chamber size or wall thickness due to the considerable low metabolic demand of fatty tissue compared to muscle. The point of discussion here is that indexing for BSA when the individuals are overweight or obese may result in an underestimation of the degree of cardiac remodeling. Likewise, in healthy individuals who exercise and have adequate daily physical activity, there is a reduction in fat tissue of the heart and an increase in the size of heart muscle. Hence, an athlete's heart should not be based only on echocardiographic measurements, other relevant clinical information requires attention too (Engel et al., 2016). Studies that provide normative data related to the heart for athletes and sportsmen maintain that present scaling approaches mostly standardize cardiovascular structures to the body surface area (BSA). Some authors state that BSA also quantifies extravascular fluid volumes, along with both muscle and adipose tissues. However, the impact of adipose tissue and extravascular fluid on BSA, may vary widely between both genders and is dependent on age (Chang et al., 2018).

Thus, insufficient indexing recommendations for countries where the reference values are based on ASE or EACVI guidelines, the cardiologists end up applying the same normal range of heart chamber dimensions for everyone, including a sportsperson e.g. an athlete or a gymnast, and the aged or the frail e.g. those suffering from a chronic disease. For instance, in a patient with small body stature, heart enlargement may not be identified due to inaccurate underestimation, leading to treatment delay and unfavorable prognosis. In such cases, the reference values stated for normal heart size may not apply due to smaller hearts at baseline (Pfaffenberger et al., 2013).

1.6 Hypothesis

1.6.1 Null hypothesis:

Cardiac size cannot be depicted on a chest X-ray and cannot be compared with cardiac size on echocardiography

1.6.2. Alternate hypothesis:

Cardiac size can be depicted on a chest X-ray and can be compared with cardiac size on echocardiography

1.7 Objective(s) of study:

1. To determine heart size measurements on chest X-ray (PA view) in a local population
2. To correlate these measurements with echocardiographic measurements for the same person
3. To determine the specificity and sensitivity of the measurement of cardiothoracic ratio (CTR) on a chest X-ray (PA view) in determining heart enlargement

1.7 Problem Statement/ Problem of Study:

80% of cardiovascular diseases are preventable, by aiming at addressing the risk factors and screening for prevention of recurrence in subjects with a history of cardiovascular disease. By applying the basic tools available, a doctor working in primary health care can address modifiable risk factors, screen for prevention of recurrence, and detect early the acute manifestation of cardiovascular disease for prompt referral to the next level of care. Primary health care centers in the rural and remote areas of a developing country are not well set up. They lack instruments, machinery and trained personnel. The doctors working in such settings have to make the most of what is available to them. It is not always possible to decide a treatment plan for a patient due to lack of investigations, nor it is always affordable for the patient to be referred to a higher level of healthcare. The lack of trust in certain investigations that may be available and actually be useful, necessitates research to demonstrate their

effectiveness or at least point towards a reasonable alternative. Frequent referrals with insufficient information for conditions that may be treatable at primary or secondary health care centers place a burden on the tertiary health centers, and also lead to delay in initiation of treatment. Both the referral process and the delayed initiation of treatment add to the suffering of the patients.

1.9 Significance of the study

This study will help verify the usefulness of chest radiography as a screening tool for an enlarged heart and also investigate cardiothoracic ratio (CTR) as a reliable diagnostic parameter. In clinical practice, a history of presenting complaints together with physical examination offers the physician a rational list of differential diagnoses, which can be further shortlisted with the help of appropriate investigations to decide a treatment plan. This study will help determine whether a simple investigation like chest radiography can be used as an alternate or a preliminary investigation to echocardiography in patients who are clinically suggestive of heart enlargement, especially in circumstances when resources are inadequate, or there is unavailability of echocardiography machine or an echocardiologist. It will help doctors working in rural healthcare facilities utilize a basic tool available to them for better therapeutic decisions. It will also help in streamlining patients, for a timely referral to a higher center. The study will ascertain the mean radiographic values at which the cardiac silhouette appears normal or enlarged, and thus serve as a baseline for establishing cardiomegaly within the Pakistani population. It will help confirm if foreign radiographic and echocardiographic reference values apply to the local population.

1.10 Operational definitions

1. *Cardiomegaly:* Cardiomegaly means an enlarged heart size. It is present if the ratio of transverse diameter of the cardiac silhouette to the transverse diameter of the chest is greater than 0.5 (referred to as an increase in cardiothoracic ratio) on a PA view of chest X-ray or computerized tomography (CT) (Amin & Siddiqui, 2020)
2. *Transverse Cardiac Diameter*: The transverse diameter of the heart that is obtained as the sum of the horizontal distance between the left and right lateral most borders of the heart and the mid-sagittal plane (Mensah et al., 2015)
3. *Transverse Thoracic Diameter:* The maximum transverse internal diameter of the thoracic cavity between the internal surfaces of the ribs on both sides (Mensah et al., 2015)
4. *Cardiothoracic Ratio:* The transverse diameter of the heart divided by the transverse thoracic diameter expressed as a ratio or percentage (Sinha et al., 2013)
5. *Heart Failure:* It is defined as an abnormal state which renders the heart incapable of pumping blood at a rate required to meet the metabolic needs of the tissues or can do so with elevated filling pressure. It may be due to the inability of the left ventricle (LV) to fill (poor diastolic performance) and/or eject (poor systolic performance) (Fukuta & Little, 2008)
6. *Systolic Heart Failure:* When heart failure is associated with a reduced ejection fraction (EF), the abnormal state may be called systolic heart failure (Fukuta & Little, 2008)
7. *Diastolic Heart Failure:* When heart failure is associated with diastolic dysfunction in the absence of a reduced EF, the abnormal state may be termed diastolic heart failure (Fukuta & Little, 2008)
8. *Ejection Fraction:* It is a measure of how much blood the left ventricle (LV) pumps out with each contraction, expressed as a percentage. The ability of the LV to empty can be quantified as LV emptying or ejection fraction (a ratio of stroke volume to end-diastolic volume) (Fukuta & Little, 2008)
9. *Left Ventricular Remodeling:* A pathophysiological process characterized by four basic patterns: normal geometry, concentric remodeling, concentric hypertrophy and

eccentric hypertrophy. Current guidelines recommend that LV geometry be classified using LV mass index (LVMi) and relative wall thickness (RWT), determined on echocardiography. A normal geometry is characterized by a normal LVMi and RWT. In concentric remodeling, only RWT is increased. In both concentric and eccentric hypertrophy, LVMi is increased, with a normal RWT in eccentric hypertrophy and an increased RWT in concentric hypertrophy (Nauta et al., 2020)

10. *Acute Coronary Syndrome (ACS):* It is a medical emergency condition, which is subdivided into several types. An ACS where there is no cell death is called unstable angina, and when there is cell death it is called a myocardial infarction (MI), which is further classified as a STEMI (ST-Elevation MI) and NSTEMI (Non-ST Elevation MI) based on ECG results. If the ECG shows an absence of ST-segment elevation, there are two possibilities. First, the cardiac markers are elevated in blood indicating heart damage and the chest pain is attributed to NSTEMI. Second, the cardiac markers are within normal limits indicating there is no evidence of heart damage and the chest pain is due to unstable angina. In contrast, when ST-segment is elevated it is strongly indicative of STEMI (Kumar & Cannon, 2009)
11. *End-Diastole*: Diastole begins when the aortic and pulmonary valves close, and ends with the closure of the mitral and tricuspid valves. This period represents ventricular relaxation and filling. The end-diastole is observed on echocardiography when the ventricle is largest, i.e. shortly before the mitral valve closes and the mitral annulus descends (Pollock & Makaryus, 2021)
12. *End-Systole*: Systole begins when the mitral and tricuspid valves close, and concludes with the closure of the aortic and pulmonary valves. This period represents ventricular contraction, forcing blood into the arteries. The end-systole is observed on echocardiography when the ventricle is smallest, i.e. shortly before the mitral valve opens (Pollock & Makaryus, 2021)

CHAPTER 2

LITERATURE REVIEW

It is often stated in literature that a human heart is approximately equal to the size of a clenched fist for that person. In a retrospective study, this claim was investigated by measuring the volume of the heart and hands using postmortem CT imaging. Other relevant data, such as heart weight, cause of death, and presence of cardiomegaly, was obtained from postmortem examination reports (Ampanozi et al., 2018). The mean hand volume was compared to the heart weight and volume. The study was conducted with a sample size of 64 cases using four categories, males and females with cardiomegaly (24 males and 8 females) or without cardiomegaly (18 males and 14 females). The results showed that in both cases, i.e. with or without cardiomegaly, the heart volume exceeded that of the fist. In all four categories, the mean hand volumes had a statistically significant difference from the mean heart volumes, in that the hands were smaller. Thus, the use of fist size for the appraisal of heart size is meaningless. In contrast, another study investigated to validate if the palm size can be used as a reference tool for determining the normal heart size. 275 healthy subjects (123 males and 152 females, with a mean age of 28.16 ± 16.18) were enrolled between the ages of 15 to 80 years. Both the palms were measured with a ruler from the medial side towards the lateral, extending from the edge of the secondary palm line or head-line to the edge of the first palmar crease or the heart-line. The 2D echocardiographic measurements of the heart were taken in the parasternal long-axis (PLAX) view, by measuring the largest diameter of the heart in two dimensions from the anterior fibrous pericardium to the lowest part of the posterior fibrous pericardium. The study concluded that the size of both palms when measured correlated with the heart diameter, and thus the size of the hand can be used for preliminary assessment of the heart for enlargement. The study stated that it was logical to expect such a relation between the heart and palm sizes as they are both mesodermal derivatives (George & Firulli, 2019). However, this correlation seized to exist for older participants, and those previously diagnosed with prehypertension (Fakoya et al., 2017). But for a timely diagnosis and making therapeutic decisions, assessment of disease progression,

and for evaluating the effectiveness of a medical or surgical intervention, a physician will need more than a few measurements of the hand (Clarke et al., 2019).

Cardiovascular diseases are considered an epidemic of the 21st century, a recognized global phenomenon with an alarming increased incidence and prevalence in low and middle-income countries (Gersh et al., 2010). According to WHO statistics, cardiovascular diseases are the number one cause of death globally, taking an estimated 17.9 million lives each year (Mc Namara et al., 2019). Mortality from heart disease is the number one cause of all deaths in the United States of America, accounting for about 20.57% of all deaths (Virani et al., 2021). Although the worldwide prevalence of heart diseases is very high, the incidence for a specific heart condition varies, e.g. heart failure with preserved ejection fraction represents more than half of these cases (Pfeffer et al., 2019). In Pakistan, the leading cause of death is attributed to ischemic heart disease (8%), cancer (8%), and lower respiratory tract infections (8%), followed by stroke (6%) and diarrheal diseases (6%). A cross-sectional study to determine the prevalence of cardiovascular disease in a study population of Punjab (Pakistan), enrolled 6351 subjects (3127 (49.2%) males and 3224 (50.8%) females) during a span of one year. The results revealed that 1109 (17.5%) subjects (519 (16.6%) males and 590 (18.3%) females) from the entire study population suffered from cardiovascular diseases (Zubair et al., 2018). Given the burden of cardiovascular diseases and limited resources at hand, it will be helpful to have a simple tool to differentiate between the normal and abnormal hearts, or being able to identify those potentially at risk. Available more readily to physicians, chest X-rays are generally used to investigate many conditions involving the structures contained within the thoracic cavity, e.g. the heart and lungs, and also any structural defect of the chest wall (Kelly & Frauenfelder, 2019). However, for some conditions, chest X-rays are effective in screening but not in diagnosis. Often further investigations are required for reaching a definitive diagnosis or for obtaining evidence in favor of the diagnosis suggested by the initial chest radiography (Ellis & Aziz, 2016).

Cardiomegaly is a frequently identified and reported chest X-ray finding and it has several causes, including coronary artery disease, kidney diseases, hypertension, inherited disorders, infections, and cardiomyopathies. The radiographic index used to measure heart size and screen for cardiomegaly is called the cardiothoracic ratio (CTR). It is a classic and most widely known chest X-ray index of cardiac function that was first conceived in 1919 for the

screening of military recruits. Numerous studies over the years have shown that a CTR of more than 0.5 on chest X-ray (PA view) is prognostically significant in the healthy and those with congenital or acquired heart diseases (Chana et al., 2015). It is still a useful tool today and a relevant index for evaluating heart size. It can be easily calculated as a ratio or percentage and can predict cardiomegaly with a 95.8% accuracy (Alghamdi et al., 2020). It is calculated from the maximum transverse cardiac diameter (TCD) and the widest internal transverse thoracic diameter (TTD). TCD is measured by drawing vertical parallel lines at the most lateral points of the heart silhouette and measuring in between them. More commonly the TCD is measured as a sum of two horizontal lines that extend from a central line passing through all the spinous processes of the vertebrae, to the lateral most margins of the heart. The distance measured from the right lateral most margin of the heart to the midline is called the transverse right cardiac diameter (TRCD or TCD) or the maximum right diameter (MRD). The distance measured from the left lateral most margin of the heart to the midline is called the transverse left cardiac diameter (TLCD or TLD) or the maximum left diameter (MLD). The TTD is measured as the widest inner diameter of the thorax by drawing vertical parallel lines at the inner aspect of the widest points of the rib cage and measuring in between them. A CTR (or TCD: TTD ratio) value of 0.5 is thought to represent the upper limit for normal. Earlier research studies have revealed ethnic differences in the CTR of Caucasians, Asians, and people of African descent (Nickol & Wade, 1982). These studies have provided an upper limit of normal for Caucasians as 50% and that for people of African descent as 55%, which is generally accepted in most African countries (Mensah et al., 2015).

A retrospective study to determine the normal mean CTR on chest X-rays (PA view) in a Ghanian population established the mean CTR to be 0.459 ± 0.04 (0.452 ± 0.04 in males and 0.467 ± 0.05 in females). A total of 1989 radiographs of indigenous Ghanaians were evaluated for the study out of which 998 (50.2%) were that of males and 991(49.8%) of females. The mean age of the study population was 30.9 ± 12.4 years (30.6 ± 11.8 years for males and 31.2 ± 13.0 years for females). The mean TCD of the study population was 126.1 ± 14.1 mm (129.8 ± 13.9 mm for males and 122.1 ± 13.1 mm for females), the mean TTD of the study population was 276.0 ± 58.1 mm (287.7 ± 19.3 mm for males and 263.7 ± 78.9 mm for females). The mean CTR of all subjects less than 60 years was less than 0.50, while that for the elderly was above 0.50. The mean CTR for males of all the age groups and females

less than 60 years was less than 0.50, while for females aged 60 years or more it was 0.52 ± 0.05. The mean TCD increased gradually with age, with males having slightly greater diameters than females. The mean TTD increased gradually with age till the fifth decade and then decreased thereafter, males having greater diameters. The mean CTR increased gradually with age, with females having greater values than males (Mensah et al., 2015).

A cross-sectional study in a Nigerian population focused on determining the normal values of CTR and its relationship with age, height, weight, and BMI in 80 undergraduate university students (40 males and 40 females, with a mean age of 19.19 ± 2.146). The ages of the participants ranged between 16 to 24 years. The parameters measured on chest X-ray (PA view) were TCD, TTD, and CTR. The degree of correlation was assessed for all the study parameters. The mean TCD for the entire study population was found to be 12.23 ± 1.06 cm, the mean TTD was found to be 26.54 ± 2.04 cm, and the average CTR was 0.46 ± 0.026. The CTR was found to correlate significantly only with TCD, implying that as the TCD increased so did the CTR. The TTD did not correlate with CTR. The TCD and TTD correlated significantly with age, height, weight, and BMI. The CTR was least affected by variation of body built or body parameters, hence it was stated to be a better indicator in predicting cardiac enlargement than TCD on a chest X-ray (PA view) (Longbak et al., 2017).

Mehra and Kumar (2019) investigated a population in Eastern Rajasthan, India to determine if heart diameter (i.e. TCD) and CTR on chest X-ray (PA view) were affected by variations in body habitus (i.e. weight, height, BMI, and BSA). 800 subjects with ages between 20 to 70 years (and above) were enrolled (350 males and 450 females, with a mean age of 58.43 ± 5.42 years), free from any cardiovascular and respiratory diseases. The radiological parameters (TCD and CTR) were correlated with weight, height, BMI, and BSA. A TCD value of more than 15.5 cm and a CTR of 50% (0.5) on a chest X-ray (PA view) were considered to represent the upper limit of normal. The maximum TCD observed in males was 16.5 cm among those aged between 30 to 40 years, and in females, it was 12.9 cm among those aged between 71 to 80 years. The CTR measured was expressed in percentage, for those aged under 30 years it was 43.1% in males and 45.9% in females, for those aged between 30 to 40 years it was 44.31% in males and 46.2% in females, for those aged between 41 and 50 years it was 44.9% in males and 46.4% in females, for those aged between 51 to 60 years it was 45.9% in males and 47.9% in females, for those aged between 61 to 70 years

it was 46.8% for males and 48.1% in females, and for those aged between 71 to 80 years it was 46% for males and 48.2% in females (Mehra & Kumar, 2019).

While chest radiography is a cheap and relatively safe method for investigating chest diseases, a serious medical condition may be associated with a normal chest X-ray. For example, a patient with acute myocardial infarction (MI) may have a completely normal chest X-ray (Tsakok & Gleeson, 2018). Thus, a normal-sized heart does not indicate the absence of any pathology, and an enlarged heart may not always be indicative of an underlying pathology, necessitating supplementary or more advanced investigations to reach a definitive diagnosis. Different studies have reiterated the screening potential of chest X-rays (PA view) for estimating heart size (Monfared et al., 2015). And as for any screening test, its validity is based on its accuracy in identifying those with a normal heart size from those with an enlarged heart. The accuracy is determined by comparing it to a gold standard which is definitive in establishing the true status of heart size, and it is recognized to be echocardiography (Alberg et al., 2004). Thus for validating the accuracy of chest X-ray (PA view) measurements, they have to be compared with 2D echocardiography. For the interpretation of echocardiography results, comparisons are usually made with standard reference values that define the measurements seen in healthy persons. The American Society of Echocardiography (ASE) and European Association of Cardiovascular Imaging (EACVI) have provided standard reference values for various echocardiographic parameters along with the guidelines of how to measure them so as to quantify cardiac chamber size and function (Douglas et al., 2019; Lang et al., 2015). Although these values are applied throughout the world, they are derived from North American and European populations. It is now known that echocardiographic measurements in a healthy person are influenced by several variables, such as age, gender, race, and geographic region (Cosyns & Lancellotti, 2016). For this reason, it is recommended that these reference values be stratified for gender and age in clinical practice (Ilercil et al., 2001; Ryu, 2016). Considering the racial differences that exist in echocardiographic measurements, there are no reference values currently available for adults or children in many countries, and therefore Western data are used as a reference for interpreting these measurements. Defining normal for a population should be based on the estimation of local normal reference values (Majonga et al., 2018). Several studies from different countries have focused on obtaining normal reference values for their

populations regarding the dimensions of the heart chambers and the great arteries, and the Doppler parameters as well (Choi et al., 2015; Yao et al., 2015).

Before proceeding to the review of different echocardiography-based studies, a description of the different echocardiographic measurements is necessary. Using 2D transthoracic echocardiography, the heart chambers are measured individually and for this purpose, each chamber has its own standard set of measurements that quantifies it and permit for its structural and functional assessment. These measurements are obtained by directing the transducer or probe at the heart and manipulating it in different angles to give multiple views of the heart. There is a wide range of measurements that have been used, measured at different stages of the cardiac cycle, e.g. during end-diastole or end-systole. Only a few of these measurements have been standardized by international societies and associations of echocardiography. Not all of these measurements are routinely taken unless specified or specially requested for research purposes (Figure 2.1 and 2.2).

The measurements taken to determine the right atrial (RA) dimensions are the RA area (RAA), the RA major (or longitudinal) axis, and the RA minor (or transverse) axis. These measurements are taken in apical 4-chamber view at the end of the ventricular systole. The left atrial (LA) dimensions are determined by measuring the LA area (LAA), the LA volume (maximum, LAV_{max}; and minimum, LAV_{min}), and the LA anterior-posterior (AP) diameter (LAD) in the end-systolic phase of the cardiac cycle. The LAA and LAV are measured in apical 4-chamber view, and the LAD is measured in parasternal long axis (PLAX) view (Mitchell et al., 2019). The indexed LAV is derived from the value of LAV divided by the body surface area (BSA) to give an independent and more powerful predictor of mortality (Patel et al., 2011).

The Right ventricular (RV) dimensions are determined by measuring the RV end-diastolic area (RV EDA), the RV end-systolic area (RV ESA), the RV outflow tract (RVOT) diameter, and the RV wall thickness (WT) in end-diastole. All these measurements are made in apical 4-chamber view, except the diameter of RVOT and RVWT. The proximal diameter of RVOT is measured from inner edge to inner edge in parasternal short-axis (PSAX) and long-axis (PLAX) views, and the distal diameter (at the level of pulmonic valves) is measured in parasternal short axis (PSAX) view only. Previously, both the diastolic RVWT and the

diastolic right ventricular internal diameter (RVIDd) were measured on M-mode echocardiography (Baker et al., 1983), which was a standard before 2D echocardiography took its place. Current guidelines recommend the RVWT to be measured in subcostal view. The RV ejection fraction, for routine clinical purposes, can be determined by several morphological parameters such as TAPSE (Tricuspid Annular Plane Systolic Excursion), RV free wall systolic velocity (s') via tissue Doppler, and fractional area change (FAC). Linear parameters (or dimensions) have also been used to quantify RV function, e.g. AP diameter measured in PLAX and PSAX views. These linear dimensions include the basal diameter (RV_1 or RV_b), the mid-cavity diameter (RV_2 or RV_m), and the base-to-apex or longitudinal length (RV_3 or RV_l). The apical 4-chamber view is used to measure the transverse diameters at different levels of the long-axis of RV, and the longitudinal diameter is measured along the long-axis of RV. The RV mid-cavity diameter has also been used to assess the dilatation of RV (Lang et al., 2015).

Left ventricular (LV) dimensions are determined by measuring LV end-diastolic diameter or LV internal diameter in end-diastole (LVEDD or LVIDd), LV end-systolic diameter or LV internal diameter in end-diastole (LVESD or LVIDs), and posterior wall thickness in end-diastole (PWd). All these measurements are taken in PLAX view. The LV ejection fraction (LV EF) can be determined by either applying the modified or biplane Simpson's method using the apical 4-chamber and apical 2-chamber views (which measure the end-diastolic (EDV) and end-systolic (ESV) volumes of the LV), or by applying the Teichholz method using the PLAX view of the LV for the calculation of M-mode LV EF. The interventricular septal wall thickness (IVS) is measured at end-diastole in the PLAX view. Its measurement is necessary for LVM (LV mass) determination. It is usually measured together with other LV dimensions, i.e. LVIDd and PWd. LV mass (LVM), which represents the weight of the left ventricle, is calculated by applying the Devereux and Reichek's 'cube' formula that incorporates the following measurements: IVSd, LVIDd, and LV PWd. This method of measuring LVM is often referred to as the linear method and the formula used is, $LVM = 0.8\{1.04\ [([LVIDd+ IVSd+PWd]^3-LVIDd^3)]\} + 0.6$. The current guidelines recommend the use of LV tissue-blood interface for LVM measurement, and there are ASE and EACVI proposed values derived from this approach. The linear method has been recommended to be implemented as the best screening technique for LV hypertrophy, due to its simplicity, ease

of acquisition, and lower variability. LVM values are usually indexed to BSA for a better predictive value of cardiovascular disease outcomes and reduced variability among normal individuals. It can also be indexed to height for better detection of LV hypertrophy in obese persons. The relative wall thickness (RWT) is a ratio determined by the formula, RWT = (2 x PWd) / LVIDd. It allows further classification of LV mass increase as either concentric hypertrophy (RWT > 0.42) or eccentric hypertrophy (RWT ≤ 0.42) (Lang et al., 2005).

The aortic root diameter is assessed in the PLAX view at multiple levels that include the level of the aortic annulus, sinuses of Valsalva, sinotubular junction, and proximal ascending aorta. The main pulmonary artery is measured in the PSAX view at the level of maximum diameter above the level of pulmonary root. Regarding the roots of great vessels, the measurements of both the aorta and pulmonary artery are performed during end-diastole, perpendicular to the long axis of the vessel being measured, by applying the leading edge method. The pulmonary artery systolic pressure (PASP) is measured using the modified Bernoulli equation, PASP (mmHG) = $4(V_{max})^2$ + RAP, where V_{max} is the maximum velocity of tricuspid regurgitation (TR) and RAP is the right atrial pressure (Figure 2.4). RAP is estimated from the diameter and collapsibility of inferior vena cava, observed in subcostal IVC (SIVC) or subcostal long axis (SLAX) views (Mitchell et al., 2019).

The Doppler echocardiography relies on detecting the shift in frequency of ultrasound signals reflected off moving structures. It makes use of two conventional modalities, which are often used in conjunction, i.e. the continuous wave (CW) and the pulsed wave (PW) Doppler. Most echocardiography machines are equipped with both types of Doppler. The CW Doppler technique assesses the velocity of blood flow by measuring signals that have high frequency and low amplitude reflected off from the blood cells. In tissue Doppler imaging (TDI), the same Doppler principles are used to quantify the higher amplitude and lower velocity signals of myocardial tissue motion. Hence, the main difference between CW Doppler and TDI is that the former is used to assess blood flow velocity as seen in e.g. aortic stenosis or tricuspid regurgitation, while the latter is used to assess the velocity of cardiac structures throughout the cardiac cycle e.g. when evaluating the global or regional myocardial systolic or diastolic function, and to detect abnormalities such as wall motion abnormalities seen in a variety of medical conditions, e.g. coronary artery disease, congestive heart failure. A CW Doppler transducer has a separate receiver and transmitter because it transmits continuously. Due to

its continuous transmission, there is no depth resolution. Tissue Doppler imaging (TDI) is obtained using pulsed wave (PW) tissue Doppler or color tissue (CT) Doppler imaging. Pulsed wave TDI measures peak longitudinal myocardial velocity from a single segment. Color TDI examines velocities from multiple sites simultaneously, representing the mean peak velocity (Moorthy, 2002). The conventional Doppler echocardiography analyzes the 'mitral inflow' for peak velocities of early (E) and late (A) diastolic flow, and the deceleration time (DT) of the E (early diastolic) wave. Using the measurements obtained, the E/A ratio (the ratio of early (E) diastolic to late (A) diastolic velocity of mitral inflow) is calculated. In contrast, the TDI evaluates longitudinal myocardial tissue velocities during LV diastole and systole, and thus evaluates the diastolic and systolic function. It analyzes the mitral annular motion sequentially at the septal and lateral portions of the mitral annulus. Measurements are taken for early (e') and late (a') diastolic annular velocities, and the E/e' ratio (i.e. the ratio of early (E) diastolic mitral flow measured by conventional Doppler to the early (e) diastolic mitral flow measured by TDI). Velocities can be measured either from the septal or lateral annulus, but a mean of both the measurements is recommended (Mitchell et al., 2019).

A study in India sought to investigate the magnitude of error resulting in echocardiographic interpretation in Indian subjects when using Western data as reference (Bansal et al., 2016). The study did not intend to establish normative data, and 100 healthy subjects (59% males and 41% females, with a mean age of 34 ± 8.8 years) were enrolled. Compared with reference values published by the ASE, the Indian subjects in the study had a much smaller LVIDd and LVIDs, and LVEDV. Only 58%, 61%, and 61% of the subjects had these parameters within ASE defined normal values, respectively. When indexed to BSA, these proportions increased to 81%, 90%, and 68% respectively. Although the pattern was similar for both males and females, a slightly greater proportion of women had these values within the normal ASE-specified ranges when indexed to BSA, i.e. indexed LVIDd in females was 82.9% and males 79.7%, indexed LVIDs in females was 95.1% and males 86.4%, and indexed LVEDV in females was 75.6% and in males 62.7%. In contrast, LV EF and most other parameters of LV diastolic function coincided with the ASE reference values for age and gender (≥ 52% in males and ≥ 54% in females). Among LV diastolic function parameters, the E/A ratio was within the normal range in the majority of subjects (86%) but the E wave deceleration time was out of range in almost two-thirds of the individuals.

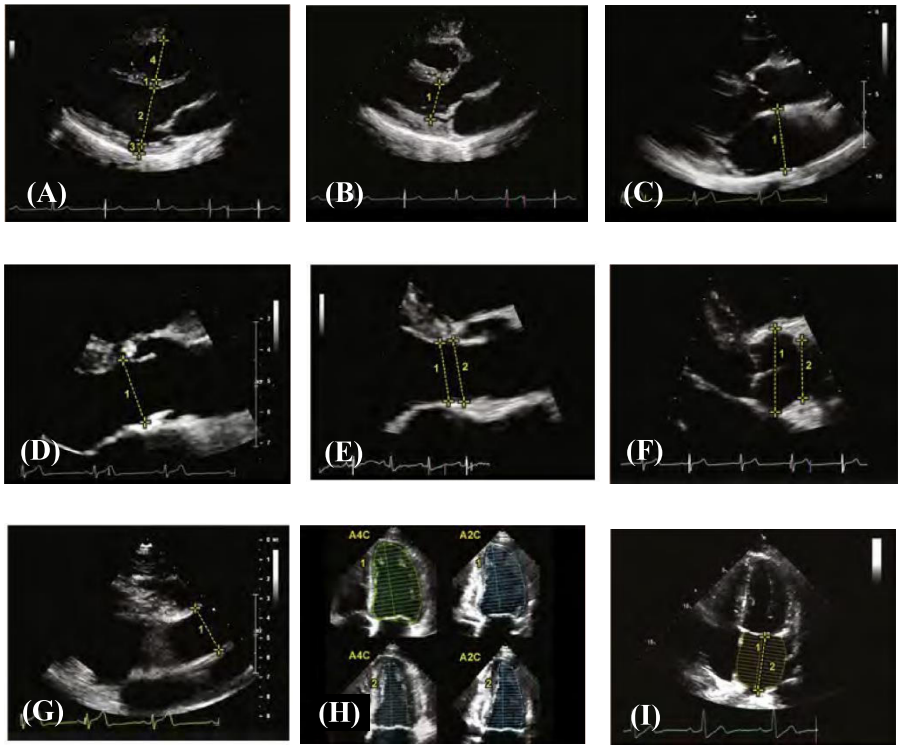

Figure 2.1 Echocardiographic Measurements: (A) PLAX view, measurements made (in end-diastole): IVSd, LVIDd, LVPWd, and RVD; (B) PLAX view, measurement made: LVIDs; (C) PLAX view, measurement made: LA diameter (D) PLAX view (Zoomed Aortic Annulus), measurement made (in mid-systole): AV annular diameter; (E) PLAX view (Zoomed LVOT), measurement made (in mid-systole): LVOT diameter and AV annular diameter; (F) PLAX view (Zoomed AoV and Asc Ao), measurement made: SoVAo diameter, STJ diameter; (G) PLAX view (Zoomed Asc Ao), measurement made: Diameter of Asc Ao; (H) A4C and A2C views, measurements made (using Biplane disk summation): LV end-diastolic volume, LV end-systolic volume; (I) A4C view, measurements made: LA length and LA area (Mitchell et al., 2019)

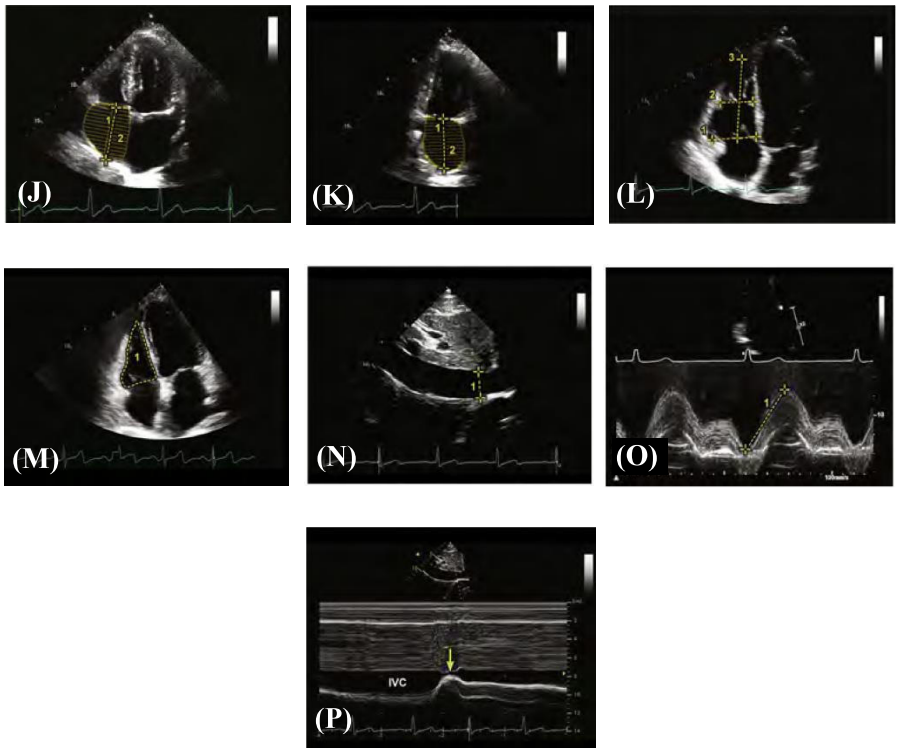

Figure 2.2 Echocardiographic Measurements: (J) A4C view, measurements made: RA length and RA area; (K) A2C view, measurements made: RA length and RA area; (L) A4C view (RV Focused), measurements made: RV base diameter, RV mid-cavity diameter, and RV length; (M) A4C view (RV Focused), measurement made: RV area; (N) SIVC view, measurement made: IVC diameter; (O) A4C view (RV Focused), M-mode measurement made: TAPSE; (P) SIVC view, demonstrating IVC reactivity (Arrow demonstrates patient sniffing maneuver or IVC collapsibility). Abbreviations: Aortic Valve (AoV); ascending aorta (Asc Ao); sinus of Valsalva (SoVAo) (Mitchell et al., 2019)

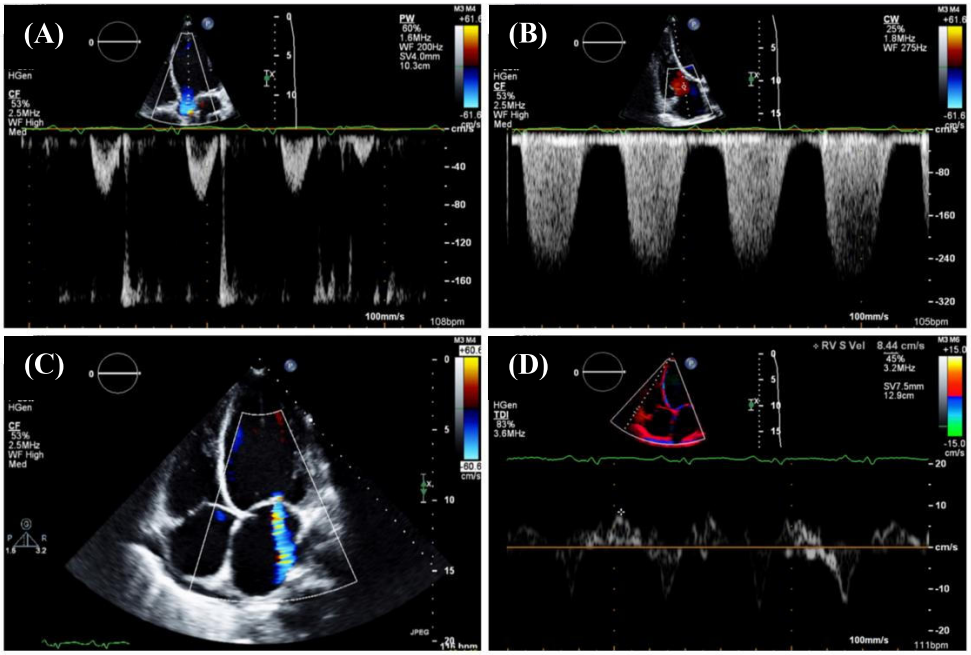

Figure 2.3 Doppler echocardiography: (A) Pulsed wave Doppler; (B) Continuous wave Doppler; (C) Color Doppler; and (D) Tissue Doppler Imaging (Sarullo, 2017)

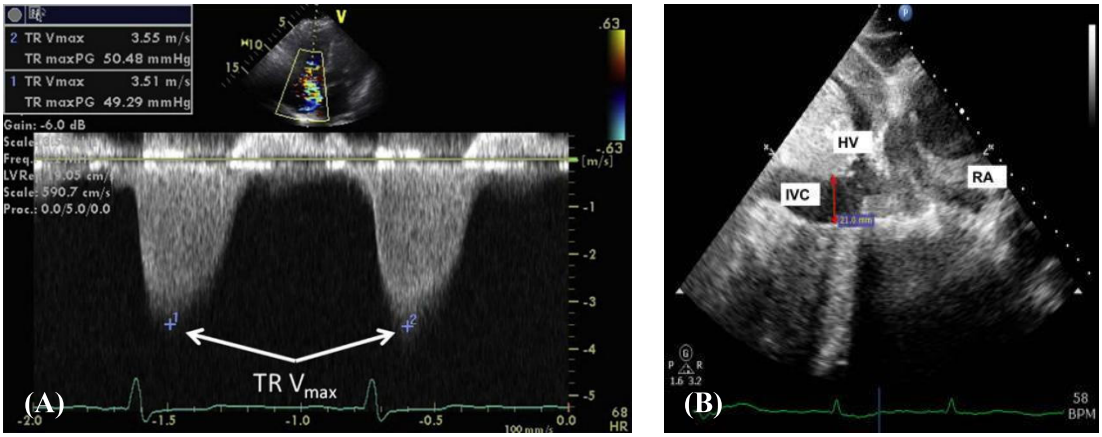

Figure 2.4 Estimation of the pulmonary artery systolic pressure (PASP) by using modified Bernoulli equation, PASP (mmHG) = 4(V_{max} of the TR)^2 +RAP. (A) The maximum velocity (V_{max}) of TR is obtained from continuous-wave Doppler echo (François & Schiebler, 2016) (B) The right atrial pressure (RAP) is estimated from IVC collapsibility (or sniff) obtained in SIVC view. Abbreviations: Hepatic vein (HV); right atrium (RA) (Garijo et al., 2017)

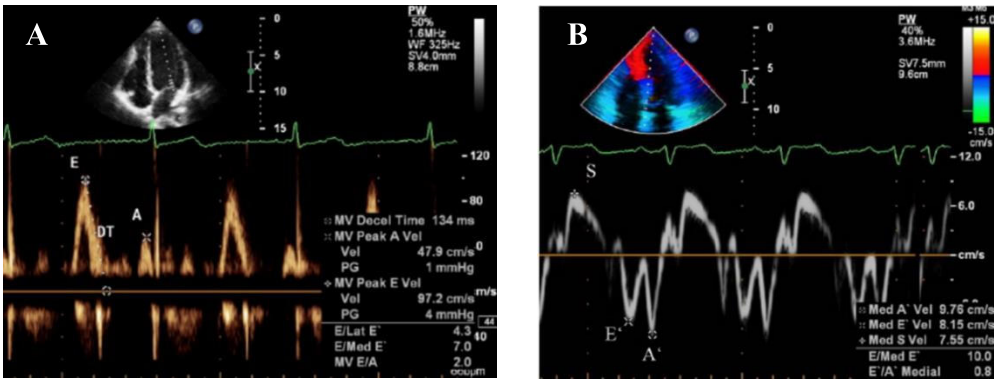

Figure 2.5 Doppler Echocardiography. (A) Pulsed wave Doppler of mitral filling. E wave: early diastolic filling; A wave: late diastolic filling; DT: deceleration time of the E wave (early mitral filling). (B) Pulsed tissue Doppler of the medial mitral annulus. S wave: systolic velocity above the baseline as a result of the annular movement toward the apex; E'm: early diastolic velocity below the baseline due to annular movement away from the apex; A'm: late diastolic velocity, at the time of atrial contraction (Kinova & Goudev, 2012)

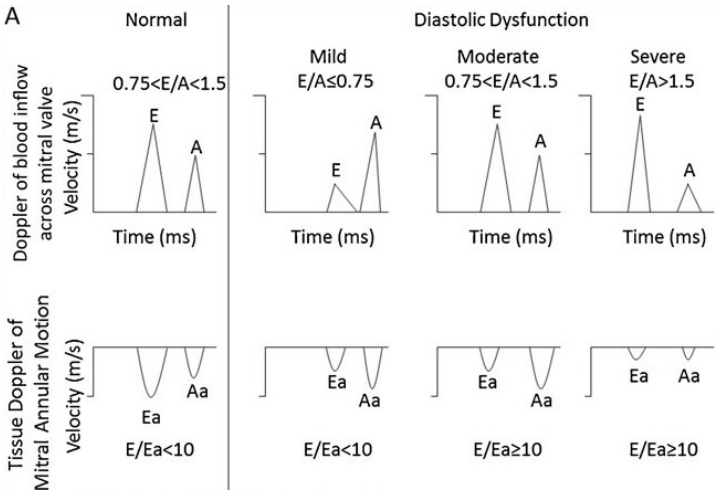

Figure 2.6 Doppler Echocardiography E/A ratio. It will initially decrease with mild diastolic dysfunction, but increases with worsening diastolic dysfunction, making moderate-to-severe diastolic dysfunction indistinguishable from normal-to-enhanced diastolic function. Ea is the peak heart muscle relaxation tissue-Doppler during early diastole about mitral valve annulus. Ea monotonically decreases with worsening diastolic dysfunction. Aa is the peak heart muscle expansion tissue-Doppler during the atrial contraction phase of diastole. In severe diastolic dysfunction, the Ea is severely slowed (Tong et al., 2014)

In comparison, the values for E/e’ septal (i.e. conventional mitral E: TDI septal e’ ratio), the E/e’ lateral (i.e. conventional mitral E: TDI lateral e’ ratio), and the E/e' average (i.e. conventional mitral E: TDI average e' ratio) were normal in most of the study subjects, 65%, 93%, and 90%, respectively. None of the subjects had an elevated value for any of these three ratios. The LV filling pressures and indexed LA volume (LAVi) were normal in all subjects. The study reinforced previous observations that Indian subjects have much smaller cardiac chamber dimensions as compared to the Western populations (Trivedi et al., 1993). However, LV systolic and diastolic functional parameters were not different. In contrast to Bansal et al, a study by Mukherjee et al presented the normal reference values of echocardiographic chamber dimensions in young eastern Indian adults. They found that LV EF was significantly higher in the Indian population, and the values of LVIDd, LVIDs, LVEDV, iLVESV, LAD, aortic diameter, and RVIDd were also significantly lower. LVM was lower in males but more in females compared to Western values (Mukherjee et al., 2021).

A similar study was conducted in Iran to ascertain the normal values of echocardiographic measurements for the healthy Iranian population, and to evaluate the relationship of these measurements with age and gender, by utilizing the three basic modes of echocardiography used in imaging the heart, i.e. the 2D and M-mode echocardiography, and Doppler (conventional and tissue) imaging (Ashley & Niebauer, 2004). A total of 368 healthy participants aged between 30 to 70 years were enrolled (171 males with a mean age of 47.6 ± 9.9, and 197 females with a mean age of 47.6 ± 9.5). The measurements obtained were indexed to BSA, and both the absolute (non-indexed) and indexed values were compared to those provided by ASE. The mean of all measurements obtained was less than the reference values published in the ASE guidelines, especially the parameters measuring LV and RV dimensions. Thus it indicated a smaller heart dimensions among the Iranian population. LAD and LAA increased with age, and the mean values for the two were significantly smaller than those cited in other references. The study did not investigate all the echocardiographic parameters of the left heart such as LV volume, LV mass, aortic root diameter, and indexed LA volume (LAVi). The right atrium was also omitted in the study. The left heart Doppler parameters showed there was a decrease in E/A ratio after the age of 60 years. Tissue Doppler parameters showed that lateral e’ was higher than septal e’ in both genders. There was an

increase in tissue velocities and an increase in E/e' septal and average ratios with age (Sadeghpour et al., 2013).

Qureshi et al investigated the echocardiographic measurements of LA and LV in the Hispanic and Latino populations in the United States, comparing them with the reference values provided by the ASE 2005 and 2015 guidelines (Gottdiener et al., 2004; Lang et al., 2005, 2015). The study was called ECHO-SOL (The Echocardiographic Study of Latinos), conducted with a sample size of 1818 (including 525 healthy) adults that consisted mostly of females (65%), with a mean age of 56.0 ± 21.3 years (i.e. for the entire cohort). The ethnic groups included Hispanics with Mexican, Puerto Rican, Cuban, Dominican, and Central and South American backgrounds. Those with Mexican background were highest in number (25%) and those with a South American background were the least in number (8%). Compared to Mexican Hispanics, the Cuban Hispanics had the highest values for LVMi, IVSd, PWd, RWT, LVIDd, LVESV, and LVEDV, whereas Central American Hispanics had the lowest values for these parameters. The values for IVSd, PWd, RWT, LVESV, and LVEDV in Caribbean-Hispanics were compared to the rest of the groups. They had significantly higher values for all the echocardiographic parameters except LVMi and LVIDd, and the values for LAVi were significantly lower. There were significant differences between all the values in both genders except for the value of RWT. All the values were smaller in females except for LAVi, which was larger compared to males. In both genders, the cardiac measurement for LVMi, IVSd, PWd, and RWT were higher when compared to the upper limit of normal reference values given in ASE 2005 and 2015 guidelines. The values were lower for LVEDV and LVIDd in both genders when compared to values specified for the same by ASE 2005 and 2015 guidelines. LVESV values were lower in both genders when compared to the upper limit given in ASE 2015 guidelines, but lower only in females when compared to the upper limit mentioned in ASE 2005 guidelines. LVESV values were similar to the ASE 2005 upper limit for males. LAVi was higher than the specified values of ASE 2005 guidelines for both genders, but similar to those specified in ASE 2015. Similar differences were found when comparisons were made for other parameters with the reference values provided in ASE 2005 guidelines. Females were more likely to be classified as having abnormal values for LVMi, RWT, IVSd and PWd. Men were

more likely to be categorized as having abnormal values for LVEDV, LVESV and LVIDd (i.e. the measures of LV volume) (Qureshi et al., 2016).

Similarly, comparisons against ASE and EACVI reference values were investigated in an Egyptian study by Missiri et al, which focused on defining the normal echocardiographic reference values for various measurements of cardiac dimensions and function in young, healthy Egyptian adults belonging to Dakahlia Governorate. The study proposed normal values for absolute and indexed echocardiographic measurements based on their results. The study included 1364 healthy Egyptian adults between the ages of 18 to 35 years (616 (45.2%) males and 748 (54.8%) females, with a mean age of 24.5 ± years). The main difference from international values was a higher upper reference limit for LV mass especially in females and relatively smaller LAD in young Egyptians (Elmissiri et al., 2016). The JAMP study (Japanese Normal Values for Echocardiographic Measurements Project) reported normal values for echocardiographic dimensions and Doppler measurements in a large, healthy Japanese population. There were several systolic and diastolic parameters that varied with age. An interesting finding of the study was that Japanese hearts were small when compared to the reference values in ASE guidelines, e.g. the mean LVIDd in Japanese men was only 4.4 ± 0.3 cm, whereas the reference range for the same in the guidelines is 4.2 to 5.9 cm (Daimon et al., 2008). A meta-analysis of echo measurements of LA and LV size, LV mass, and LV systolic function was undertaken by researchers in Auckland, New Zealand. It was called the EchoNoRMAL study (Echocardiographic Normal Ranges Meta-analysis of the Left Heart), which involved data from 43 studies around the world, representing 22,404 healthy adults aged between 18 to 80 years, without any comorbidity. All the studies included were published between 1st January 1990 and 31st December 2011. The study showed that the upper reference values for LVEDV, LVESV, and LV stroke volume were highest in Europeans and lowest in South Asians (including Pakistanis). For these measurements, the gender and ethnic differences remained after indexation by body surface area or height. LVEDV and LV stroke volume decreased with increasing age. LV EF differed by ethnicity, and the values were lower in Europeans and higher in Asians. The upper reference values for LVIDd and LVIDs were higher for Europeans than those for East Asians, South Asians and African populations, especially in males. Similarly, the upper reference values for LAD and LAV were highest for Europeans (Poppe et al., 2015).

Several studies have compared heart size measured on different imaging modalities, e.g. heart size measured on a chest X-ray (PA view) compared to measurements obtained by echocardiography for the same heart (Alam et al., 1989; Samuelsson et al., 1989; Sinha et al., 2013). Other studies have compared electrocardiography (ECG) to echocardiography, or chest X-rays and ECG to echocardiography (Agrawal et al., 2019; Ellis et al., 2007). Most of these studies consist of a small number of subjects with under-representation of women, the participants being healthy and/or diseased, and date back three to four decades when spatial 2D echocardiography was limited. Additionally, many of these researches focus only on the LV cavity size, not taking into account the RV or the atria. Thus, the dimensions of RV and both the atria have been omitted frequently in research studies (Pfaffenberger et a1., 20l3). Later studies have compared imaging techniques with a more modified version of the same technique, e.g. 2D echocardiography compared with 3D echocardiography (Correale et al., 2009; Ruddox et al., 2013). The more recent studies have compared both chest X-ray and echocardiography with MRI and CT (Alì et al., 2020; Gollub et al., 2012). Different studies suggest that MRI is emerging as the new gold standard (Salerno et al., 2017). For now, there is a consensus among many authors that echocardiography cannot be replaced as a gold standard, and that chest X-ray and ECG are invaluable alternatives only when resources are scarce. Chest X-ray lacks the ability to diagnose accurately when compared to echocardiography, but due to ease of accessibility, straightforward interpretation, and high specificity for identifying cardiomegaly, makes it very useful (Alghamdi et al., 2020).

A cross-sectional study in Iran compared CTR on chest X-ray (PA view) to ventricular dimensions (RVEDD and LVEDD) on echocardiography between patients with or without cardiomegaly. 197 patients (99 (50.3%) males and 98 (49.7%) females, with a mean age of 57.47 ± 10.75 years) were enrolled, aged between 34 to 86 years. History of ischemic heart disease and hypertension was observed in 52.3% and 38.6% of the patients, respectively. According to the radiographs and echocardiography results, 49 (24.9%) and 100 (50.8%) subjects had cardiomegaly, respectively. The sensitivity and specificity of CTR in identifying cardiomegaly were 34% and 84.5%, respectively. The median of LVEDD and RVEDD were 50 mm (34 - 70 mm) and 24 mm (15 - 40 mm), respectively. Additionally, when the means for these parameters were compared in those with or without an enlarged heart size, the results demonstrated a statistically significant difference (Monfared et al., 2015).

Sinha et al carried a comparative study in India with 35 males only, aged between 25 to 60 years. All the subjects underwent chest X-rays (PA and lateral views) and M-mode echocardiography. The study did not determine the sensitivity or specificity of chest X-ray as a screening test, but compared different chest X-ray parameters to echocardiography. The chest X-ray (PA view) parameters studied were CTR (expressed in percentage), TCD (by measuring TLD and TRD) and TTD. Two more measurements considered were the oblique and broad diameters, the oblique diameter was measured from the left cardiophrenic angle to the junction of right atrium and superior vena cava, and the broad diameter was measured from the right cardiophrenic angle to the junction of the pulmonary artery and left atrial appendage. The chest X-ray (lateral view) parameter studied was the anterior-posterior (AP) diameter, measured from the anterior border of the heart to the maximum convexity of the posterior border. The echocardiographic parameters measured were IVS thickness, LV PWd, right ventricular dimension (RVID), left ventricular internal dimension (LVID), left atrial dimension (LAD), and the total ventricular dimension (TVD). The TVD was calculated by adding the values of the two ventricular dimensions, IVS thickness and PWd. The subjects were divided into three groups based on the provisional diagnosis, group A subjects had a clinical history not suspected of any cardiac enlargement, group B subjects had a clinical history suggestive of LV enlargement, and group C subjects had a clinical history suggestive of RV enlargement. There were 15 subjects in groups A and B, and only 5 in group C. The study found a weak correlation between the parameters of echocardiography and chest X-rays in group A. However, there was a strong positive correlation observed between TVD and TLD. In group B (with enlarged LV), a very strong positive correlation was observed between the TVD and CTR. However, the LVID showed a very poor correlation with the different variables on the chest X-rays. In group C (with enlarged RV), the TVD and RVID had a very strong positive correlation with CTR and TCD, and showed a stronger correlation with TLD than the TRD. The study concluded that CTR is a good indicator of LV and RV enlargement. The TCD is a good indicator of RV enlargement and a fair indicator of LV enlargement. TLD correlates more with the RV enlargement than LV enlargement, whereas the TRD is a poor indicator of RV and LV enlargement. The study proposed that chest X-ray is a reliable alternative for the diagnosis of cardiomegaly, when better investigative options are limited (Sinha et al., 2013).

A study by Alam et al in Bangladesh focused on comparing chest X-ray (PA view) and 12-lead ECG findings to LV ejection fraction on echocardiography, to ascertain the diagnostic worth of the former two in LV systolic dysfunction (characterized by LV ejection fraction ≤ 45%). The study enrolled 70 patients (40 males and 30 females, with a mean age of 62.66 ± 10.70 years). 60 (85.7%) patients had enlarged cardiac silhouette on chest X-ray, and 20 (28.6%) patients had congestion and upper lobe diversion. 56 (80%) patients had abnormal 12-lead ECG and 50 (71.4%) patients had LV ejection fraction less than 45% on echocardiography suggestive of LV dysfunction. On chest X-ray (PA view), a CTR of more than 0.5 had a sensitivity of 92%, specificity of 30% and a positive predictive value of 76.7% in diagnosing cardiomegaly. A set of pre-selected ECG abnormalities had a sensitivity of 100%, specificity of 70% and a positive predictive value of 89.3% in diagnosing LV systolic dysfunction. The study concluded that abnormal ECG findings related to LV function and a CTR of more than 0.5 on chest X-ray (PA view) can reflect LV systolic dysfunction with high precision among patients with clinical features of heart failure (Siddiqui et al., 2013).

Researchers in New Zealand investigated a study population following non-ST segment elevation MI (NSTEMI) for cardiomegaly with chest X-ray (PA view) and 2D echocardiography. The radiological parameter investigated was CTR, and the echocardiographic parameters measured were the right and left ventricular dimensions. BSA was also taken into consideration to explore if it was a significant explanatory variable. From a cohort of 244 patients with a mean age of 67.2 ± 12.6 years, 39 patients had cardiomegaly on chest X-ray (PA view), while 55 had cardiomegaly on echocardiography. Of the 39 patients with an enlarged heart on chest X-ray (PA view), 22 (56%) patients did have cardiomegaly (true positive) based on echocardiography, while 17 (44%) patients did not have cardiomegaly (false positive) on echocardiography. The sensitivity of chest X-ray (PA view) to determine cardiomegaly was 40%, and the specificity was 91%. The study showed that chest X-ray (PA view) was accurate in 80% of the cases, the positive predictive value was 56%, while the negative predictive value was 84%. The true positive rate of cardiomegaly on chest X-ray (PA view) was not too dissimilar to the false positive rate, suggesting that a diagnosis of cardiomegaly cannot be made purely based on a CTR of greater than 50% on chest X-ray (PA view) (McKee & Ferrier, 2017).

A retrospective descriptive study in Zambia was carried out with a sample size of 124 adults (40 (32%) males and 84 (68%) females, with a mean age of 56.78 ± 18.38 years). The radiological parameter measured on chest X-ray (PA view) was CTR, and the parameters measured on echocardiography were atrial and ventricular dimensions, IVSd, LV PWd, and LV EF. An assessment of the atrial and mitral valves was also done. A total of 88% of patients showed cardiomegaly on chest X-ray (PA view) and had abnormal echocardiographic findings, while 12% of the patients showed normal echocardiographic measurements. Younger patients aged less than 35 years had minimal cardiomegaly, while the older patients had more severely enlarged hearts. Thus there was a positive and strong correlation between cardiomegaly and age. The list of common cardiovascular diseases that presented with cardiomegaly included LV diastolic dysfunction, LA dilatation, LV systolic dysfunction and LV hypertrophy (Gwaba, Isaacs, & Harneck, 2018). A cross-sectional study in Basrah, Iraq investigated CTR on chest X-ray (PA view), comparing it to LVIDd and LVIDs on echocardiography. The study enrolled 150 adult patients (99 (66%) males and 51 (44%) females), and showed that the ability of CTR to detect (sensitivity) or exclude (specificity) cardiomegaly when compared to LVIDd was 85.71% and 13.79%, respectively. It had a positive predictive value of 41.86% and a negative predictive value of 42.85% for cardiac enlargement. There was a significant correlation between CTR and LVIDd. Similarly, CTR had a sensitivity of 90.4% and a specificity of 17.24% when compared to LVIDs in determining cardiomegaly. It had a positive predictive value of 44.18% and a negative predictive value of 28.57%. The study found CTR to be highly sensitive but of very low specificity in measuring heart size (Abd-Hazaa et al., 2007).

In Bedford, UK a retrospective, dual center study enrolled 272 inpatients (153 males and 119 females, with a mean age of 70 ± 19.9 years), to investigate the diagnostic accuracy of CTR on both PA and AP chest X-rays in predicting LV or RV dysfunction determined on echocardiography. The LV measurements included LVIDd, LVIDs, LV EF and LV fractional shortening (FAC). The RV function was assessed by tricuspid annular plane systolic excursion (TAPSE). An LV ejection fraction of less than 45% and a TAPSE of less than 1.6 cm were considered abnormal. There was a significant difference in the mean CTR obtained from PA and AP view films (0.52 and 0.56, respectively). The prevalence of moderate to severe ventricular systolic dysfunction was 20% in the PA film group and 30% in the AP

film group. In the PA film group, CTR correlated strong positive with age, strong negative with LV EF, and there was a significant difference in the mean CTR between those who had and those who did not have moderate-to-severe ventricular dysfunction on echocardiography. In the AP film group, CTR correlated poorly with age and was not predictive of ventricular dysfunction on echocardiography as it did not correlate with LV EF. In both PA and AP film groups, CTR did not correlate with fractional shortening and LVIDd. In chest X-rays (PA view), a CTR value of more than 0.50, had a sensitivity of 73.9%, specificity of 47.4%, the positive predictive value of 25.4%, and a negative predictive value of 88.2%. For a CTR value of more than 0.55, the values for the same were 56.5%, 77.9%, 38.2% and 88.1%, respectively. In chest X-rays (AP view), a CTR value of more than 0.50, had a sensitivity of 93.5%, specificity of 26.2%, the positive predictive value of 35.2%, and a negative predictive value of 90.3% (Chana et al., 2015).

A study in Nepal compared CTR with LVEDV, LVESV, LV PWd and LV mass for LV enlargement. The study enrolled 39 patients (29 males and 10 females, with a median age of 51 years), who had an enlarged cardiac size based on CTR on chest X-ray (PA view). Using the values of LV mass obtained from the Devereux formula, 44.8% of males and 30% of females had enlarged LV mass, i.e. a combined 41% of the total study population. Using the values of LV mass obtained by the monogram method (Werther et al., 1983), 20.7% of males and no females had enlarged LV mass, representing a total study population of 15.4%. Using LVEDV to estimate heart size, 24.2% of males and 40% of females had an end-diastolic volume of more than 90 ml/m^2 (the upper limit of normal). This accounted for 28.3% of the total study population. Using LVESV to estimate heart size, 38.0% of males and 60% of females had end-systolic volume of more than 34 ml/m^2 (the upper limit of normal). This accounted for 43.6% of the total study population. Using the American College of Cardiology (ACC) criteria for LV mass, with the upper limit set at $90g/m^2$, it was found that 58.7% males and 30% females had an enlarged LV, corresponding to 51.3% of the total study population. An average of 33.5% of patients had enlarged cardiac size without any obvious radiographic markers or signs of cardiac illness on chest X-ray (PA view), who were proven to have cardiomegaly when echocardiography was performed (Adhikary et al., 2003).

Fonseca et al investigated the assumption that a normal ECG or a normal heart size on chest X-ray virtually rules out a diagnosis of heart failure. It was a prospective study in which data

was collected at the time of patient enrolment in the EPICA study. A total of 1058 patients aged over 25 years were enrolled, with probable heart failure, and investigated through chest X-ray (PA view), 12-lead ECG and 2D echocardiography. A definitive diagnosis of heart failure was established in 551 patients (males 208 and females 343) with echocardiographic evidence of cardiac dysfunction at rest. The 12-lead ECGs were classified as normal or abnormal, and the abnormal ECGs were analyzed for nineteen variables. In chest X-ray (PA view), the presence of six signs was evaluated related to lung fields and included CTR. For identifying patients with heart failure among those with suspected diagnosis, an abnormal ECG had a sensitivity of 81%, specificity of 51%, a positive predictive value of 59%, and a negative predictive value of 75%. For the diagnosis of LV systolic dysfunction, an abnormal ECG had a sensitivity of 80%, specificity of 40%, a positive predictive value of 17%, and a negative predictive value of 93%. Individual ECG variables had high specificity (74% to 99%) but low sensitivity (1% to 42%) for the overall diagnosis of heart failure. For identifying patients with heart failure, an abnormal chest X-ray (PA view) had an estimated sensitivity of 57%, specificity of 78%, a positive predictive value of 50%, and a negative predictive value of 83%. The radiographic parameters had a high specificity (79% to 99%) but modest sensitivity (1% to 54%) for the diagnosis of heart failure. The most sensitive ECG abnormalities were non-specific ST-segment or T-wave changes (43%), LV hypertrophy (30%), LV strain (26%) and LA enlargement (18%). The most sensitive abnormality identified on the chest X-ray (PA view) was cardiomegaly (54%). The study concluded that ECG and radiographic features are not sufficient to allow heart failure to be reliably predicted or excluded in the community and recommended that all patients with suspected heart failure should undergo echocardiography (Fonseca et al., 2004).

CHAPTER 3

METHODOLOGY

3.1 Study Design

This study was designed as a comparative cross-sectional study. It was a non-experimental, observational study that involved the investigation of heart size using one imaging modality and comparing it to a gold standard. The imaging modality being compared was chest X-ray (PA view) and the gold standard to which it was being compared was 2D transthoracic echocardiography (TTE or 2D echocardiography).

3.2 Subjects

The study was approved by the Ethics Committee of Bahria University Medical and Dental College, Karachi via approval reference number ERC 29/2021. It was a non-interventional study, and since patients' records were used after their consent, all the information was kept confidential. The subjects were patients (male and female) with heart-related complaints or diseases, aged between 18 to 75 years.

3.3 Setting

The study was conducted at PNS Shifa Hospital and the National Institute of Cardiovascular Diseases (NICVD), both located in the city of Karachi, Pakistan.

3.4 Inclusion Criteria

1. Subjects aged ≥ 18 and ≤ 75 years, from both genders
2. Subjects admitted or referred for both Chest X-ray (PA view) and 2D echocardiography
3. Subjects with heart-related complaints

4. Subjects with signs and symptoms suggestive of cardiovascular disease

3.5 Exclusion Criteria

1. Subjects with abnormal shape and size of the thorax
2. Subjects with cervical and thoracic spinal deformities
3. Previous history of surgery of thoracic region or any past intervention performed on the heart
4. Subjects with severe respiratory diseases e.g. pneumonia with pleural effusion, pneumothorax
5. Subjects who had a missing measurement of any study parameter on 2D echocardiography
6. Subjects who had either chest X-ray (PA view) or 2D echocardiography done, but not both
7. Subjects who had chest X-ray (AP view) and 2D echocardiography done
8. Subjects who had a timeframe between chest X-ray (PA view) and 2D echocardiography of greater than 3-7 days

3.6 Duration of Study

The total period of the study was 06 months. The individual study period was approximately 02 hours each day, during weekdays.

3.7 Sample Size Estimation

The sample size was calculated using OpenEpi (Version 3, open-source calculator). The equation used was, sample size (n) = [DEFF * Np(1-p)] / [($d^2/Z^2_{1-\alpha/2}$ * (N-1)+p * (1-p)]. Of the total population size of 120 subjects, a total of 79 subjects were enrolled at a confidence level of 95%. The patients excluded were those who lacked a chest X-ray (PA view) or an echocardiography report, or the echocardiography reports were deficient, or had a previous history of intervention performed on the heart.

3.8 Sampling Technique

The sampling technique chosen for the study was non-probability convenience sampling. 79 inpatients who met the inclusion criteria and consented to the study were selected at convenience.

3.9 Human Subjects and Consent

The subjects of the study were adult males and females aged between 18 to 75 years, who were admitted to the hospital with various cardiac complaints and had undergone both chest radiography (PA view) and echocardiography. An informed consent was obtained from the participants after explaining the benefits and associated risks of the study. The consent forms were provided to the participants in English and Urdu, whichever they preferred.

3.10 Materials Used

1. Informed Consent Form
2. Participant Evaluation Proforma
3. Chest X-ray (PA view) Images
4. 2D Transthoracic Echocardiography Reports
5. Equipment Used:
    i. *Toshiba X-Ray Machine KXO-15R*: X-ray tube, DRX-1603B; Beam limiting device, TF-6TL-6; Floor-To-Ceiling X-ray tube stand, DS-TA-5A; input, 110V~ 50/60Hz; Max input power, 0.3kVA filtration 1.2 mm
    ii. *Cannon Aplio i600 CV Echocardiography Machine*: Frequency range, 1-22 Mhz; iBeam, ApliPure+; CEUS: Quad View; Display modes 2D, 3D
    iii. *Stadiometer*
    iv. *Radiograph Illuminator* : SL-288A Soft Video Light; input, 12-16.8V, 4.8A; power, 40W; luminance, 800Lux/1m; color temperature, 3200K/5600K

v. *Samsung Galaxy Camera A31 and Tripod Stand*: 48 MP, f/2.0, 26 mm (wide), 1/2.0", 0.8 µm, PDAF 8MP, f/2.2, 123˚, (ultrawide), 1/4.0", 1.12 µm, 5MP, f/2.4, (macros), 5 MP, f/2.4, (depth), HDR
vi. *Fiji ImageJ Software*: ImageJ 1.53h (Wayne Rasband and contributors, National Institute of Health, USA), Java 1.8.0_172 (32bit). An open-source image processing software package that supports Windows, Linux, and Mac OS X platforms (both Intel 32-bit and 64-bit)
vii. *Lenovo Thinkpad T420s*: OS, Microsoft Windows 8.1 Pro (32 Bit)

3.11 Parameters of Study

The demographic (gender, ethnicity, marital status, education and occupation) and physical (weight (Kg), height (m), BMI (Kg/m^2) and BSA (m^2)) characteristics of the study participants were evaluated. The study involved parameters that belonged to two different imaging techniques, i.e. radiological parameters and echocardiographic parameters:

I. Radiological Parameters: Chest X-ray (PA view)

These included measurements related to the heart size, which were:

i. *Transverse Cardiac Diameter (TCD):* The maximum horizontal distance between the most lateral points of the heart silhouette
ii. *Transverse Right Cardiac Diameter (TRCD or TRD), also called Maximum Right Diameter (MRD):* The distance between the right lateral most margin of the heart and the midline passing through the spinous processes of the vertebral bodies
iii. *Transverse Left Cardiac Diameter (TLCD or TLD), also called Maximum Left Diameter (MLD):* The distance between the left lateral most margin of the heart to the midline passing through the spinous processes of the vertebral bodies
iv. *Transverse Thoracic Diameter (TTD):* The widest most internal transverse diameter of the thoracic cavity
v. *Cardiothoracic Ratio (CTR):* Calculated as a ratio of maximum Transverse Cardiac Diameter (TCD) and widest internal Transverse Thoracic Diameter (TTD)

(A)

(B)

(C)

(D)

(E)

Figure 3.1: Instruments used for measuring weight and radiographic parameters. (A) Stadiometer; (B) Tripod stand for holding the camera; (C) Radiograph illuminator (SL-288A Soft Video Light); (D) Samsung Galaxy Camera A31; (E) Lenovo T420s Laptop

Figure 3.2: Toshiba Radiography Equipment installed in the X-ray department of NICVD, Karachi

Figure 3.3: Canon Aplio i600 Echocardiography Machine used in Transthoracic Echocardiography Department at NICVD, Karachi

For TTD, TRD, TLD and TCD, there were no standard reference values available. For the CTR, a ratio value of 0.5 was considered to represent the upper limit of normal. Thus, a ratio value of ≤ 0.5 was considered normal, and a value of > 0.5 represented the presence of cardiomegaly. Other parameters that were also evaluated on the chest X-rays (PA view) were:

i. *Pulmonary vascular congestion or edema:* The lung fields were evaluated for:

a) Normal/ Abnormal changes
b) Pulmonary Congestion
c) Pulmonary Oligemia

ii. *Assessment for signs of pulmonary disease:* The lung fields were evaluated for any evidence (e.g. fibrosis, scarring) of past or current pulmonary illness, e.g. pulmonary tuberculosis, interstitial lung disease (occupational, drug-induced or autoimmune), or airway diseases

II. Echocardiographic Parameters: 2D Transthoracic Echocardiography

These included measurements related to the atria, the ventricles, the aortic root diameter and the pulmonary artery systolic pressure (PASP). The parameters used were:

i. Atrial Measurements:

For the right atrium (RA), the measurement recorded was RA minor axis or transverse diameter (RAD) taken in apical 4-chamber view. For the left atrium (LA), the measurement recorded was LA anterior-posterior diameter (LAD) taken in the PLAX (parasternal long axis) view. All the measurements were measured in millimeters (mm).

ii. Ventricular Measurements:

For the right ventricle (RV), the measurements recorded were RV linear dimension (RVD) in the PLAX view, and TAPSE measured on M-mode tracing in the apical 4-chamber view, between end-diastole and peak systole. For the left ventricle (LV), the measurements recorded were LV internal diameter at end-diastole (LVIDd), LV internal diameter at end-systole (LVIDs), LV posterior wall thickness at end-diastole (PWd), and interventricular septal wall thickness (IVS or IVSd) at end-diastole were taken in the PLAX view. The LV ejection fraction (EF) was determined in the apical 4-chamber and apical 2-chamber views by applying the biplane (Simpson's) method. The LV mass (LVM) was calculated by the linear method, applying the Devereux and Reichek 'cube' formula: LVM= 0.8{1.04 [([LVIDd+ IVSd+PWd]^3-LVIDd^3)]} + 0.6. The relative wall thickness (RWT) was calculated as a ratio by the formula: RWT= (2 x PWd) / LVIDd. The units of measurement for all the ventricular measurements, with their reference normal values, are mentioned in Table 3.1.

iii. Aortic Diameter Measurement and Pulmonary Artery Systolic Pressure (PASP) Estimation:

The aortic root diameter was assessed at the level of the annulus during end-diastole in the PLAX view. The pulmonary artery systolic pressure (PASP) was estimated from the tricuspid regurgitant (TR) jet or maximum velocity (V_{max}) using the modified Bernoulli equation and adding the right atrial pressure (RAP), which was estimated based on inferior vena cava (IVC) diameter and collapsibility (or respiratory variation). The V_{max} was obtained by continuous-wave (CW) tissue Doppler echocardiography, and the size of IVC was measured in the subcostal IVC (SIVC) view. The equation used was, PASP (mmHg) = 4(V_{max} of the TR)^2 +RAP. The RAP (mmHg) is generally assigned a value using different classification schemes, such as those proposed by Kuppahally et al (2010), Rudski et al (2010), Brennan et al (2007) and Lang et al (2005). In this study, the classification proposed by Rudski et al was used (Table 3.2).

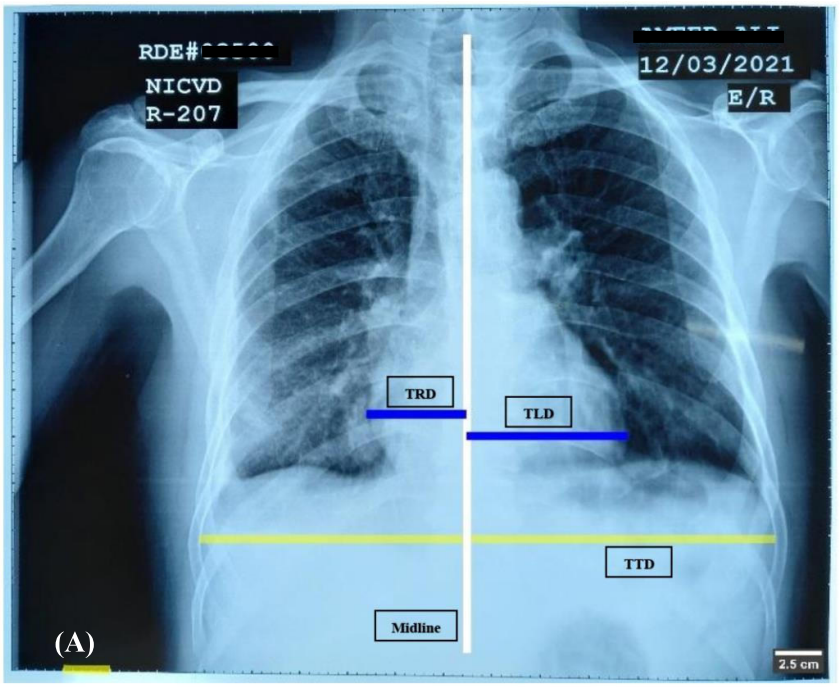

(B)

Results

File Edit Font Results

	Area	Mean	Min	Max	Angle	Length
1	13.861	208.020	144	221	0	30.851
2	2.407	195.895	99	223	0	5.344
3	3.879	185.529	42	222	180	8.622

(C)

Results.csv

FILE HOME INSERT PAGE LAYOUT FORMULAS DATA REVIEW VIEW

Cut Copy Format Painter Paste Clipboard

Calibri 11 Font

Wrap Text Merge & Center Alignment

E14

	A	B	C	D	E	F	G	H
1		Area	Mean	Min	Max	Angle	Length	
2	1	13.861	208.02	144	221	0	30.851	
3	2	2.407	195.895	99	223	0	5.344	
4	3	3.879	185.529	42	222	180	8.622	
5								
6								
7								

Figure 3.4: Radiographic parameters. (A) Labeled chest X-ray (PA view); (B) An output of measurements in Fiji ImageJ software; (C) Results displayed in Microsoft Excel

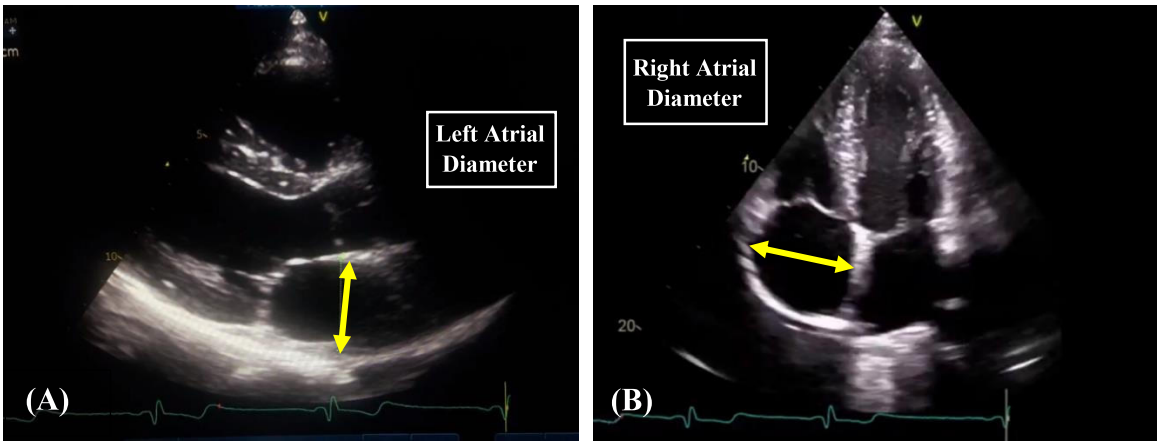

Figure 3.5: Echocardiographic Parameters. (A) Shows the LA Anterior-posterior diameter (LAD) measurement in PLAX view. (B) Shows the measurement of RA Minor/Short axis diameter (RAD), also called the transverse diameter, in apical 4-chamber view

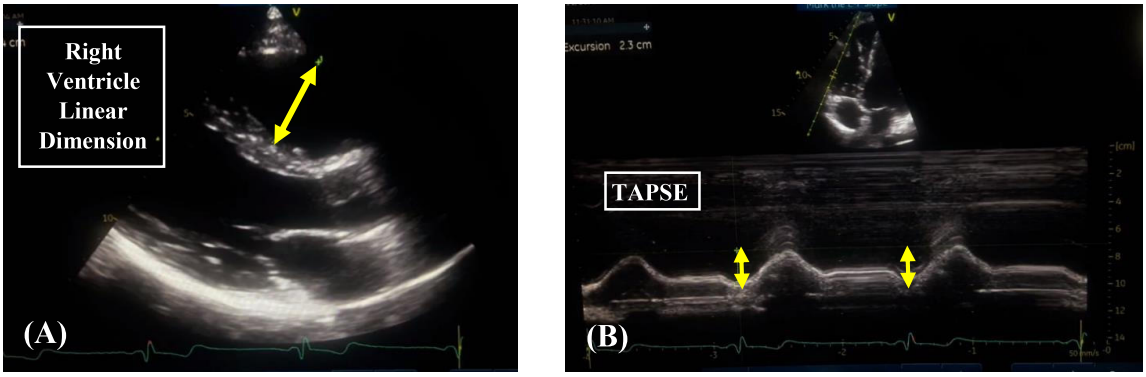

Figure 3.6: Echocardiographic Parameters. (A) Show the measurement of RV linear dimension (RVD) in PLAX view. (B) Shows the M-mode tracing of TAPSE, using the apical 4-chamber view.

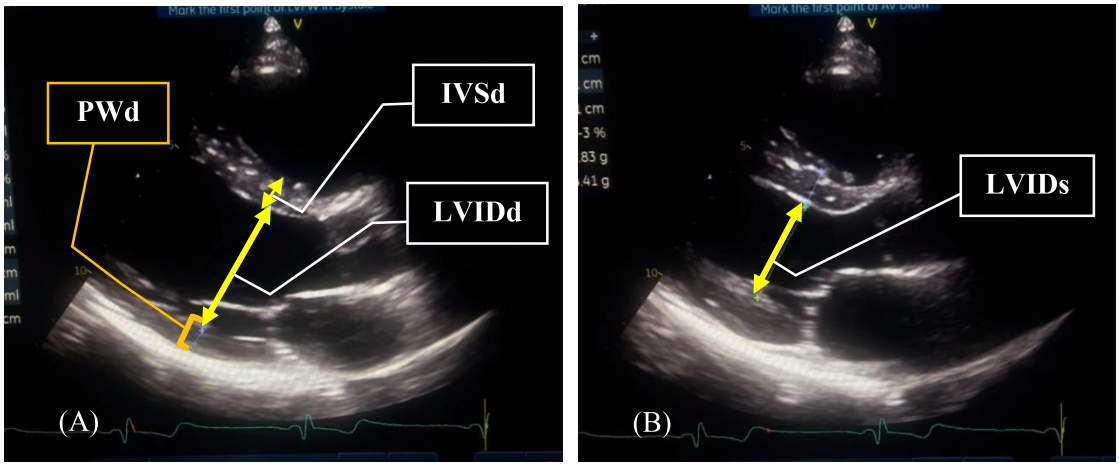

Figure 3.7: Echocardiographic Parameters. (A) Shows the LV end-diastolic measurements (i.e. LVIDd), PWd, and IVSd in the PLAX view. (B) Shows the LV end-systolic measurement (i.e. LVIDs) in the PLAX view

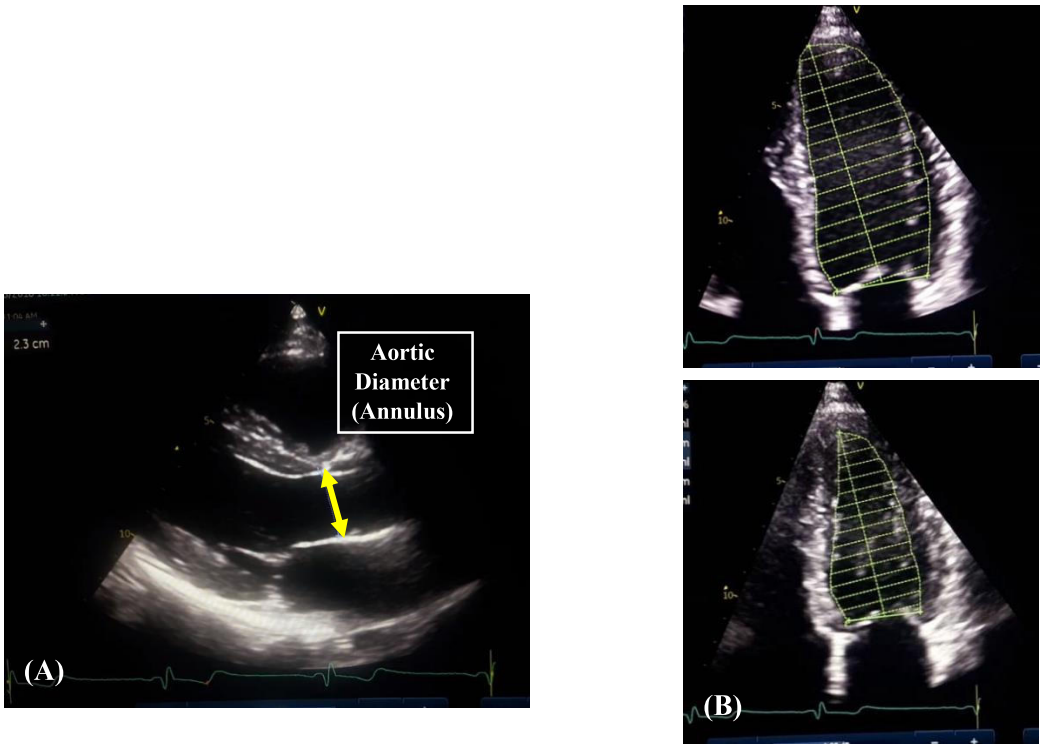

Figure 3.8: Echocardiographic Parameters. (A) Shows the measurement of Aortic diameter at the aortic annulus in the PLAX view. (B) Shows the measurement of LV ejection fraction using biplane (Simpson's) method (only apical 2-chamber view shown)

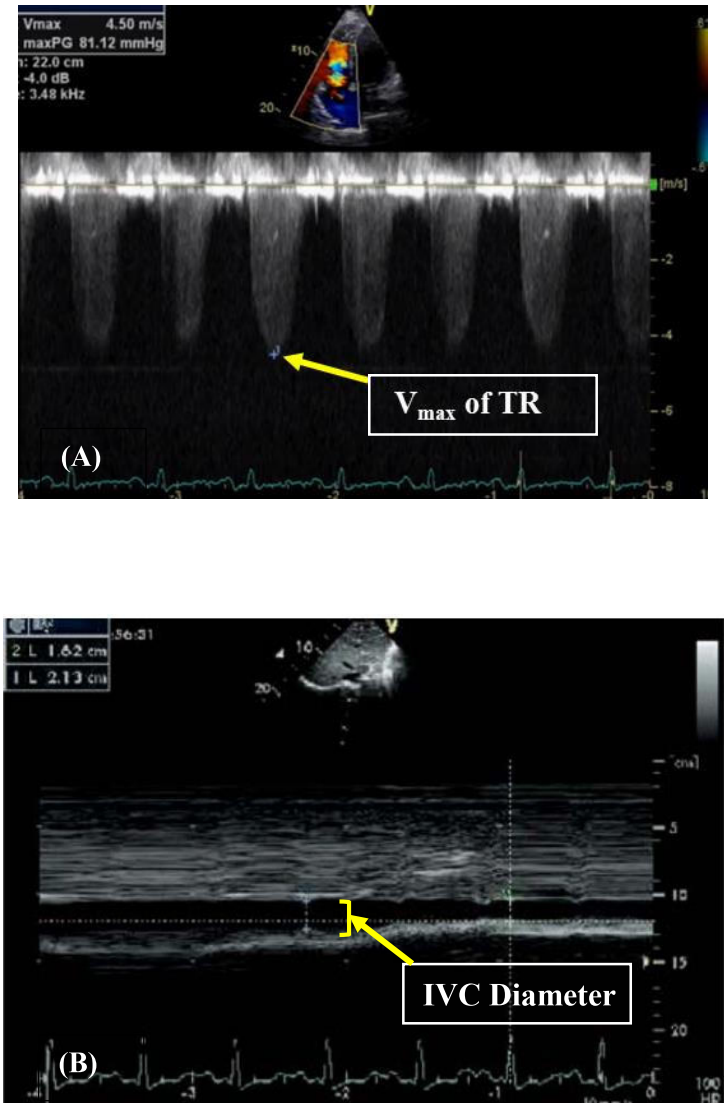

Figure 3.9: Echocardiographic Parameters. (A) Shows the measurement of maximum velocity (V_{max}) of TR using continuous-wave tissue Doppler, utilizing the apical 4-chamber view. (B) Shows the estimation of IVC size and collapsibility in the SCIVC (subcostal IVC) view

Table 3.1: The normal reference values (according to ASE) of the study parameters determined by 2D echocardiography

Parameter	***Normal Reference Value***
RAD (minor-axis)	*< 36 mm*
LAD (anterior-posterior)	*< 41 mm*
RVD (PLAX)	*< 25 mm*
TAPSE	*15 – 25 mm*
LVIDd	*< 55 mm*
LVIDs	*< 41 mm*
IVSd	*≤ 11 mm*
LV PWd	*≤ 11 mm*
LV Ejection Fraction (EF)	*> 55 %*
Aorta	*< 40 mm*
PASP	*≤ 35 mmHg*
LV Mass index (LVMi)	*≤ 115 g/m^2 (Males)* *≤ 95 g/m^2 (Females)*
RWT	*> 0.42 (concentric)* *≤ 0.42 (normal or eccentric)*

Table 3.2: Classification of RAP values based on IVC size and collapsibility (Rudski et al., 2010)

Inferior Vena Cava Diameter (cm) & Collapsibility (%)	***Right Atrial Pressure (mm Hg)***
When IVC diameter is ≤ 2.1 cm and collapsibility >50%	*RAP of 3mmHg is added*
When the IVC diameter is >2.1 cm and collapsibility ≤50%	*RAP of 15 mmHg is added*
When the IVC diameter and collapsibility do not fit the above pattern	*RAP of 8 mmHg is added*

Table 3.3: The formulae used for calculating Body Surface Area (BSA) (Redlarski et al., 2016)

Formula	***BSA (m^2)***
Mosteller	$=\sqrt{\text{height (cm) x weight (kg)}} / 3600$
Dubois & Dubois	$= 0.007184 \times \text{Weight (kg)}^{0.425} \times \text{Height (m)}^{0.725}$
Averaged	$= \frac{\text{BSA (Mosteller Formula) + BSA (Dubois \& Dubois Formula)}}{2}$

3.12 Protocol of Study

The study was conducted in PNS Shifa Hospital and the National Institute of Cardiovascular Diseases (NICVD), which are both located in Karachi. All participants were in-patients admitted through the out-patient department (OPD) or the emergency department (ED), who presented with signs and symptoms or complaints related to any cardiac disease. The patients were examined by a consultant in the OPD or the ED and admitted for further investigation or management. Those patients who met the inclusion criteria were selected at convenience and were included in the study after their consent for participation. Their clinical history was taken and complete physical examination performed after admission to the ward. Patient proforma were filled for them by the primary researcher at the time of conducting history and physical examination. Their heights and weights were recorded at the time of admission in meters (m) and kilograms (kg), respectively. The patients had either echocardiography or chest X-ray (PA view), or both done at the time of admission, or after admission. Those who had both investigations done were included in the study, and those with either chest X-ray (PA view) or echocardiography done were included only after the missing investigation was done within three days of one another. Usually, patients had one or both investigations done within three days of admission. All echocardiograms were reported by an experienced consultant echocardiologist. The chest X-ray (PA view) measurements were taken by the primary researcher using Fiji ImageJ software and endorsed by an experienced consultant radiologist.

All chest X-rays were taken in PA view, during full inspiration, in an upright position and with the film exposure at a distance of 6 feet (72 inches). The radiographic films (14 x 17 inches) obtained from patients were placed on SL-288A LED light panel, which was used as an illuminator. Photographs of all the illuminated radiographic films were obtained at a fixed distance of 12 inches (1 foot) with Samsung Galaxy A31 Camera attached to a tripod stand. The chest X-rays (PA view) were checked for the presence of any deformity in the chest wall or thoracic spine, presence of any artifacts that would hamper measurements, and if proper X-ray positioning technique was observed. They were also checked for clear and visible costophrenic angles, if both clavicles were in the same horizontal plane, if the 5^{th} to 7^{th} anterior ribs were intersecting the diaphragm at the midclavicular line and if the

sternoclavicular joints were equidistant from the spinous processes in the midline. Those patients who took portable chest X-rays were excluded from the study, as they are taken in AP view and not considered a standard in the determination of heart size. Chest X-rays (PA view) without calibrated grid lines at the borders of the radiographic films were also excluded, as they were crucial for taking measurements. Pulmonary venous congestion or edema and any evidence of previous or current pulmonary disease were assessed on the radiographs as categorical variables of the study.

The radiographic images were transferred to a personal computer (PC) hard drive and each image was copied to a separate folder. Each image was loaded separately in Fiji ImageJ, which is an open-source image processing software package that supports Windows, Linux, and Mac OS X platforms. The measurements were taken in the same sequence for all the radiographic images, i.e. first TTD was measured, followed by TRD and TLD. The TCD was calculated separately by adding the values of TRD and TLD. The CTR was then calculated from the values obtained for TTD and TCD. The chest X-rays (PA view) with a CTR > 0.5 were considered to have cardiomegaly present, and those with a CTR ≤ 0.5 were regarded to have a normal heart size.

The echocardiography reports obtained from patients were checked for the relevant study parameters. Those reports that had all the study parameters, were included in the study. The study parameters were:

i. *Right atrium*: Minor-axis (or Transverse) diameter
ii. *Left atrium*: Anterior-Posterior (AP) diameter
iii. *Right ventricle*: Linear dimension (or PLAX diameter) and TAPSE
iv. *Left ventricle*: LVIDd, LVIDs, IVSd, PWd, and LV ejection fraction
v. *Aortic diameter*: Measured at the level of the aortic annulus
vi. *Pulmonary Artery Systolic Pressure (PASP)*: Determined by the modified Bernoulli equation and the right atrial pressure (RAP)

Those echocardiography reports that lacked any of the required parameters, were excluded. The reports were reviewed for heart size and were considered to have cardiomegaly present if any one of the echocardiographic study parameters (i.e. LVIDd, LVIDs, IVSd, PWd, LAD,

RVD and RAD) had values greater than their respective standard normal reference values. The heart size was considered to be normal if all the values for the aforementioned echocardiographic parameters were within their normal reference range. The measurements of the chamber size and other echocardiographic parameters were defined and conducted according to the internationally agreed guidelines of ASE. The measurements that were indexed to BSA (determined using the DuBois and DuBois formula) included LVIDd, LVIDs, IVSd, PWd, LAD, RVD, RAD, TAPSE, the aortic diameter, LV mass and RWT.
Initially, the Mosteller formula was used to calculate the body surface area (BSA) when the patient proforma were being filled, due to its simplicity. During result analysis, the DuBois and DuBois formula was also used to calculate the BSA for indexing echocardiographic parameters and making comparisons (Table 3.3). It was analyzed whether BSA is a significant variable for explaining discrepancies between the chest X-ray (PA view) and echocardiographic estimates in patients with cardiomegaly. The Body Mass Index (BMI) was calculated using the formula: BMI (Kg/m^2) = Weight (Kg)/ [height (m)] ^{2}. All the measurements related to chest X-rays (PA view) were recorded in centimeters (cm) and were stated in the results as such, but for comparison with echocardiographic parameters, the radiographic measurements were converted to millimeters where needed during result analysis. The study population was divided into the following four groups after comparing the findings of chest X-ray (PA view) and echocardiography. The groups were based on:

1. **Group A – *True Positive***: CTR > 0.5, and an enlarged value for **any** one of these echocardiographic parameters: LVIDd, LVIDs, IVSd, PWd, LAD, RVD and RAD
1. **Group B – *False Positive***: CTR > 0.5, and a normal value for **all** of these echocardiographic parameters: LVIDd, LVIDs, IVSd, PWd, LAD, RVD and RAD
2. **Group C – *False Negative***: CTR ≤ 0.5, and an enlarged value for **any** one of these echocardiographic parameters: LVIDd, LVIDs, IVSd, PWd, LAD, RVD and RAD
3. **Group D – *True Negative***: CTR ≤ 0.5, and a normal value for **all** of these echocardiographic parameters: LVIDd, LVIDs, IVSd, PWd, LAD, RVD and RAD

Thus, the groups were divided such that Group A consisted of subjects with an enlarged heart size both on chest X-ray (PA view) and echocardiography. Group B consisted of subjects with an enlarged heart size on chest X-ray (PA view), but a normal heart size on

echocardiography. Group C consisted of subjects with a normal heart size on chest X-ray (PA view), but an enlarged heart size on echocardiography. Group D consisted of subjects with a normal heart size on both chest X-ray (PA view) and echocardiography.

The echocardiography reports also reported the ventricular function of the heart, with a normal and abnormal heart function mentioned for each patient. Those with abnormal left ventricular function had either a diastolic or systolic dysfunction, or both. Those with abnormal right ventricular function had either depressed function or systolic dysfunction. The data was gathered for evaluation and tabulated in a table. Similarly, the diagnosis of each patient was determined from the patient charts, and the data obtained was evaluated and summarized in a table.

3.13 Algorithm of Study

The study algorithm is described in Figure 3.10.

3.14 Statistical Analysis

The data obtained was entered into Excel spreadsheets, and then transferred to SPSS 23.0 for statistical analysis. The data was evaluated to determine if chest X-rays (PA view) were adequate at precisely identifying true cardiomegaly determined on 2D echocardiography. Categorical variables were expressed as numbers and percentages and analyzed using the chi-square test. Continuous variables were expressed as mean ± SD and analyzed using Student's t-test for variables that passed normality tests and Mann–Whitney U-test for those that did not pass normality. Correlations were analyzed using Pearson's correlation (r) and Spearman's-Rho coefficient tests. A probability value $p \leq 0.05$ was considered statistically significant and a p-value ≤ 0.01 was considered highly significant. Associations were explored using correlation and regression for continuous variables, and the means were also compared. Complex multivariate analysis was carried out to investigate how a dependent variable was related to more than one explanatory variable. A binary categorical variable was modeled based on the absence or presence of cardiomegaly, determined after analysis of echocardiography reports. The standard measures of test validity which included sensitivity, specificity, and predictive values with 95% confidence intervals were calculated.

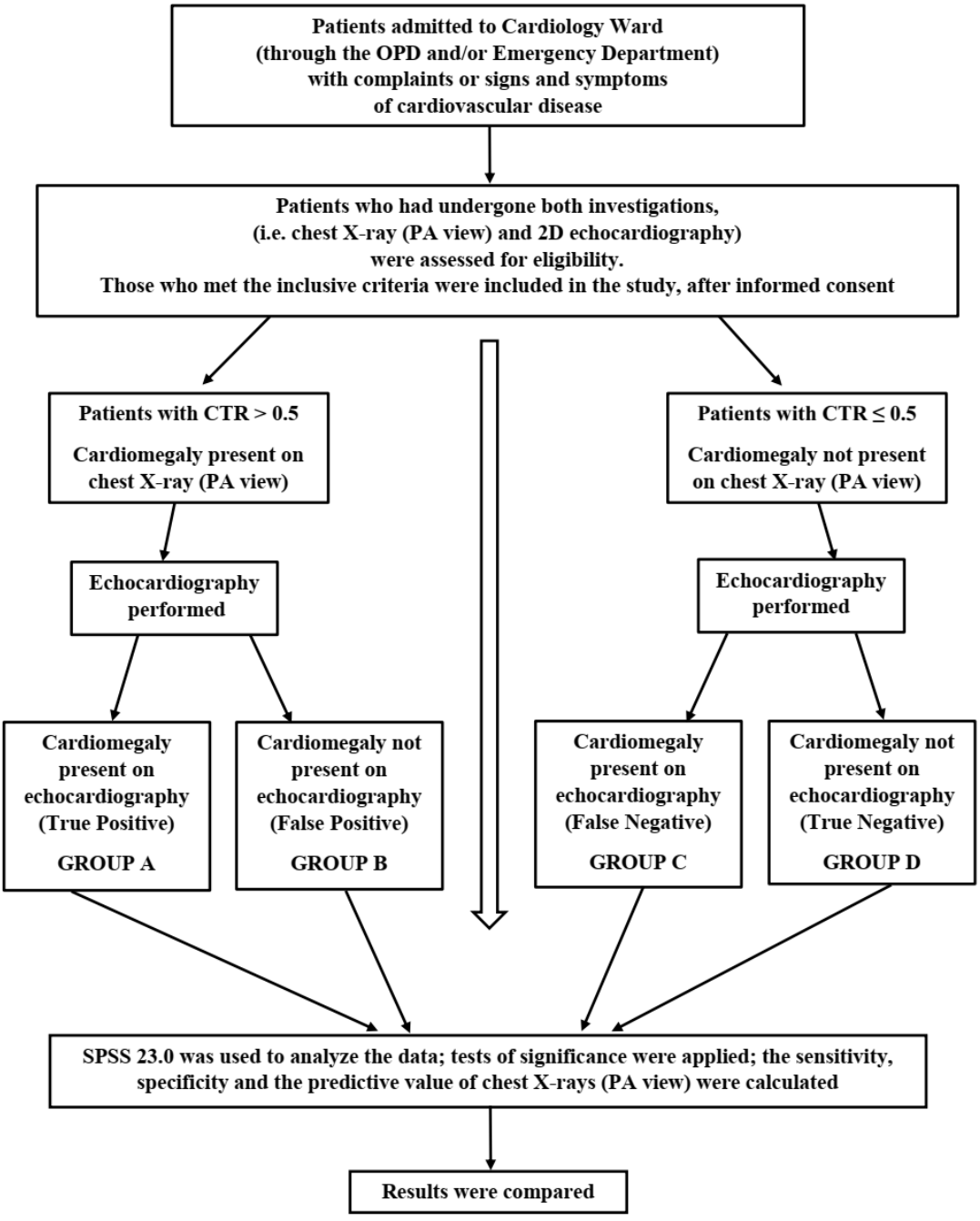

Figure 3.10: The algorithm of the study

CHAPTER 4

RESULTS

The current study was a cross-sectional study, which consisted of 79 patients with a mean age of 52.71 ± 14.54 years, ranging from 19 to 75 years. There were 44 (55.7%) males with a mean age of 55.11 ± 14.34, and 35 (44.3%) females with a mean age of 49.69 ± 14.42 (Table 4.1). The weight, height and BMI of the total study population were 65.54 ± 8.10 kg, 1.61 ± 0.09 m (161 ± 0.09 cm) and 25.54 ± 2.88 kg/m^2. The weight, height and BMI in males were 69.27 ± 7.99 kg, 1.67 ± 0.07 m (167 ± 0.07 cm), and 24.98 ± 2.94 kg/m^2 respectively, and in females, the mean values for the same were 60.86 ± 5.41 kg, 1.54 ± 0.04 m (154 ± 0.04 cm), and 26.03 ± 2.73 kg/m^2 respectively (Table 4.2). The mean body surface area (BSA) when calculated using the Mosteller formula (BSA (Mos.)), was 1.71 ± 0.14 m^2 for the total study population, 1.79 ± 0.12 m^2 in males and 1.61 ± 0.07 m^2 in females. The BSA calculated using DuBois & DuBois formula (BSA (D&D)) was 1.69 ± 0.14 m^2 for the total study population, 1.77 ± 0.12 m^2 in males and 1.58 ± 0.07 m^2 in females. The mean obtained from both the formulae was averaged, which was recorded as 'BSA (averaged)' to investigate its significance in comparison to the two parent means. The BSA calculated using BSA (averaged) was 1.70 ± 0.14 m^2 for the total study population, 1.78 ± 0.12 m^2 in males and 1.59 ± 0.07 m^2 in females. The means of the aforementioned parameters (i.e. weight, height, BMI and BSA) were compared in male and female participants of the study using one-way ANOVA (Table 4.2). The results showed a highly significant (p-value < 0.001) difference between the two genders for weight, height and BSA (all three values of BSA, i.e. BSA (Mos.), BSA (D&D) and BSA (averaged)).

The participants were grouped into different age groups, based on the age range with a class interval of 10 years (Figure 4.1). Similarly, for the purpose of analysis, the participants were also grouped for BMI and BSA (Figures 4.3 and 4.4). According to the age groups, most of the study participants belonged to the age group of 61 to 70 years (29.11%), the next most populous age group was of participants aged 51 to 60 years (25.32%). The least number of participants were observed in the age group of 21 to 30 years (3.80%). The gender distribution in each age group is shown in the bar chart in Figure 4.2. In the most populous

age group (i.e. 61 to 70 years), there were 15 males and 8 females. A similar disparity in gender population was also observed in other groups except for those aged 41 to 50 years, where an equal number of males and females were observed. In the age group of 21 to 30 years, there were only females and no males. Overall, there were more males in the study compared to females.

According to the BMI groups, 45 participants were overweight, i.e. their BMI was between 25 to 29.9 kg/m^2 (Figure 4.3). The mean BMI was higher for the females compared to males. The number of overweight females was marginally higher (21 males and 24 females). According to the BSA groups, males always had a higher BSA compared to females. When the BSA (Mos.) formula was used, males frequently had a BSA between 1.79 to 1.88 m^2, whereas females frequently had a BSA between 1.59 to 1.68 m^2. When the BSA (D & D) formula was used, males frequently had a BSA between 1.69 to 1.78 m^2, whereas females more often had a BSA between 1.49 to 1.58 m^2. When the BSA (averaged) formula was used, an equal number of males occupied the BSA groups of 1.79 to 1.88 m^2 and 1.69 to 1.78 m^2. The females more often occupied the BSA group of 1.59 to 1.68 m^2 (Figure 4.4).

The ethnic profile of the study participants is shown in Figure 4.5, and the gender distribution in each ethnic group is shown in Figure 4.6. The education level of the participants is shown in Figure 4.7. Most of the participants had no formal education (59.5%), followed by those who had an educational background of matriculation (20.3%). The occupation profile of the participants showed that 45.8% of the participants were housewives and 21.5% were retired persons (Figure 4.8). The addiction profile of the study participants showed that 70.9% had no addictions whereas 7.6% were smokers (Figure 4.9).

The physical activity level of the participants showed that a vast majority (60.8%) had infrequent physical activity (Figure 4.10). The participants who walked for less than or more than 30 minutes per week were 25.3% and 13.9%, respectively. There was a strong, statistically significant (p-value = 0.007) difference between male and female participants regarding physical activity level (Table 4.3). Males were more physically active than females. The comorbidities observed in the study participants are shown in Figure 4.11. Most of the participants (55.7%) had no associated disease, while 27.9% had both diabetes mellitus and hypertension, 11.4% had hypertension only, and 5.1% had others. The participants who did

not have any associated diseases were mostly males (32.9%). The most frequent diagnosis was NSTEMI (36.7%), followed by STEMI (16.5%) and valvular heart diseases (16.5%). The diagnosis of decompensated heart failure and dilated cardiomyopathy was observed in 10.1% and 6.3% of participants, respectively. The diagnoses observed in the remaining 13.9% of participants are shown in Figure 4.12.

The radiological signs of pulmonary congestion were observed in 63.3% of participants, while 36.7% had normal chest X-rays (PA view) for pulmonary vasculature (Figure 4.13). There was no oligemia observed in any of the chest X-rays (PA view) included in the study. Four participants had a past history of pulmonary disease, they were treated for pulmonary tuberculosis. Among the total cases observed to have an enlarged heart size (or cardiomegaly) on chest X-ray (PA view), 31.65% had pulmonary vascular congestion and 3.80% did not have congestion. Of the total cases observed with normal heart size on chest X-ray (PA view), an equal number of participants were observed to have pulmonary vascular congestion and no congestion (Figure 4.14). Among the total cases observed to have an enlarged heart size on echocardiography, 46.84% had pulmonary vascular congestion and 11.39% had no congestion. Of the total cases observed with normal heart size on echocardiography, pulmonary vascular congestion was observed less frequently and most of the chest X-rays (PA view) had no congestion (Figure 4.14).

The echocardiography reports also revealed the left and right ventricular functions. Of the total participants, 31.7% had a normal LV function and 74.7% had a normal RV function. For the left ventricle, 44.3% of participants had only systolic LV dysfunction, and 24.1% had both systolic and diastolic LV dysfunction (Figure 4.15). For the right ventricle, 16.5% of participants had depressed RV function, and 8.9% had systolic RV dysfunction (Figure 4.17). In the participants who had LV dysfunction, there was a statistically significant (p-value = 0.015) difference between both genders. In the total study population, females had a higher frequency of systolic dysfunction compared to males, who had a higher frequency of both systolic and diastolic dysfunction. A higher number of females had a normal LV function (Figure 4.16). The gender difference in right ventricular dysfunction was statistically not significant (p-value = 0.987) (Figure 4.18). In the total study population, there was a higher number of participants with a normal right ventricular function. Both genders had a similar

number of participants with depressed RV function and systolic RV dysfunction, observed slightly more in males.

The entire study population was evaluated for an enlarged heart size on both chest X-ray (PA view) and echocardiography. The data obtained was documented, compared and then correlated.

Chest X-ray (PA View) Measurements

The total number of participants with an enlarged heart size or cardiomegaly on chest X-ray (PA view) were 28 (35.4%), with 18 (22.8%) males and 10 (12.7%) females, and those with a normal heart size were 51 (64%), with 26 (32.9%) males and 25 (31.6%) females (Table 4.4). The measurements of radiological parameters of the total study participants based on gender are summarized in Table 4.5. Males had higher values compared to females except for CTR which was equal in both genders when the heart size was normal and higher in females when the heart was enlarged. The mean values of both males and females together were always lower for males and higher for females. The measurements of the radiological parameters based on heart size (normal and enlarged) are summarized in Table 4.6.

The values of TTD, TRD, TLD and TCD were highly significant when compared between both genders with normal heart size, whereas only TTD was highly significant in those with enlarged hearts, as shown in Table 4.7.

Echocardiographic Measurements

The total number of participants with an enlarged heart size or cardiomegaly on echocardiography were 46 (58.2%), with 26 (32.9%) males and 20 (25.3%) females, and those with a normal heart size were 33 (41.8%), with 18 (22.8%) males and 15 (19.0%) females (Table 4.8). The measurements of echocardiographic parameters of the total study participants based on gender and heart size are summarized in Tables 4.9 and 4.10, respectively. The echocardiographic measurements for males and females with a normal heart size are summarized in Tables 4.11 and 4.12, and for those with an enlarged heart are summarized in Tables 4.13 and 4.14.

The values of LVIDd and aortic diameter were highly significant when compared between both genders (Table 4.9). When the normal and enlarged heart sizes were compared, the

parameters that did not show any statistically significant difference were the IVSd, PWd and aortic diameter, whereas all the other parameters exhibited highly significant differences (Table 4.10).

Comparison of Chest X-ray (PA View) and Echocardiography

The ability of chest X-ray (PA view) to determine an enlarged heart was compared to echocardiography. The number of normal-sized and enlarged hearts determined on both imaging modalities were compared using a Pearson Chi-square. A two-by-two (2 x 2) contingency table was constructed (Table 4.18). The total participants who had an enlarged heart on both chest X-ray (PA view) and echocardiography (i.e. true positive) were 25 (31.6%) in number. Those with an enlarged heart on chest X-ray (PA view) but not on echocardiography (i.e. false positive) were 3 (3.8%) in number. Those with an enlarged heart on echocardiography but not on chest X-ray (PA view) (i.e. false negative) were 21 (26.6%) in number. And those with a normal-sized heart on both chest X-ray (PA view) and echocardiography were 30 (38.0%) in number.

i. Specificity and Sensitivity of Chest X-ray (PA View)

The sensitivity and specificity of chest X-ray (PA view) in determining an enlarged heart was calculated by using their respective equations, i.e. sensitivity = True Positive/ (True Positive + False Negative); and, specificity = True Negative/ (True Negative + False Positive). The sensitivity determined in the current study was 54%, and the specificity was 91% (Table 4.19 A).

ii. Determining Positive Predictive Value (PPV) and Negative Predictive Value (NPV)

The positive predictive value (PPV) and negative predictive value (NPV) were determined using their respective equations, i.e. PPV= True Positives/ (True Positives + False Positives); and, NPV= True Negatives/ (True Negatives + False Negatives). The PPV determined in the current study was 89%, and the NPV determined was 59% (Table 4.19 B). The false positive and false negative rates, probability of positive and negative tests, and the accuracy were also calculated as shown in Table 4.19 B.

The positive and negative likelihood ratios are listed in Table 4.19 C.

iii. Categorization of Study Participants into Four Groups (i.e. Group A, B, C and D)

Based on these findings (of Pearson Chi-square), the study participants were divided into four groups, namely Group A, B, C and D. The gender and ethnic characteristics of these groups are shown in Tables 4.20 and 4.21. The purpose of grouping the data was to determine the values of radiological and echocardiographic parameters which resulted in the participants being categorized into their respective groups.

iv. Measurements of Radiological Parameters in Group A, B, C and D:

The radiological parameters observed in each of these groups are summarized in Table 4.22. The difference between these groups for TRD, TLD, TCD and CTR had a strong statistical significance with a p-value of less than 0.001. The difference was not statistically significant for TTD (p-value = 0.597).

The values for the different radiological parameters in males and females in each group are summarized in Tables 4.23 and 4.24, respectively.

v. Measurements of Echocardiographic Parameters in Group A, B, C and D:

The echocardiographic parameters measured for the atria and ventricles, the aortic diameter and PASP are summarized in Table 4.25. The differences between these groups were statistically significant for RAD (p-value = 0.000), LAD (p-value = 0.000), RVD (p-value = 0.003), TAPSE (p-value = 0.049), LVIDd (p-value = 0.000), LVIDs (p-value = 0.000), EF (p-value = 0.000), LV mass (p-value = 0.000), RWT (p-value = 0.000), and PASP (p-value = 0.047). The difference was not statistically significant for IVSd (p-value = 0.494), PWd (p-value = 0.804), and aortic diameter (p-value = 0.379).

The values for the different echocardiographic parameters in males and females in each group are summarized in Tables 4.26 and 4.27, respectively.

vi. Correlation between Radiological and Echocardiographic Parameters

The chest X-ray (PA view) parameters were correlated with echocardiographic parameters using Pearson's correlation. The results for each group were tabulated, as shown in Tables 4.28 to 4.35.

a) In Group A (Tables 4.28 and 4.29), the CTR had a strong positive correlation with RVD (p-value = 0.012) and PASP (p-value = 0.012). The TCD had a positive correlation with LVIDs (p-value = 0.022) and negative correlation with EF (p-value

= 0.020). The TLD had a positive correlation with LVIDd (p-value = 0.050) and LVIDs (p-value = 0.005), and a negative correlation with IVSd (p-value = 0.016), LV EF (p-value = 0.002) and RWT (p-value = 0.014). The TTD had a positive correlation with LVIDs (p-value = 0.036) and aortic diameter (p-value = 0.014).

b) In Group B (Tables 4.30 and 4.31), the CTR did not correlate with any of the echocardiographic parameters. The TCD had a positive correlation with LVIDd (p-value = 0.020), and a negative correlation with PWd (p-value = 0.032) and RWT (p-value = 0.041). The TLD had a positive correlation with LVIDd (p-value = 0.012), and a negative correlation with PWd (p-value = 0.040) and RWT (p-value = 0.048). The TRD had a positive correlation with LVIDd (p-value = 0.049), and a negative correlation with PWd (p-value = 0.004) and RWT (p-value = 0.012). The TTD had a positive correlation with LVIDd (p-value = 0.045), and a negative correlation with PWd (p-value = 0.007) and RWT (p-value = 0.015). There were only 3 participants categorized in this group, and one of the participant's PASP could not be measured due to turbulent tricuspid blood flow (turbulent TR jet).

c) In Group C (Tables 4.32 and 4.33), only a negative correlation was observed between TLD and EF (p-value = 0.011).

d) In Group D (Tables 4.34 and 4.35), the CTR did not correlate with any of the echocardiographic parameters. The TCD had a positive correlation with RAD (p-value = 0.010) and LAD (p-value = 0.046). The TLD had a positive correlation with RAD (p-value = 0.018) and the aortic diameter (p-value = 0.043). The TTD had a positive correlation with RAD (p-value = 0.002) and LAD (p-value = 0.016).

vii. Indexed echocardiographic measurements

The echocardiographic values were indexed to BSA (D&D), to compare them with chest X-rays (PA view) (Tables 4.15 to 4.17). It was to investigate whether echocardiographic measurements standardized to BSA correlated with chest X-ray (PA view) better than the measurements that were not standardized. Pearson's correlation was used for this purpose, and the results for each group were tabulated (Tables 4.36 to 4.43).

a) In Group A (Tables 4.36 and 4.37), the CTR had positive correlation with indexed RVD (iRVD) (p-value = 0.010). The TCD had a negative correlation with indexed

RWT (RWTi) (p-value = 0.038) and indexed EF (iEF) (p-value = 0.018). The TLD had a positive correlation with indexed LVIDs (iLVIDs) (p-value = 0.023), and a negative correlation with indexed IVSd (IVSdi) (p-value = 0.010), iEF (p-value = 0.002) and RWTi (p-value = 0.006). The TTD had a negative correlation with iEF (p-value = 0.035).

b) In Group B (Tables 4.38 and 4.39), the TTD, TRD, TLD and TCD had a negative correlation with iRVD (p-value = 0.043, 0.046, 0.010 and 0.018, respectively).

c) In Group C (Tables 4.40 and 4.41), the CTR had a positive correlation with indexed aortic diameter (p-value = 0.012). The TLD had a negative correlation with iEF (p-value = 0.017). The TTD had a negative correlation with indexed LAD (iLAD) (p-value = 0.023).

d) In Group D (Tables 4.42 and 4.43), the CTR had a negative correlation with indexed RAD (iRAD) (p-value = 0.045). The TCD had a negative correlation with indexed RVD (iRVD) (p-value = 0.019), indexed TAPSE (iTAPSE) (p-value = 0.028) and iLVIDs (p-value = 0.010). The TLD had a negative correlation with iTAPSE (p-value = 0.011), iLVIDs (p-value = 0.008), iLVIDd (p-value = 0.009), IVSdi (p-value = 0.032), and indexed PWd (PWdi) (p-value = 0.027). The TRD had a negative correlation with iRVD (p-value = 0.018). The TTD had a negative correlation with iRVD (p-value = 0.031); iTAPSE (p-value = 0.026), iLVIDd (p-value = 0.044), iLVIDs (p-value = 0.018) and IVSdi (p-value = 0.017).

viii. The Ventricular Function of Participants (Group A, B, C and D)

The ventricular function of the participants in the four groups was evaluated using a Chi-square test. The results were tabulated, as shown in Tables 4.44 to 4.47.

There was a highly significant (p-value = 0.009) difference in the RV function of the four groups. The difference in the LV function of the four groups was also statistically significant (p-value = 0.01). Comparing the males and females in each group, the only statistically significant (p-value = 0.01) difference observed was for the LV function in males.

Indexed Left Ventricular (LV) Mass (LVMi) and Right Wall Thickness (RWT)

The male and female participants with normal and enlarged heart size on chest X-ray (PA view) were evaluated for LVMi and RWT. The findings are summarized in Tables 4.48 and 4.49. There was no statistically significant difference observed for both LVMi and RWT in male and female participants with a CTR value of ≤ 0.5 or > 0.5.

Left Ventricular (LV) Hypertrophy

The LV hypertrophy was identified by an increase in indexed LV mass (LVMi), and it was investigated further to identify whether it had an eccentric or hypertrophic pattern. Using the Pearson Chi-square, a two-by-two (2 x 2) contingency table was constructed using the values for LVMi and RWT (Tables 4.50 and 4.52). The number of participants with LV hypertrophy and the pattern of hypertrophy present were tabulated separately (Tables 4.51 and 4.53).

In both males and females, the most frequent pattern of LV hypertrophy observed was eccentric, followed by concentric remodeling. Concentric hypertrophy was observed in 2 females, and none in males.

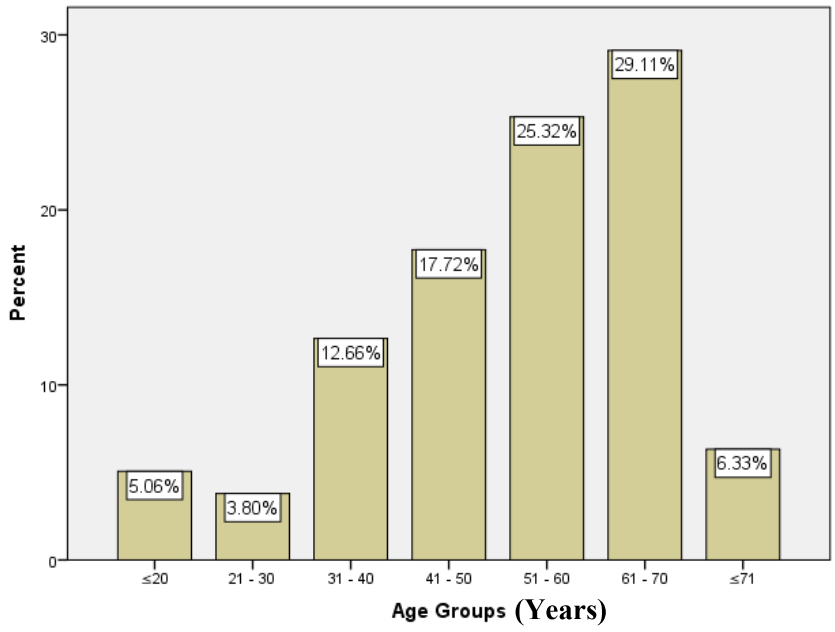

Figure 4.1: Distribution of the Study Participants into Age Groups (in years)

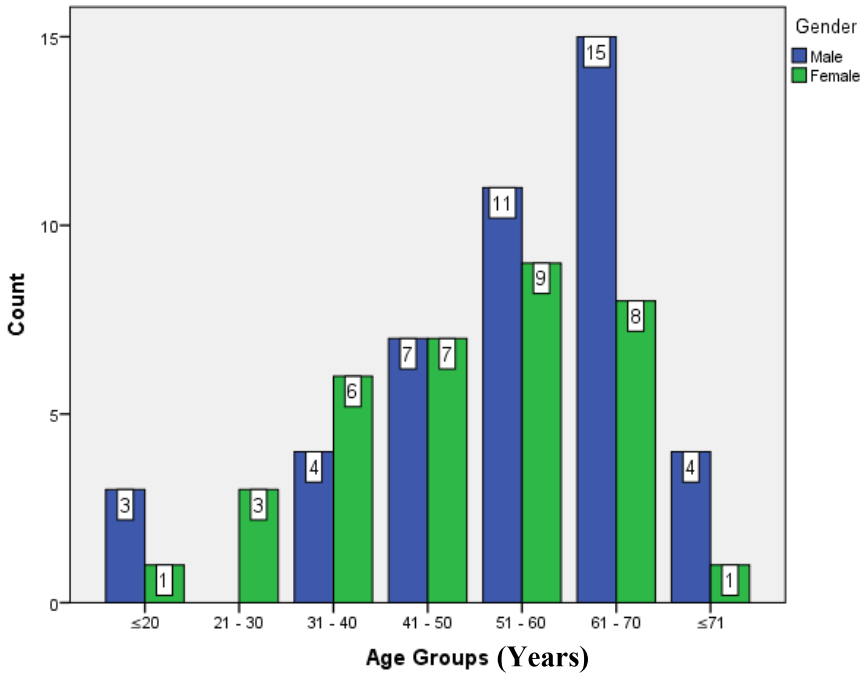

Figure 4.2: Gender Distribution Within Each Age Group (in years)

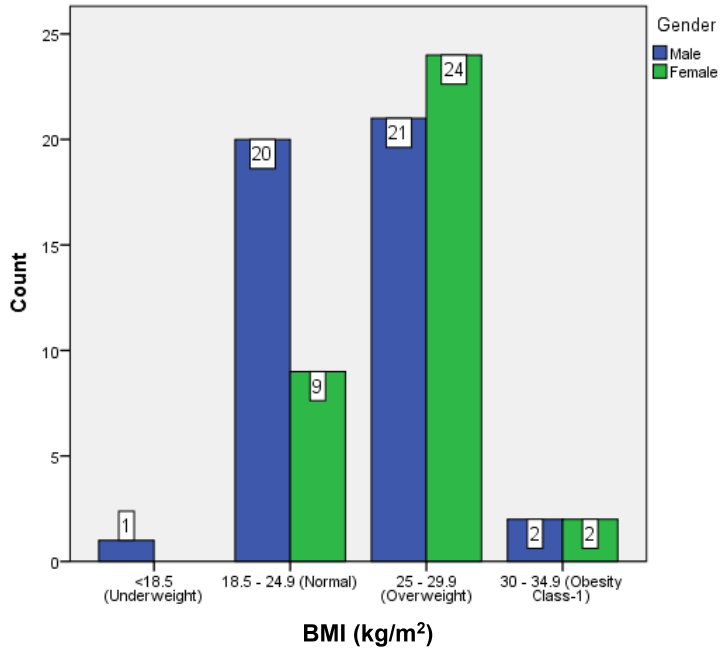

Figure 4.3: BMI Groups and Gender Comparison

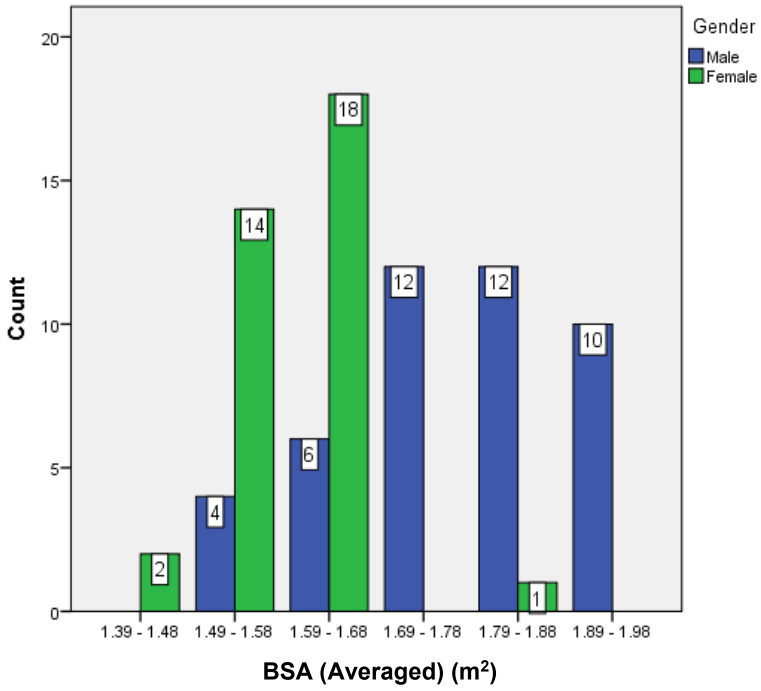

Figure 4.4: BSA (Averaged) Groups and Gender Comparison

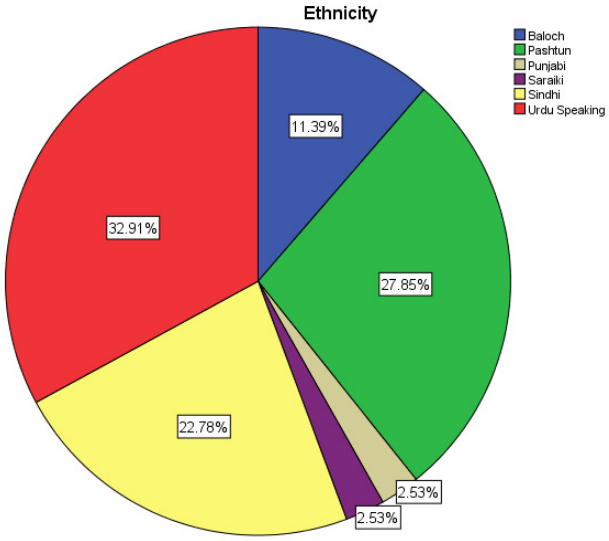

Figure 4.5: Ethnic Profile of the Total Study Participants

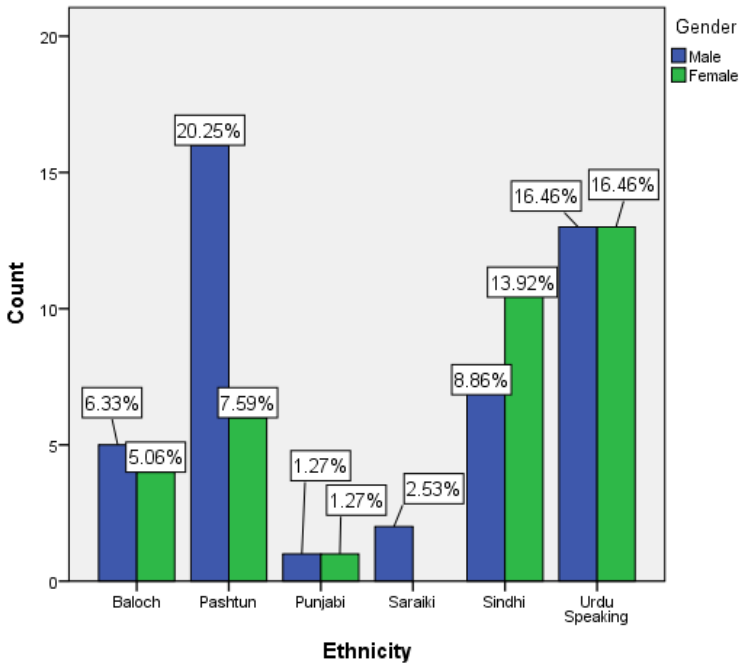

Figure 4.6: Gender Distribution in the Ethnic Groups

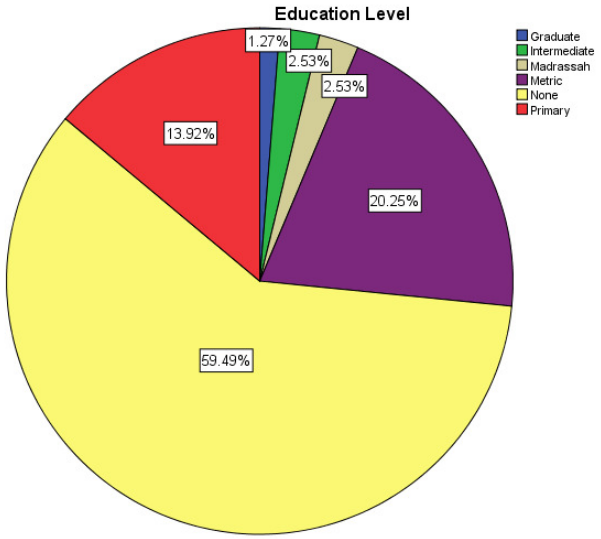

Figure 4.7: Education Level of the Total Study Participants

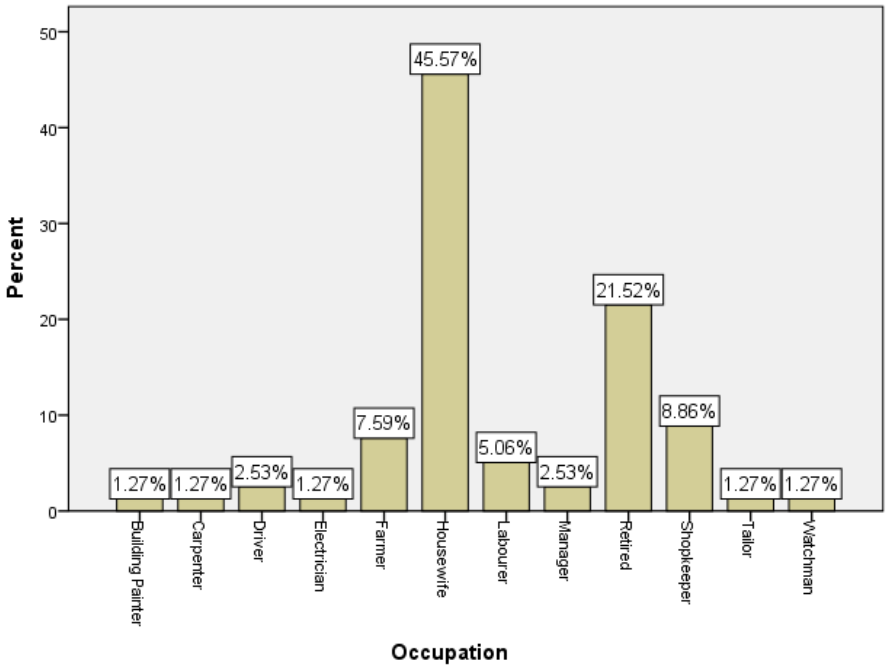

Figure 4.8: Occupation Profile of the Total Study Participants

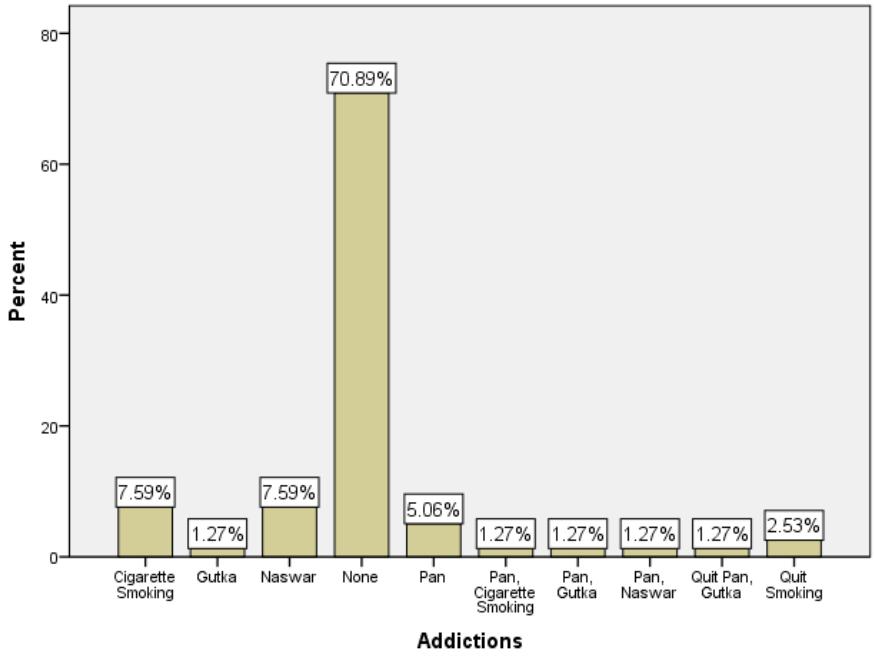

Figure 4.9: Addiction Profile of the Total Study Participants

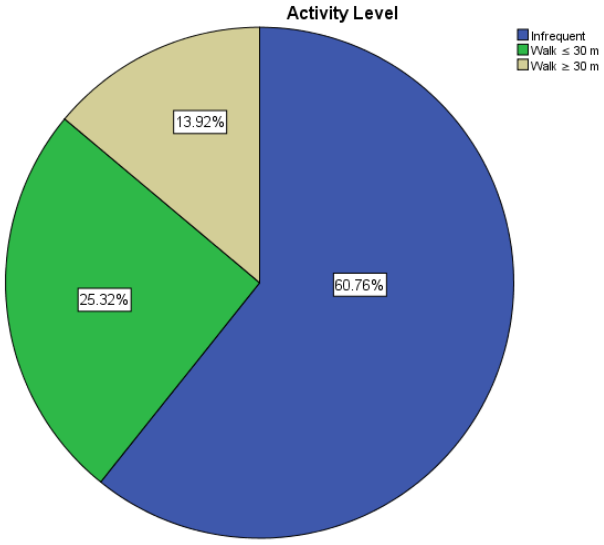

Figure 4.10: Physical Activity Level of the Total Study Participants

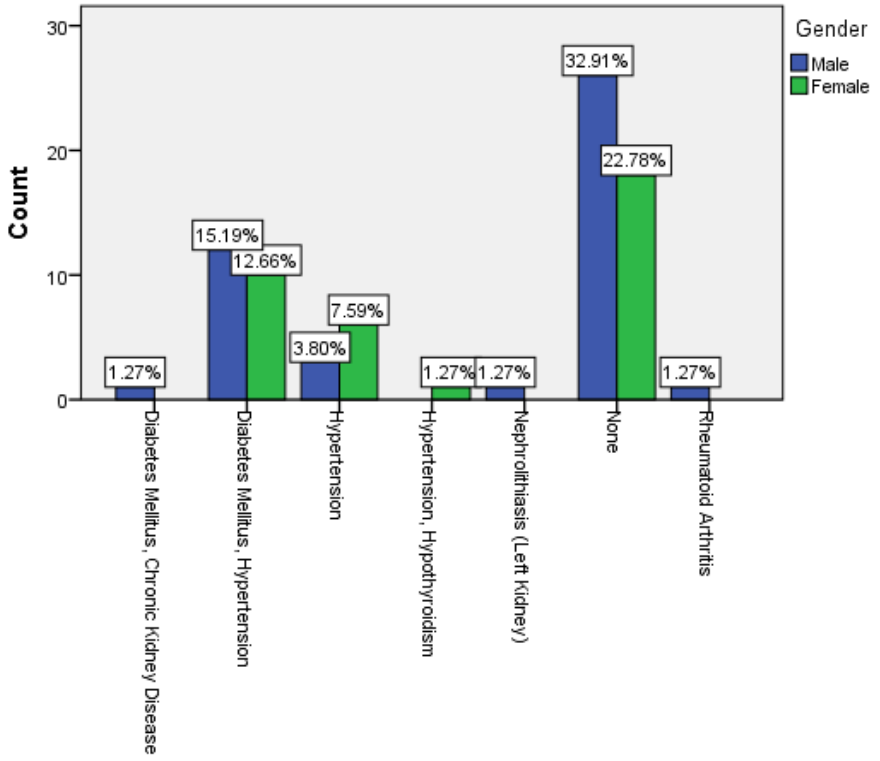

Figure 4.11: Comorbidities Present in the Total Study Participants

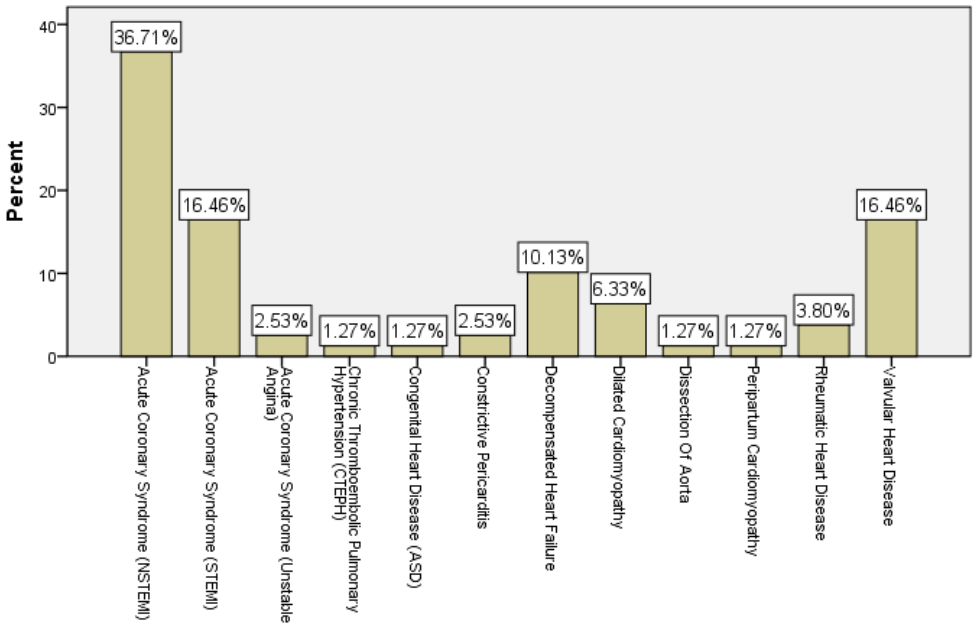

Figure 4.12: Diagnosis of the Total Study Participants

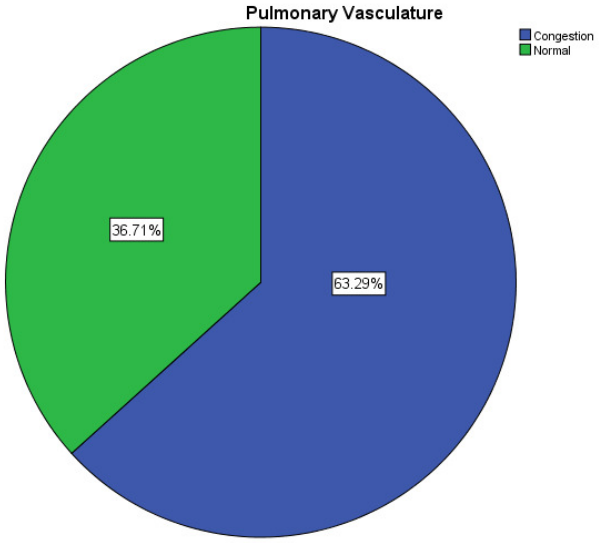

Figure 4.13: Pulmonary Vascular Status on Chest X-ray (PA view)

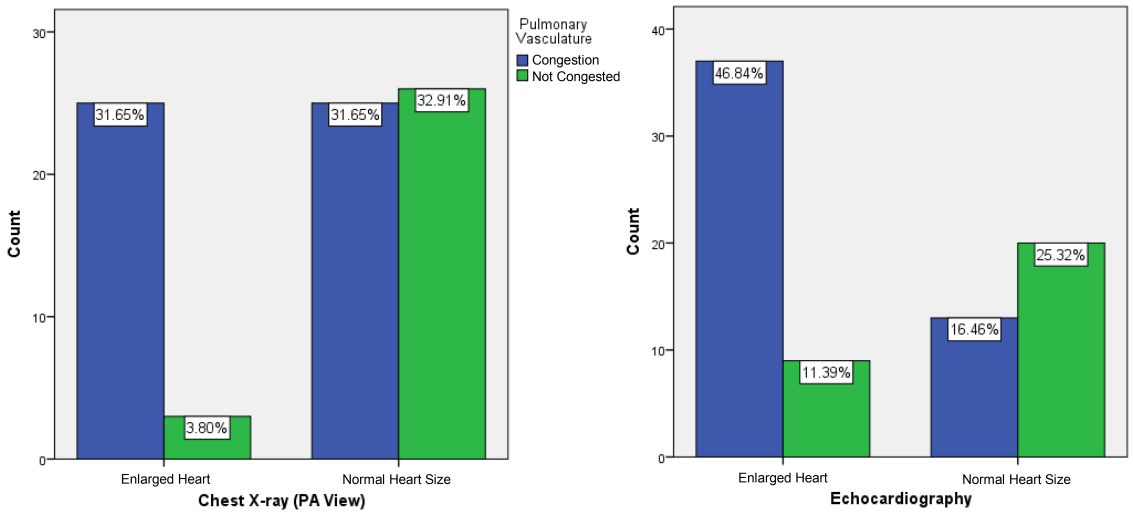

Figure 4.14: Pulmonary Vascular Status on Chest X-ray (PA view) and Echocardiography

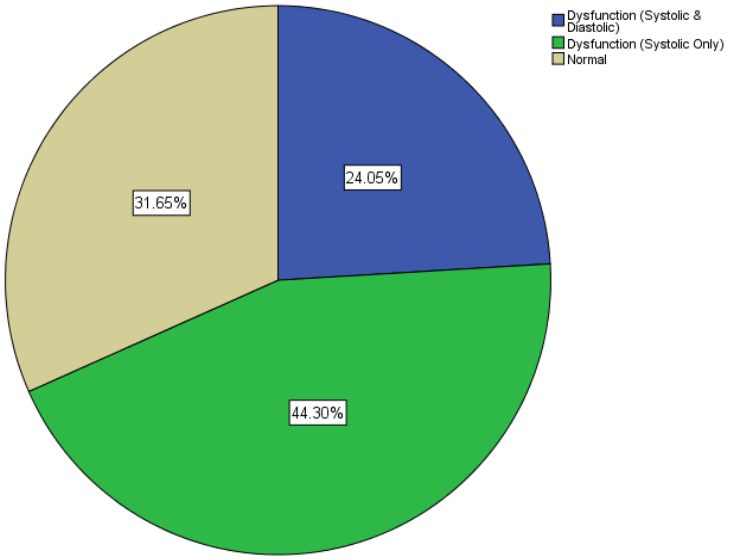

Figure 4.15: Left Ventricular (LV) Function in Total Study Participants

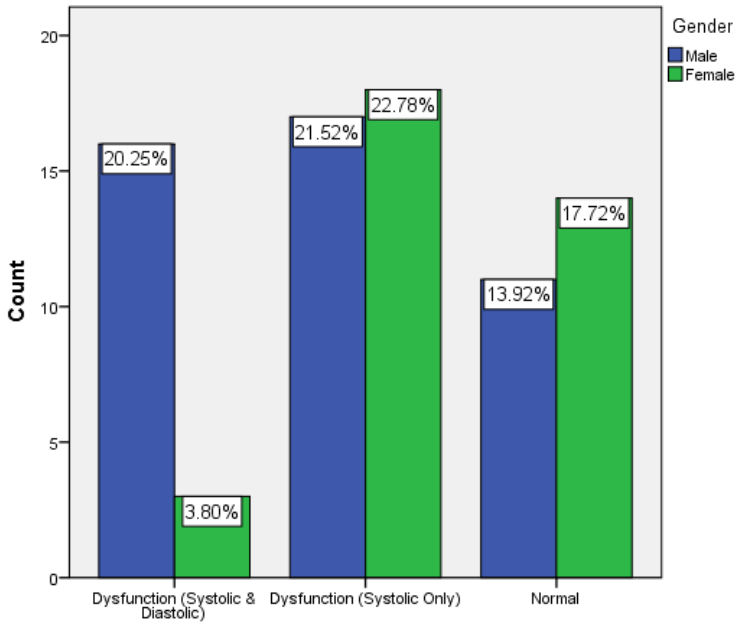

Figure 4.16: Left Ventricular (LV) Function in Male and Female Participants

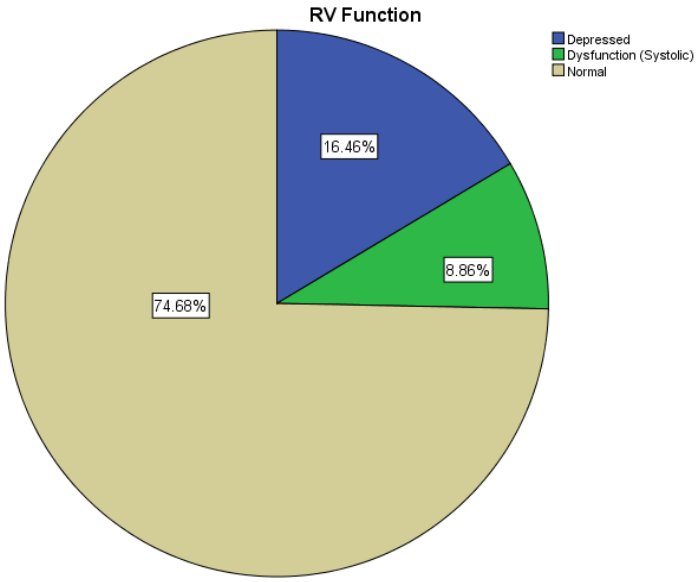

Figure 4.17: Right Ventricular (RV) Function in Total Study Participants

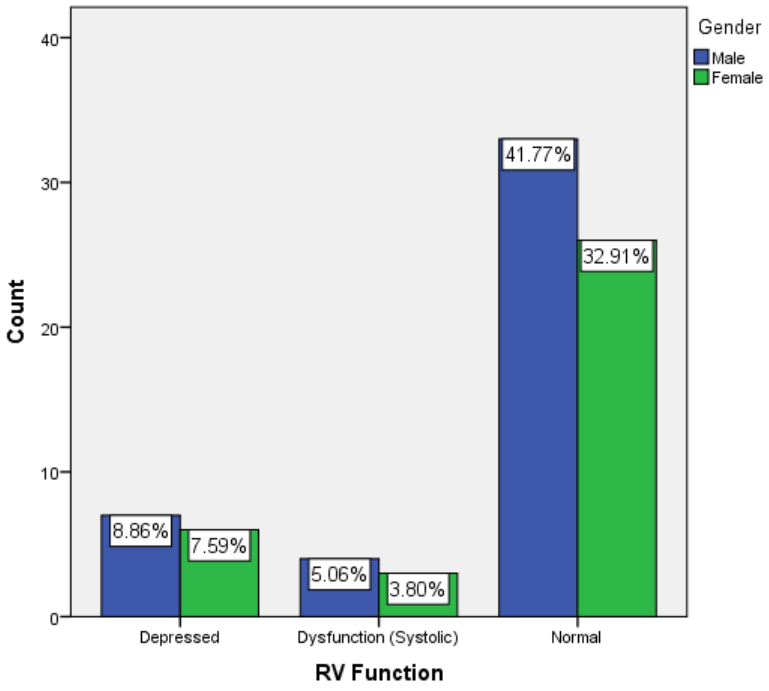

Figure 4. 18: Right Ventricular (RV) Function in Male and Female Participants

Table 4.1: Age (in years) of the Study Participants					
Gender	**n (%)**	**Minimum**	**Maximum**	**Mean**	**SD**
Male	44 (55.7%)	19.00	75.00	55.11	14.34
Female	35 (44.3%)	20.00	73.00	49.69	14.42
Total	79 (100%)	19.00	75.00	52.71	14.54

Data presented as numbers, percentages and mean ± standard deviation

Table 4.2: Demographic Characteristics of the Study Participants (Weight, Height, BMI and BSA)							
Variable	**Gender**	**n**	**Minimum**	**Maximum**	**Mean**	**SD**	**p-value**
Weight (kg)	**Male**	44	50.00	85.00	69.27	7.99	0.000**
	Female	35	45.00	78.00	60.86	5.41	
	Total	79	45.00	85.00	65.54	8.10	
Height (m)	**Male**	44	1.52	1.88	1.67	0.07	0.000**
	Female	35	1.42	1.60	1.53	0.04	
	Total	79	1.42	1.88	1.61	0.09	
BMI (kg/m^2)	**Male**	44	18.12	31.18	24.98	2.94	0.107
	Female	35	18.62	33.39	26.03	2.73	
	Total	79	18.12	33.39	25.45	2.88	
BSA (Mos.) (m^2)	**Male**	44	1.50	2.00	1.79	0.12	0.000**
	Female	35	1.39	1.83	1.61	0.07	
	Total	79	1.39	2.00	1.71	0.14	
BSA (D&D) (m^2)	**Male**	44	1.51	1.98	1.77	0.12	0.000**
	Female	35	1.41	1.77	1.58	0.07	
	Total	79	1.41	1.98	1.69	0.14	
BSA (Averaged) (m^2)	**Male**	44	1.51	1.99	1.78	0.12	0.000**
	Female	35	1.40	1.80	1.59	0.07	
	Total	79	1.40	1.99	1.70	0.14	

Abbreviations: see ‘List of Abbreviations’; p-value ≤ 0.05: significant (*); p-value ≤ 0.01: highly significant (**); Test applied: ANOVA

Table 4.3: Physical Activity Level and its Significance					
		Gender		Total	p-value
		Male	Female		
Activity Level	Infrequent	20	28	48	0.007**
		25.3%	35.4%	60.8%	
	Walk ≤ 30 m	16	4	20	
		20.3%	5.1%	25.3%	
	Walk ≥ 30 m	8	3	11	
		10.1%	3.8%	13.9%	
Total		44	35	79	
		55.7%	44.3%	100.0%	

p-value ≤ 0.05: significant (*); p-value ≤ 0.01: highly significant (**); Test applied: Pearson's Chi-square

Table 4.4: Gender-based Comparison of Heart Size on chest X-ray (PA View)					
		Gender		Total	p-value
		Male	Female		
Chest X-ray (PA View)	Enlarged (CTR > 0.5)	18	10	28	0.255
		22.8%	12.7%	35.4%	
	Normal (CTR ≤ 0.5)	26	25	51	
		32.9%	31.6%	64.6%	
Total		44	35	79	
		55.7%	44.3%	100.0%	

p-value ≤ 0.05: significant (*); p-value ≤ 0.01: highly significant (**); Test applied: Pearson's Chi-square

Table 4.5: Measurement of Radiological Parameters in Total Study Population (Based on Gender)							
Parameter	**Gender**	**n**	**Minimum**	**Maximum**	**Mean**	**SD**	**p-value**
TTD (cm)	Male	44	24.08	36.90	29.23	2.70	0.000**
	Female	35	21.44	32.13	25.09	2.57	
	Total	79	21.44	36.90	27.39	3.34	
TRD (cm)	Male	44	2.80	8.59	5.20	1.17	0.000**
	Female	35	2.31	7.67	4.26	0.98	
	Total	79	2.31	8.59	4.78	1.18	
TLD (cm)	Male	44	6.75	14.20	9.71	1.64	0.001**
	Female	35	6.54	11.78	8.41	1.53	
	Total	79	6.54	14.20	9.14	1.71	
TCD (cm)	Male	44	10.60	19.66	14.91	2.16	0.000**
	Female	35	10.03	19.45	12.67	2.12	
	Total	79	10.03	19.66	13.92	2.41	
CTR	Male	44	0.43	0.68	0.51	0.06	0.729
	Female	35	0.44	0.72	0.51	0.07	
	Total	79	0.43	0.72	0.51	0.07	

Abbreviations: see 'List of Abbreviations'; p-value ≤ 0.05: significant (*); p-value ≤ 0.01: highly significant (**); Test applied: ANOVA

Table 4.6: Measurement of Radiological Parameters in Total Study Population (Based on Heart Size)							
Parameter	**Heart Size**	**n**	**Minimum**	**Maximum**	**Mean**	**SD**	**p-value**
TTD (cm)	Normal	51	21.44	35.35	27.32	3.38	0.798
	Enlarged	28	22.23	36.90	27.53	3.33	
	Total	79	21.44	36.90	27.39	3.34	
TRD (cm)	Normal	51	2.31	6.84	4.38	1.03	0.000**
	Enlarged	28	3.63	8.59	5.50	1.09	
	Total	79	2.31	8.59	4.78	1.18	
TLD (cm)	Normal	51	6.54	10.59	8.43	1.20	0.000**
	Enlarged	28	6.75	14.20	10.41	1.78	
	Total	79	6.54	14.20	9.14	1.71	
TCD (cm)	Normal	51	10.03	16.95	12.82	1.71	0.000**
	Enlarged	28	11.76	19.66	15.92	2.20	
	Total	79	10.03	19.66	13.92	2.41	
CTR	Normal	51	0.43	0.50	0.47	0.02	0.000**
	Enlarged	28	0.51	0.72	0.58	0.06	
	Total	79	0.43	0.72	0.51	0.07	

Abbreviations: see 'List of Abbreviations'; p-value ≤ 0.05: significant (*); p-value ≤ 0.01: highly significant (**); Test applied: ANOVA

Table 4.7: Comparison of the Radiological Parameters of Heart Size in Males & Females									
Parameter	**Gender**	**Normal Sized Heart**				**Enlarged Heart**			
		n	**Mean**	**SD**	**p-value**	**n**	**Mean**	**SD**	**p-value**
TTD (cm)	Male	26	29.39	2.66	0.000**	18	28.99	2.81	0.001**
	Female	25	25.17	2.64		10	24.88	2.50	
TRD (cm)	Male	26	4.87	1.11	0.000**	18	5.66	1.11	0.310
	Female	25	3.88	0.64		10	5.22	1.04	
TLD (cm)	Male	26	8.94	1.07	0.002**	18	10.83	1.71	0.099
	Female	25	7.91	1.12		10	9.67	1.74	
TCD (cm)	Male	26	13.81	1.47	0.000**	18	16.49	2.03	0.063
	Female	25	11.79	1.30		10	14.89	2.22	
CTR	Male	26	0.47	0.02	0.852	18	0.57	0.06	0.237
	Female	25	0.47	0.02		10	0.60	0.06	

Abbreviations: see 'List of Abbreviations'; p-value ≤ 0.05: significant (*); p-value ≤ 0.01: highly significant (**); Test applied: ANOVA

Table 4.8: Gender-based Comparison of Heart Size on Echocardiography					
		Gender		**Total**	**p-value**
		Male	**Female**		
Echocardiography	**Enlarged Heart**	26	20	46	0.862
		32.9%	25.3%	58.2%	
	Normal Sized Heart	18	15	33	
		22.8%	19.0%	41.8%	
Total		44	35	79	
		55.7%	44.3%	100.0%	

p-value ≤ 0.05: significant (*); p-value ≤ 0.01: highly significant (**); Test applied: ANOVA

Table 4.9: Echocardiographic Measurements in Total Study Participants (Based on Gender)							
	Gender	**n**	**Minimum**	**Maximum**	**Mean**	**SD**	**p-value**
RAD (mm)	Male	44	23.00	42.00	31.39	5.47	0.644
	Female	35	21.00	60.00	32.20	9.88	
	Total	79	21.00	60.00	31.75	7.70	
LAD (mm)	Male	44	28.00	57.00	38.25	7.48	0.828
	Female	35	26.00	61.00	37.86	8.34	
	Total	79	26.00	61.00	38.07	7.82	
RVD (mm)	Male	44	16.00	50.00	23.05	7.65	0.795
	Female	35	15.00	66.00	22.51	10.42	
	Total	79	15.00	66.00	22.81	8.93	
TAPSE (mm)	Male	44	10.00	22.00	16.73	3.12	0.814
	Female	35	9.00	26.00	16.54	3.84	
	Total	79	9.00	26.00	16.65	3.43	
LVIDd (mm)	Male	44	33.00	69.00	52.02	8.66	0.036*
	Female	35	34.00	80.00	47.77	9.00	
	Total	79	33.00	80.00	50.14	9.01	
LVIDs (mm)	Male	44	20.00	62.00	38.98	10.71	0.082
	Female	35	22.00	50.00	35.03	8.78	
	Total	79	20.00	62.00	37.23	10.04	
IVSd (mm)	Male	44	5.00	17.00	8.35	1.88	0.680
	Female	35	5.00	12.00	8.51	1.58	
	Total	79	5.00	17.00	8.42	1.74	
PWd (mm)	Male	44	5.00	11.00	8.25	1.28	0.750
	Female	35	5.00	13.00	8.14	1.57	
	Total	79	5.00	13.00	8.20	1.41	
EF (%)	Male	44	20.00	60.00	37.27	13.31	0.072
	Female	35	20.00	64.00	42.97	14.37	
	Total	79	20.00	64.00	39.80	13.99	
LVM (g)	Male	44	62.71	275.16	156.70	54.11	0.118
	Female	35	65.78	381.90	136.69	58.03	
	Total	79	62.71	381.90	147.83	56.41	
RWT	Male	44	0.19	0.48	0.33	0.07	0.147
	Female	35	0.20	0.63	0.35	0.10	
	Total	79	0.19	0.63	0.34	0.08	
Aorta (mm)	Male	44	23.00	37.00	29.60	3.63	0.000**
	Female	35	16.00	32.00	26.09	3.58	
	Total	79	16.00	37.00	28.04	3.99	
PASP (mm Hg)	Male	36	20.00	90.00	34.58	13.33	0.155
	Female	29	20.00	105.00	40.17	18.00	
	Total	65	20.00	105.00	37.08	15.71	

Abbreviations: see 'List of Abbreviations'; p-value ≤ 0.05: significant (*); p-value ≤ 0.01: highly significant (**); Test applied: ANOVA

Table 4.10: Echocardiographic Measurements in Total Study Participants (Based On Heart Size Determined On Echocardiography)							
	Heart Size	**n**	**Minimum**	**Maximum**	**Mean**	**SD**	**p-value**
RAD (mm)	Enlarged	46	22.00	60.00	35.41	7.79	0.000**
	Normal	33	21.00	34.00	26.64	3.58	
	Total	79	21.00	60.00	31.75	7.70	
LAD (mm)	Enlarged	46	28.00	61.00	41.97	7.66	0.000**
	Normal	33	26.00	40.00	32.64	3.80	
	Total	79	26.00	61.00	38.07	7.82	
RVD (mm)	Enlarged	46	15.00	66.00	25.26	10.97	0.003**
	Normal	33	16.00	23.00	19.39	2.08	
	Total	79	15.00	66.00	22.81	8.93	
TAPSE (mm)	Enlarged	46	9.00	26.00	15.78	4.03	0.008**
	Normal	33	11.00	20.00	17.85	1.82	
	Total	79	9.00	26.00	16.65	3.43	
LVIDd (mm)	Enlarged	46	33.00	80.00	53.76	9.45	0.000**
	Normal	33	35.00	54.00	45.09	5.22	
	Total	79	33.00	80.00	50.14	9.01	
LVIDs (mm)	Enlarged	46	21.00	62.00	42.11	10.02	0.000**
	Normal	33	20.00	40.00	30.42	4.72	
	Total	79	20.00	62.00	37.23	10.04	
IVSd (mm)	Enlarged	46	5.00	17.00	8.33	2.06	0.599
	Normal	33	7.00	11.00	8.55	1.18	
	Total	79	5.00	17.00	8.42	1.74	
PWd (mm)	Enlarged	46	5.00	13.00	8.08	1.52	0.386
	Normal	33	7.00	11.00	8.36	1.25	
	Total	79	5.00	13.00	8.20	1.41	
EF (%)	Enlarged	46	20.00	64.00	35.30	13.22	0.001**
	Normal	33	25.00	60.00	46.06	12.73	
	Total	79	20.00	64.00	39.80	13.99	
LVM (g)	Enlarged	46	62.71	381.90	164.58	63.45	0.001**
	Normal	33	78.36	234.82	124.50	33.63	
	Total	79	62.71	381.90	147.83	56.41	
RWT	Enlarged	46	0.19	0.52	0.31	0.08	0.000**
	Normal	33	0.26	0.63	0.38	0.08	
	Total	79	0.19	0.63	0.34	0.08	
Aorta (mm)	Enlarged	46	16.00	37.00	28.01	4.48	0.927
	Normal	33	20.00	34.00	28.09	3.25	
	Total	79	16.00	37.00	28.04	3.99	
PASP (mm Hg)	Enlarged	38	25.00	105.00	43.03	17.42	0.000**
	Normal	27	20.00	55.00	28.70	7.15	
	Total	65	20.00	105.00	37.08	15.71	

Abbreviations: see 'List of Abbreviations'; p-value ≤ 0.05: significant (*); p-value ≤ 0.01: highly significant (**); Test applied: ANOVA

Table 4.11: Total Male Participants with Normal Heart Size (18) on Echocardiography				
Parameter	**Minimum**	**Maximum**	**Mean**	**SD**
RAD (mm)	23.00	34.00	27.72	3.16
LAD (mm)	28.00	39.00	33.06	3.52
RVD (mm)	16.00	23.00	19.89	1.97
TAPSE (mm)	15.00	20.00	17.89	1.41
LVIDd (mm)	40.00	54.00	45.56	4.74
LVIDs (mm)	20.00	38.00	30.33	4.21
IVSd (mm)	7.00	11.00	8.22	1.17
PWd (mm)	7.00	11.00	8.28	1.23
EF (%)	25.00	60.00	44.44	12.23
LV Mass (g)	78.36	234.82	123.36	37.69
RWT	0.27	0.45	0.37	0.06
Aorta (mm)	23.00	34.00	29.11	2.97
PASP (mm Hg)	20.00	40.00	27.67	4.95

Abbreviations: see ‘List of Abbreviations’. Data presented as mean ± standard deviation

Table 4.12: Total Female Participants with Normal Heart Size (15) On Echocardiography				
Parameter	**Minimum**	**Maximum**	**Mean**	**SD**
RAD (mm)	21.00	33.00	25.33	3.72
LAD (mm)	26.00	40.00	32.13	4.17
RVD (mm)	16.00	23.00	18.80	2.11
TAPSE (mm)	11.00	20.00	17.80	2.27
LVIDd (mm)	35.00	54.00	44.53	5.85
LVIDs (mm)	22.00	40.00	30.53	5.41
IVSd (mm)	8.00	11.00	8.93	1.10
PWd (mm)	7.00	11.00	8.47	1.30
EF (%)	25.00	60.00	48.00	13.47
LV Mass (g)	78.77	168.92	125.87	29.26
RWT	0.26	0.63	0.39	0.09
Aorta (mm)	20.00	32.00	26.87	3.25
PASP (mm Hg)	20.00	55.00	30.00	9.29

Abbreviations: see ‘List of Abbreviations’. Data presented as mean ± standard deviation

Table 4.13: Total Male Participants with Enlarged Heart (26) on Echocardiography				
Parameter	**Minimum**	**Maximum**	**Mean**	**SD**
RAD (mm)	24.00	42.00	33.92	5.33
LAD (mm)	30.00	57.00	41.84	7.42
RVD (mm)	16.00	50.00	25.23	9.26
TAPSE (mm)	10.00	22.00	15.92	3.71
LVIDd (mm)	33.00	69.00	56.50	7.91
LVIDs (mm)	21.00	62.00	44.97	9.70
IVSd (mm)	5.00	17.00	8.44	2.26
PWd (mm)	5.00	10.20	8.22	1.34
EF (%)	20.00	60.00	32.31	11.85
LV Mass (g)	62.71	275.16	179.78	52.11
RWT	0.19	0.48	0.30	0.06
Aorta (mm)	23.00	37.00	29.93	4.04
PASP (mm Hg)	25.00	90.00	39.52	15.24

Abbreviations: see ‘List of Abbreviations’. Data presented as mean ± standard deviation

Table 4.14: Total Female Participants with Enlarged Heart (20) on Echocardiography				
Parameter	**Minimum**	**Maximum**	**Mean**	**SD**
RAD (mm)	22.00	60.00	37.35	9.97
LAD (mm)	28.00	61.00	42.15	8.15
RVD (mm)	15.00	66.00	25.30	13.12
TAPSE (mm)	9.00	26.00	15.60	4.51
LVIDd (mm)	34.00	80.00	50.20	10.26
LVIDs (mm)	25.00	50.00	38.40	9.41
IVSd (mm)	5.00	12.00	8.20	1.82
PWd (mm)	5.00	13.00	7.90	1.74
EF (%)	20.00	64.00	39.20	14.17
LV Mass (g)	65.78	381.90	144.81	72.34
RWT	0.20	0.52	0.32	0.09
Aorta (mm)	16.00	30.00	25.50	3.79
PASP (mm Hg)	25.00	105.00	47.35	19.37

Abbreviations: see ‘List of Abbreviations’. Data presented as mean ± standard deviation

Table 4.15: Indexed Echocardiographic Parameters in Total Study Participants				
Parameter	**Minimum**	**Maximum**	**Mean**	**SD**
iRAD (mm/m^2)	12.62	37.34	18.96	5.05
iLAD (mm/m^2)	15.37	37.17	22.70	5.00
iRVD (mm/m^2)	8.84	42.57	13.63	5.69
iTAPSE (mm/m^2)	5.20	16.77	9.94	2.25
iLVIDd (mm/m^2)	19.46	50.38	29.75	5.03
iLVIDs (mm/m^2)	10.40	32.42	22.07	5.67
IVSdi (mm/m^2)	2.80	9.37	5.04	1.14
PWdi (mm/m^2)	2.98	8.30	4.89	0.94
iEF (%/m^2)	11.21	40.63	23.91	9.11
iAorta (mm/m^2)	10.32	21.28	16.65	2.25
LVMi (g/m^2)	36.97	240.53	87.57	32.70
RWTi	0.11	0.40	0.20	0.06

Abbreviations: see 'List of Abbreviations'. Data presented as mean ± standard deviation

Table 4.16: Indexed Echocardiographic Parameters in Total Study Participants (Based on Gender)						
Parameter	**Gender**	**n**	**Mean**	**SD**	**S.E.**	**p-value**
iRAD (mm/m^2)	**Male**	44	17.76	3.30	0.50	0.017*
	Female	35	20.47	6.37	1.08	
iLAD (mm/m^2)	**Male**	44	21.63	4.37	0.66	0.032*
	Female	35	24.05	5.47	0.92	
iRVD (mm/m^2)	**Male**	44	13.10	4.74	0.72	0.354
	Female	35	14.30	6.70	1.13	
iTAPSE (mm/m^2)	**Male**	44	9.50	2.02	0.30	0.052
	Female	35	10.49	2.43	0.41	
iLVIDd (mm/m^2)	**Male**	44	29.35	4.62	0.70	0.426
	Female	35	30.26	5.53	0.93	
iLVIDs (mm/m^2)	**Male**	44	21.98	5.88	0.89	0.871
	Female	35	22.19	5.49	0.93	
IVSdi (mm/m^2)	**Male**	44	4.73	1.09	0.16	0.006**
	Female	35	5.43	1.10	0.19	
PWdi (mm/m^2)	**Male**	44	4.67	0.81	0.12	0.018*
	Female	35	5.17	1.03	0.17	
iEF (%/m^2)	**Male**	44	21.26	8.31	1.25	0.003**
	Female	35	27.24	9.07	1.53	
LVMi (g/m^2)	**Male**	44	88.21	29.63	4.47	0.846
	Female	35	86.76	36.61	6.19	
RWTi	**Male**	44	0.18	0.05	0.01	0.002**
	Female	35	0.22	0.06	0.01	
iAorta (mm/m^2)	**Male**	44	16.75	2.30	0.35	0.666
	Female	35	16.53	2.22	0.37	

Abbreviations: see 'List of Abbreviations'; p-value ≤ 0.05: significant (*); p-value ≤ 0.01: highly significant (**); Test applied: ANOVA

Table 4.17: Indexed Echocardiographic Parameters in Total Study Participants (Based on Heart Size Determined on Echocardiography)						
Parameter	**Heart Size**	**n**	**Mean**	**SD**	**S.E.**	**p-value**
iRAD (mm/m^2)	**Enlarged**	46	21.21	5.34	0.79	0.000**
	Normal	33	15.82	2.17	0.38	
iLAD (mm/m^2)	**Enlarged**	46	25.06	4.99	0.74	0.000**
	Normal	33	19.42	2.62	0.46	
iRVD (mm/m^2)	**Enlarged**	46	15.12	6.99	1.03	0.005**
	Normal	33	11.56	1.58	0.28	
iTAPSE (mm/m^2)	**Enlarged**	46	9.42	2.56	0.38	0.016*
	Normal	33	10.65	1.51	0.26	
iLVIDd (mm/m^2)	**Enlarged**	46	31.86	5.02	0.74	0.000**
	Normal	33	26.80	3.29	0.57	
iLVIDs (mm/m^2)	**Enlarged**	46	24.91	5.39	0.79	0.000**
	Normal	33	18.12	3.14	0.55	
IVSdi (mm/m^2)	**Enlarged**	46	4.98	1.28	0.19	0.575
	Normal	33	5.12	0.93	0.16	
PWdi (mm/m^2)	**Enlarged**	46	4.82	0.97	0.14	0.410
	Normal	33	5.00	0.91	0.16	
iEF (%/m^2)	**Enlarged**	46	21.30	8.81	1.30	0.002**
	Normal	33	27.55	8.34	1.45	
LVMi (g/m^2)	**Enlarged**	46	97.18	36.66	5.40	0.002**
	Normal	33	74.17	19.95	3.47	
RWTi	**Enlarged**	46	0.19	0.05	0.01	0.002**
	Normal	33	0.23	0.06	0.01	
iAorta (mm/m^2)	**Enlarged**	46	16.62	2.37	0.35	0.868
	Normal	33	16.70	2.11	0.37	

Abbreviations: see ‘List of Abbreviations’; p-value ≤ 0.05: significant (*); p-value ≤ 0.01: highly significant (**); Test applied: ANOVA

Table 4.18: Comparison of Chest X-ray (PA View) and Echocardiography Findings					
		Echocardiography		Total	p-value
		Enlarged Heart	Normal Sized Heart		
Chest X-ray (PA View)	Enlarged Heart	25	3	28	0.000**
		31.6%	3.8%	35.4%	
	Normal Sized Heart	21	30	51	
		26.6%	38.0%	64.6%	
Total		46	33	79	
		58.2%	41.8%	100.0%	

p-value ≤ 0.05: significant (*); p-value ≤ 0.01: highly significant (**); Test applied: Pearson's Chi-square

Table 4.19 (A): Comparison of Chest X-ray (PA View) and Echocardiography Findings	
	n (%)
True Positive (**TP**) or **Group A**	25 (31.6%)
False Positive (**FP**) or **Group B**	3 (3.8%)
False Negative (**FN**) or **Group C**	21 (26.6%)
True negative (**TN**) or **Group D**	30 (38.0%)

Data presented as numbers and percentages

Table 4.19 (B): Comparison of Chest X-ray (PA View) and Echocardiography Findings	
	Percentage
Sensitivity **[TP/(TP + FN)]**	54%
Specificity **[TN/(TN + FP)]**	91%
Prevalence (of Cardiomegaly) **[(TP+FN)/ Total No. of Subjects]**	58.2%
Positive Predictive Value (PPV) **[TP/(TP+FP)]**	89%
Negative Predictive Value (NPV) **[TN/(TN+FN)]**	59%
False Positive Rate **[FP/(FP+TN)]**	9.1%
False Negative Rate **[FN/(FN+TP)]**	45.7%
Probability of Positive Test **[(TP+FP)/ Total No. of Subjects]**	35.4%
Probability of Negative Test **[(TN+FN)/ Total No. of Subjects]**	64.6%
Accuracy (of Chest X-ray (PA view)) **[(TP+TN)/ (TP+FP+FN+TP)]**	69.6%

Data presented as percentages

Table 4.19 (C): Comparison of Chest X-ray (PA View) and Echocardiography Findings		
		Ratio
Positive Likelihood Ratio	**[Sensitivity/ (1-Specificity)]**	5.98
Negative Likelihood Ratio	**[(1-Sensitivity)/ Specificity]**	0.50

Data presented as ratios

Table 4.20: Gender Distribution in Group A, B, C and D				
Groups		**Gender**		**Total**
		Male	**Female**	
A	Count	16	9	25
	% of Total	20.3%	11.4%	31.6%
B	Count	2	1	3
	% of Total	2.5%	1.3%	3.8%
C	Count	10	11	21
	% of Total	12.7%	13.9%	26.6%
D	Count	16	14	30
	% of Total	20.3%	17.7%	38.0%
Total	Count	44	35	79
	% of Total	55.7%	44.3%	100.0%

Data presented as numbers and percentages

Table. 4.21. Ethnic distribution in the Group A, B, C, and D										
Ethnicity	**Males**				**Total**	**Females**				**Total**
	A	**B**	**C**	**D**		**A**	**B**	**C**	**D**	
Baloch	2	1	0	2	5	1	0	1	2	4
	4.5%	2.3%	0.0%	4.5%	11.4%	2.9%	0.0%	2.9%	5.7%	11.4%
Pashtun	7	0	3	6	16	0	0	3	3	6
	15.9%	0.0%	6.8%	13.6%	36.4%	0.0%	0.0%	8.6%	8.6%	17.1%
Punjabi	0	0	1	0	1	1	0	0	0	1
	0.0%	0.0%	2.3%	0.0%	2.3%	2.9%	0.0%	0.0%	0.0%	2.9%
Saraiki	1	0	0	1	2	0	0	0	0	0
	2.3%	0.0%	0.0%	2.3%	4.5%	0.0%	0.0%	0.0%	0.0%	0.0%
Sindhi	4	0	1	2	7	5	0	5	1	11
	9.1%	0.0%	2.3%	4.5%	15.9%	14.3%	0.0%	14.3%	2.9%	31.4%
Urdu Speaking	2	1	5	5	13	2	1	2	8	13
	4.5%	2.3%	11.4%	11.4%	29.5%	5.7%	2.9%	5.7%	22.9%	37.1%
Total	16	2	10	16	44	9	1	11	14	35
	36.4%	4.5%	22.7%	36.4%	100.0%	25.7%	2.9%	31.4%	40.0%	100.0%

Data presented as numbers and percentages

Table. 4.22: Measurement of Radiological Parameters in the Four Groups (A, B, C, and D)				
TTD (cm)				
Groups	**n**	**Mean**	**SD**	**p-value**
A	25	27.27	2.74	0.597
B	3	29.62	7.24	
C	21	27.73	3.00	
D	30	27.03	3.65	
Total	79	27.39	3.34	
TRD (cm)				
Groups	**n**	**Mean**	**SD**	**p-value**
A	25	5.51	1.13	0.000**
B	3	5.44	0.80	
C	21	4.38	1.08	
D	30	4.38	1.02	
Total	79	4.78	1.17	
TLD (cm)				
Groups	**n**	**Mean**	**SD**	**p-value**
A	25	10.45	1.67	0.000**
B	3	10.09	2.96	
C	21	8.88	1.04	
D	30	8.12	1.23	
Total	79	9.14	1.71	
TCD (cm)				
Groups	**n**	**Mean**	**SD**	**p-value**
A	25	15.97	2.06	0.000**
B	3	15.53	3.76	
C	21	13.26	1.34	
D	30	12.51	1.89	
Total	79	13.92	2.41	
CTR				
Groups	**n**	**Mean**	**SD**	**p-value**
A	25	0.59	0.06	0.000**
B	3	0.52	0.01	
C	21	0.48	0.02	
D	30	0.46	0.02	
Total	79	0.51	0.07	

Abbreviations: see ‘List of Abbreviations’; p-value ≤ 0.05: significant (*); p-value ≤ 0.01: highly significant (**); Test applied: ANOVA

Table. 4.23: Radiological Measurements in Males of Group A, B, C and D						
Groups		**TTD (cm)**	**TRD (cm)**	**TLD (cm)**	**TCD (cm)**	**CTR**
A	Mean	28.47	5.64	10.74	16.38	0.58
	SD	2.12	1.17	1.69	2.00	0.06
	Minimum	24.08	4.06	8.54	13.19	0.52
	Maximum	31.37	8.59	14.20	19.66	0.68
B	Mean	33.21	5.84	11.51	17.35	0.52
	SD	5.22	0.57	2.32	2.89	0.01
	Minimum	29.52	5.44	9.87	15.31	0.52
	Maximum	36.90	6.25	13.15	19.40	0.53
C	Mean	29.37	5.01	9.13	14.13	0.48
	SD	1.81	0.99	0.95	0.70	0.02
	Minimum	26.59	3.80	7.00	13.19	0.45
	Maximum	32.54	6.75	10.24	15.69	0.50
D	Mean	29.40	4.79	8.82	13.61	0.46
	SD	3.14	1.21	1.15	1.79	0.02
	Minimum	24.10	2.80	6.75	10.60	0.43
	Maximum	35.35	6.84	10.59	16.95	0.49
Total	Mean	29.23	5.20	9.71	14.91	0.51
	SD	2.70	1.17	1.64	2.16	0.06
	Minimum	24.08	2.80	6.75	10.60	0.43
	Maximum	36.90	8.59	14.20	19.66	0.68
p-value		0.123	0.159	0.001**	0.000**	0.000**

Abbreviations: see ‘List of Abbreviations’; p-value ≤ 0.05: significant (*); p-value ≤ 0.01: highly significant (**); Test applied: ANOVA

Table 4.24 : Radiological Measurements in Females of Group A, B, C and D						
Groups		**TTD (cm)**	**TRD (cm)**	**TLD (cm)**	**TCD (cm)**	**CTR**
A	Mean	25.15	5.28	9.94	15.22	0.61
	SD	2.49	1.08	1.60	2.07	0.06
	Minimum	22.23	3.63	6.75	11.76	0.51
	Maximum	30.60	7.67	11.78	19.45	0.72
B	Mean	22.43	4.64	7.24	11.88	0.53
	SD	[a]	[a]	[a]	[a]	[a]
	Minimum	22.43	4.64	7.24	11.88	0.53
	Maximum	22.43	4.64	7.24	11.88	0.53
C	Mean	26.25	3.82	8.65	12.46	0.48
	SD	3.15	0.83	1.10	1.30	0.02
	Minimum	22.73	2.31	6.75	10.60	0.44
	Maximum	32.13	5.23	10.33	14.60	0.50
D	Mean	24.33	3.92	7.33	11.25	0.46
	SD	1.88	0.46	0.75	1.05	0.02
	Minimum	21.44	3.20	6.54	10.03	0.44
	Maximum	27.67	4.87	8.91	13.78	0.50
Total	Mean	25.09	4.26	8.41	12.67	0.51
	SD	2.57	0.98	1.53	2.12	0.07
	Minimum	21.44	2.31	6.54	10.03	0.44
	Maximum	32.13	7.67	11.78	19.45	0.72
p-value		0.212	0.001**	0.000**	0.000**	0.000**

Abbreviations: see 'List of Abbreviations'; p-value ≤ 0.05: significant (*); p-value ≤ 0.01: highly significant (**); Test applied: ANOVA; [a]: not computed due to a single value

Table. 4.25: Measurement of Echocardiographic Parameters in the Four Groups (A, B, C, And D)						
	RAD (mm)			**LAD (mm)**		
	Mean	**SD**	**p-value**	**Mean**	**SD**	**p-value**
A	37.36	8.69	0.000**	42.95	7.74	0.000**
B	28.33	2.08		34.67	3.51	
C	33.10	5.97		40.81	7.57	
D	26.47	3.67		32.43	3.82	
Total	31.75	7.70		38.07	7.82	
	RVD (mm)			**TAPSE (mm)**		
	Mean	**SD**	**p-value**	**Mean**	**SD**	**p-value**
A	27.84	12.63	0.003**	15.44	4.57	0.049*
B	19.33	0.58		17.00	2.00	
C	22.19	7.81		16.19	3.34	
D	19.40	2.18		17.93	1.81	
Total	22.81	8.93		16.65	3.43	
	Aorta (mm)			**PASP (mmHg)**		
	Mean	**SD**	**p-value**	**Mean**	**SD**	**p-value**
A	28.93	4.93	0.379	18.20	45.24	0.001**
B	29.00	2.65		21.21	40.00	
C	26.91	3.70		16.53	40.29	
D	28.00	3.33		5.02	27.80	
Total	28.04	3.99		15.71	37.08	
	LVId (mm)			**LVIDs (mm)**		
	Mean	**SD**	**p-value**	**Mean**	**SD**	**p-value**
A	58.60	8.65	0.000**	46.96	7.55	0.000**
B	45.33	3.51		30.00	2.00	
C	48.00	6.85		36.33	9.65	
D	45.07	5.40		30.47	4.93	
Total	50.14	9.01		37.23	10.04	

Abbreviations: see ‘List of Abbreviations’; p-value ≤ 0.05: significant (*); p-value ≤ 0.01: highly significant (**); Test applied: ANOVA

Table. 4.25 (Continued): Echocardiographic Parameter Measurements in the Four Groups (A, B, C, And D)

	IVSd (mm)			PWd (mm)		
	Mean	**SD**	**p-value**	**Mean**	**SD**	**p-value**
A	8.02	1.60	0.494	8.05	1.25	0.804
B	8.00	1.73		8.00	1.00	
C	8.71	2.49		8.12	1.82	
D	8.60	1.13		8.40	1.28	
Total	8.42	1.74		8.20	1.41	
	LV Mass (g)			**RWT**		
	Mean	**SD**	**p-value**	**Mean**	**SD**	**p-value**
A	184.46	62.92	0.000**	0.28	0.05	0.000**
B	114.35	12.06		0.36	0.07	
C	140.90	56.79		0.34	0.09	
D	125.51	35.02		0.38	0.08	
Total	147.84	56.41		0.34	0.08	
	EF (%)					
	Mean		**SD**	**p-value**		
A	31.76		11.23	0.000**		
B	31.67		5.77			
C	39.52		14.40			
D	47.50		12.37			
Total	39.80		13.99			

Abbreviations: see ‘List of Abbreviations’; p-value ≤ 0.05: significant (*); p-value ≤ 0.01: highly significant (**); Test applied: ANOVA

Table 4.26: Echocardiographic Measurements in Males of Group A, B, C and D							
Groups		**RAD (mm)**	**LAD (mm)**	**RVD (mm)**	**TAPSE (mm)**	**LVIDd (mm)**	**LVIDs (mm)**
A	**Mean**	34.31	42.74	26.75	15.06	60.93	49.57
	SD	4.54	7.05	9.81	3.86	3.88	5.47
	Minimum	28.00	32.00	16.00	10.00	57.00	42.00
	Maximum	42.00	57.00	50.00	22.00	69.00	62.00
B	**Mean**	27.50	33.00	19.50	17.00	47.00	30.00
	SD	2.12	2.83	0.71	2.83	2.83	2.83
	Minimum	26.00	31.00	19.00	15.00	45.00	28.00
	Maximum	29.00	35.00	20.00	19.00	49.00	32.00
C	**Mean**	33.30	40.40	22.80	17.30	49.40	37.60
	SD	6.62	8.13	8.20	3.16	7.62	10.66
	Minimum	24.00	30.00	19.00	11.00	33.00	21.00
	Maximum	42.00	51.00	46.00	21.00	56.00	50.00
D	**Mean**	27.75	33.06	19.94	18.00	45.38	30.38
	SD	3.32	3.68	2.08	1.26	4.96	4.43
	Minimum	23.00	28.00	16.00	15.00	40.00	20.00
	Maximum	34.00	39.00	23.00	20.00	54.00	38.00
Total	**Mean**	31.39	38.25	23.05	16.73	52.02	38.98
	SD	5.47	7.48	7.65	3.12	8.66	10.71
	Minimum	23.00	28.00	16.00	10.00	33.00	20.00
	Maximum	42.00	57.00	50.00	22.00	69.00	62.00
p-value		0.001**	0.000**	0.071	0.050*	0.000**	0.000**

Abbreviations: see 'List of Abbreviations'; p-value ≤ 0.05: significant (*); p-value ≤ 0.01: highly significant (**); Test applied: ANOVA

Table 4.26 (Continued): Echocardiographic Measurements in Males of Group A, B, C and D								
Groups		**IVSd (mm)**	**PWd (mm)**	**EF (%)**	**LVM (g)**	**RWT**	**Aorta (mm)**	**PASP (mm Hg)**
A	**Mean**	7.84	8.45	29.06	196.68	0.28	30.52	38.93
	SD	1.60	1.23	8.41	40.06	0.04	4.32	10.59
	Minimum	5.00	7.00	20.00	140.27	0.21	23.00	25.00
	Maximum	10.00	10.20	55.00	275.16	0.35	37.00	60.00
B	**Mean**	7.00	7.50	30.00	107.63	0.32	30.50	25.00
	SD	0.00	0.71	7.07	4.43	0.05	0.71	[a]
	Minimum	7.00	7.00	25.00	104.50	0.29	30.00	25.00
	Maximum	7.00	8.00	35.00	110.76	0.36	31.00	25.00
C	**Mean**	9.40	7.86	37.50	152.75	0.33	29.00	40.71
	SD	2.88	1.50	14.95	59.58	0.08	3.56	22.99
	Minimum	7.00	5.00	20.00	62.71	0.19	24.00	25.00
	Maximum	17.00	10.00	60.00	272.40	0.48	36.00	90.00
D	**Mean**	8.38	8.38	46.25	125.32	0.37	28.94	27.86
	SD	1.15	1.26	11.62	39.64	0.06	3.11	5.08
	Minimum	7.00	7.00	30.00	78.36	0.27	23.00	20.00
	Maximum	11.00	11.00	60.00	234.82	0.45	34.00	40.00
Total	**Mean**	8.35	8.25	37.27	156.70	0.33	29.60	34.58
	SD	1.88	1.28	13.31	54.11	0.07	3.63	13.33
	Minimum	5.00	5.00	20.00	62.71	0.19	23.00	20.00
	Maximum	17.00	11.00	60.00	275.16	0.48	37.00	90.00
p-value		0.145	0.556	0.001**	0.000**	0.000**	0.596	0.063

Abbreviations: see 'List of Abbreviations'; p-value ≤ 0.05: significant (*); p-value ≤ 0.01: highly significant (**); Test applied: ANOVA; [a]: not computed due to a single value

Table 4.27: Echocardiographic Measurements in Females of Group A, B, C and D							
Groups		**RAD (mm)**	**LAD (mm)**	**RVD (mm)**	**TAPSE (mm)**	**LVIDd (mm)**	**LVIDs (mm)**
A	**Mean**	42.78	43.33	29.78	16.11	54.44	42.33
	SD	11.67	9.29	17.09	5.84	12.89	8.80
	Minimum	28.00	32.00	17.00	9.00	34.00	26.00
	Maximum	60.00	61.00	66.00	26.00	80.00	50.00
B	**Mean**	30.00	38.00	19.00	17.00	42.00	30.00
	SD	[a]	[a]	[a]	[a]	[a]	[a]
	Minimum	30.00	38.00	19.00	17.00	42.00	30.00
	Maximum	30.00	38.00	19.00	17.00	42.00	30.00
C	**Mean**	32.91	41.18	21.64	15.18	46.73	35.18
	SD	5.63	7.41	7.79	3.31	6.15	9.00
	Minimum	22.00	28.00	15.00	10.00	37.00	25.00
	Maximum	42.00	56.00	42.00	22.00	57.00	48.00
D	**Mean**	25.00	31.71	18.79	17.86	44.71	30.57
	SD	3.62	3.99	2.19	2.35	6.03	5.61
	Minimum	21.00	26.00	16.00	11.00	35.00	22.00
	Maximum	33.00	40.00	23.00	20.00	54.00	40.00
Total	**Mean**	32.20	37.86	22.51	16.54	47.77	35.03
	SD	9.88	8.34	10.42	3.84	9.00	8.78
	Minimum	21.00	26.00	15.00	9.00	34.00	22.00
	Maximum	60.00	61.00	66.00	26.00	80.00	50.00
p-value		0.000**	0.001**	0.089	0.382	0.060	0.011*

Abbreviations: see 'List of Abbreviations'; p-value ≤ 0.05: significant (*); p-value ≤ 0.01: highly significant (**); Test applied: ANOVA; [a]: not computed due to a single value

Table 4.27 (Continued): Echocardiographic Measurements in Females of Group A, B, C and D								
Groups		**IVSd (mm)**	**PWd (mm)**	**EF (%)**	**LVM (g)**	**RWT**	**Aorta (mm)**	**PASP (mm Hg)**
A	**Mean**	8.33	7.33	36.56	162.74	0.28	26.11	57.86
	SD	1.66	1.00	14.34	89.65	0.07	4.88	24.13
	Minimum	5.00	6.00	20.00	65.78	0.23	16.00	35.00
	Maximum	11.00	9.00	64.00	381.90	0.41	30.00	105.00
B	**Mean**	10.00	9.00	35.00	127.81	0.43	26.00	55.00
	SD	[a]	[a]	[a]	[a]	[a]	[a]	[a]
	Minimum	10.00	9.00	35.00	127.81	0.43	26.00	55.00
	Maximum	10.00	9.00	35.00	127.81	0.43	26.00	55.00
C	**Mean**	8.09	8.36	41.36	130.13	0.36	25.00	40.00
	SD	2.02	2.11	14.33	54.66	0.09	2.76	11.55
	Minimum	5.00	5.00	25.00	68.82	0.20	21.00	25.00
	Maximum	12.00	13.00	60.00	247.60	0.52	30.00	65.00
D	**Mean**	8.86	8.43	48.93	125.73	0.39	26.93	27.73
	SD	1.10	1.34	13.47	30.36	0.10	3.36	5.18
	Minimum	8.00	7.00	25.00	78.77	0.26	20.00	20.00
	Maximum	11.00	11.00	60.00	168.92	0.63	32.00	35.00
Total	**Mean**	8.51	8.14	42.97	136.69	0.35	26.09	40.17
	SD	1.58	1.57	14.37	58.03	0.10	3.58	18.00
	Minimum	5.00	5.00	20.00	65.78	0.20	16.00	20.00
	Maximum	12.00	13.00	64.00	381.90	0.63	32.00	105.00
p-value		0.501	0.352	0.201	0.497	0.045*	0.637	0.002**

Abbreviations: see 'List of Abbreviations'; p-value ≤ 0.05: significant (*); p-value ≤ 0.01: highly significant (**); Test applied: ANOVA, [a]: not computed due to a single value

Table 4.28: Correlation of Radiological & Echocardiographic Parameters (A)

		TTD (cm)	TRD (cm)	TLD (cm)	TCD (cm)	CTR
LVIDd (mm)	Pearson Correlation	.248	-.058	.396*	.290	.107
	Sig. (2-tailed)	.232	.782	.050	.160	.610
LVIDs (mm)	Pearson Correlation	.421*	.029	.542**	.457*	.132
	Sig. (2-tailed)	.036	.891	.005	.022	.528
IVSd (mm)	Pearson Correlation	-.124	.370	-.478*	-.185	-.090
	Sig. (2-tailed)	.553	.068	.016	.376	.670
EF (%)	Pearson Correlation	-.355	.035	-.594**	-.464*	-.238
	Sig. (2-tailed)	.082	.868	.002	.020	.253
PWd (mm)	Pearson Correlation	.169	.009	-.172	-.135	-.338
	Sig. (2-tailed)	.420	.966	.412	.521	.098
LVM (g)	Pearson Correlation	.112	.106	.070	.115	.042
	Sig. (2-tailed)	.593	.615	.741	.585	.842
RWT	Pearson Correlation	-.197	.028	-.485*	-.379	-.258
	Sig. (2-tailed)	.345	.895	.014	.062	.213

Abbreviations: see 'List of Abbreviations'; *: Correlation is significant at the 0.05 level (2-tailed); **: Correlation is highly significant at the 0.01 level (2-tailed)

Table 4.29: Correlation of Radiological & Echocardiographic Parameters (A)

		TTD (cm)	TRD (cm)	TLD (cm)	TCD(cm)	CTR
RAD (mm)	Pearson Correlation	-.141	.354	-.011	.185	.363
	Sig. (2-tailed)	.502	.083	.959	.375	.074
LAD (mm)	Pearson Correlation	.077	.331	.063	.233	.169
	Sig. (2-tailed)	.714	.107	.765	.263	.418
RVD (mm)	Pearson Correlation	-.086	.281	.171	.294	.493*
	Sig. (2-tailed)	.684	.173	.413	.154	.012
TAPSE (mm)	Pearson Correlation	-.157	-.246	-.105	-.220	-.067
	Sig. (2-tailed)	.453	.236	.617	.290	.750
Aorta (mm)	Pearson Correlation	.484*	.221	.269	.340	-.072
	Sig. (2-tailed)	.014	.289	.193	.096	.734
PASP (mm Hg)	Pearson Correlation	-.016	.320	.318	.407	.537*
	Sig. (2-tailed)	.947	.158	.160	.067	.012

Abbreviations: see 'List of Abbreviations'; *: Correlation is significant at the 0.05 level (2-tailed); **: Correlation is highly significant at the 0.01 level (2-tailed)

Table 4.30: Correlation of Radiological & Echocardiographic Parameters (B)

		TTD (cm)	TRD (cm)	TLD (cm)	TCD (cm)	CTR
LVIDd (mm)	Pearson Correlation	.997*	.997*	1.000*	1.000*	-.272
	Sig. (2-tailed)	.045	.049	.012	.020	.824
LVIDs (mm)	Pearson Correlation	.510	.505	.554	.543	.636
	Sig. (2-tailed)	.659	.663	.627	.634	.561
IVSd (mm)	Pearson Correlation	-.860	-.863	-.833	-.839	.772
	Sig. (2-tailed)	.341	.337	.373	.366	.439
EF (%)	Pearson Correlation	-.872	-.869	-.896	-.890	-.165
	Sig. (2-tailed)	.326	.329	.293	.301	.895
PWd (mm)	Pearson Correlation	-1.000**	-1.000**	-.998*	-.999*	.351
	Sig. (2-tailed)	.007	.004	.040	.032	.772
LVM (g)	Pearson Correlation	-.699	-.702	-.661	-.670	.910
	Sig. (2-tailed)	.508	.504	.540	.533	.272
RWT	Pearson Correlation	-1.000*	-1.000*	-.997*	-.998*	.363
	Sig. (2-tailed)	.015	.012	.048	.041	.764

Abbreviations: see 'List of Abbreviations'; *: Correlation is significant at the 0.05 level (2-tailed); **: Correlation is highly significant at the 0.01 level (2-tailed)

Table 4.31: Correlation of Radiological & Echocardiographic Parameters (B)

		TTD (cm)	TRD (cm)	TLD (cm)	TCD (cm)	CTR
RAD (mm)	Pearson Correlation	-.229	-.234	-.179	-.191	.993
	Sig. (2-tailed)	.853	.849	.886	.878	.074
LAD (mm)	Pearson Correlation	-.417	-.422	-.369	-.381	.997
	Sig. (2-tailed)	.726	.723	.759	.751	.053
RVD (mm)	Pearson Correlation	-.011	-.006	-.063	-.051	-.937
	Sig. (2-tailed)	.993	.996	.960	.968	.228
TAPSE (mm)	Pearson Correlation	-.510	-.505	-.554	-.543	-.636
	Sig. (2-tailed)	.659	.663	.627	.634	.561
Aorta (mm)	Pearson Correlation	.748	.752	.713	.722	-.878
	Sig. (2-tailed)	.462	.458	.494	.487	.318
PASP (mm Hg)	Pearson Correlation	-.947	-.945	-.962	-.959	.019
	Sig. (2-tailed)	.209	.212	.176	.183	.988

Abbreviations: see 'List of Abbreviations'; *: Correlation is significant at the 0.05 level (2-tailed); **: Correlation is highly significant at the 0.01 level (2-tailed)

Table 4.32: Correlation of Radiological & Echocardiographic Parameters (C)

		TTD (cm)	TRD (cm)	TLD (cm)	TCD (cm)	CTR
LVIDd (mm)	Pearson Correlation	.089	-.160	.347	.139	.142
	Sig. (2-tailed)	.700	.487	.123	.547	.540
LVIDs (mm)	Pearson Correlation	.140	-.129	.349	.166	.069
	Sig. (2-tailed)	.546	.578	.121	.472	.766
IVSd (mm)	Pearson Correlation	.363	.286	.104	.310	-.169
	Sig. (2-tailed)	.106	.208	.654	.171	.465
EF (%)	Pearson Correlation	-.217	.295	-.543*	-.183	.095
	Sig. (2-tailed)	.345	.194	.011	.428	.682
PWd (mm)	Pearson Correlation	.141	.029	.215	.190	.102
	Sig. (2-tailed)	.541	.899	.350	.410	.659
LVM (g)	Pearson Correlation	.298	.080	.319	.311	.012
	Sig. (2-tailed)	.189	.730	.159	.170	.960
RWT	Pearson Correlation	.112	.171	-.008	.131	.011
	Sig. (2-tailed)	.630	.459	.972	.572	.964

Abbreviations: see 'List of Abbreviations'; *: Correlation is significant at the 0.05 level (2-tailed); **: Correlation is highly significant at the 0.01 level (2-tailed)

Table 4.33: Correlation of Radiological & Echocardiographic Parameters (C)

		TTD (cm)	TRD (cm)	TLD (cm)	TCD (cm)	CTR
RAD (mm)	Pearson Correlation	-.235	-.040	-.123	-.127	.231
	Sig. (2-tailed)	.306	.864	.597	.584	.313
LAD (mm)	Pearson Correlation	-.381	-.075	-.219	-.229	.396
	Sig. (2-tailed)	.088	.747	.341	.318	.075
RVD (mm)	Pearson Correlation	.151	.214	.100	.250	.219
	Sig. (2-tailed)	.513	.351	.666	.275	.339
TAPSE (mm)	Pearson Correlation	.154	.296	-.116	.148	-.054
	Sig. (2-tailed)	.506	.193	.618	.522	.816
Aorta (mm)	Pearson Correlation	.209	.319	.172	.389	.384
	Sig. (2-tailed)	.364	.159	.456	.081	.085
PASP (mm Hg)	Pearson Correlation	-.130	-.179	.194	.001	.340
	Sig. (2-tailed)	.619	.492	.456	.996	.182

Abbreviations: see 'List of Abbreviations'; *: Correlation is significant at the 0.05 level (2-tailed); **: Correlation is highly significant at the 0.01 level (2-tailed)

Table 4.34: Correlation of Radiological & Echocardiographic Parameters (D)

		TTD (cm)	TRD (cm)	TLD (cm)	TCD (cm)	CTR
LVIDd (mm)	Pearson Correlation	.093	.198	.003	.108	.100
	Sig. (2-tailed)	.625	.295	.989	.569	.597
LVIDs (mm)	Pearson Correlation	-.123	-.116	-.156	-.164	-.195
	Sig. (2-tailed)	.518	.542	.411	.387	.303
IVSd (mm)	Pearson Correlation	-.081	.050	-.022	.013	.339
	Sig. (2-tailed)	.670	.792	.909	.946	.067
EF (%)	Pearson Correlation	-.002	-.012	.035	.016	.047
	Sig. (2-tailed)	.992	.951	.855	.932	.807
PWd (mm)	Pearson Correlation	.029	.331	-.100	.114	.321
	Sig. (2-tailed)	.881	.074	.601	.550	.084
LVM (g)	Pearson Correlation	.053	.289	-.052	.121	.283
	Sig. (2-tailed)	.780	.122	.783	.523	.130
RWT	Pearson Correlation	-.053	.122	-.081	.013	.216
	Sig. (2-tailed)	.783	.522	.669	.948	.252

Abbreviations: see 'List of Abbreviations'; *: Correlation is significant at the 0.05 level (2-tailed); **: Correlation is highly significant at the 0.01 level (2-tailed)

Table 4.35: Correlation of Radiological & Echocardiographic Parameters (D)

		TTD (cm)	TRD (cm)	TLD (cm)	TCD (cm)	CTR
RAD (mm)	Pearson Correlation	.553**	.342	.428*	.462*	-.168
	Sig. (2-tailed)	.002	.064	.018	.010	.374
LAD (mm)	Pearson Correlation	.436*	.293	.321	.367*	-.131
	Sig. (2-tailed)	.016	.115	.083	.046	.492
RVD (mm)	Pearson Correlation	.021	-.230	.157	-.022	-.143
	Sig. (2-tailed)	.912	.221	.407	.910	.450
TAPSE (mm)	Pearson Correlation	-.005	.065	-.054	.000	.000
	Sig. (2-tailed)	.979	.732	.779	.999	.999
Aorta (mm)	Pearson Correlation	.348	.156	.372*	.326	.054
	Sig. (2-tailed)	.060	.412	.043	.079	.775
PASP (mm Hg)	Pearson Correlation	.125	.199	-.001	.105	-.048
	Sig. (2-tailed)	.551	.339	.998	.619	.821

Abbreviations: see 'List of Abbreviations'; *: Correlation is significant at the 0.05 level (2-tailed); **: Correlation is highly significant at the 0.01 level (2-tailed)

Table 4.36: Correlation of Radiological & Indexed Echocardiographic Parameters (A)

		TTD (cm)	TRD (cm)	TLD (cm)	TCD (cm)	CTR
iRAD	Pearson Correlation	-.255	.308	-.099	.089	.360
(mm/m^2)	Sig. (2-tailed)	.219	.134	.636	.674	.077
iLAD	Pearson Correlation	-.122	.306	-.083	.101	.204
(mm/m^2)	Sig. (2-tailed)	.562	.137	.695	.631	.327
iRVD	Pearson Correlation	-.161	.272	.110	.239	.502*
(mm/m^2)	Sig. (2-tailed)	.443	.188	.599	.249	.010
iTAPSE	Pearson Correlation	-.283	-.231	-.172	-.266	.001
(mm/m^2)	Sig. (2-tailed)	.170	.267	.411	.198	.996
iAorta	Pearson Correlation	.318	.233	.160	.259	-.009
(mm/m^2)	Sig. (2-tailed)	.121	.261	.444	.212	.967

Abbreviations: see 'List of Abbreviations'; *: Correlation is significant at the 0.05 level (2-tailed); **: Correlation is highly significant at the 0.01 level (2-tailed)

Table. 4.37: Correlation of Radiological & Indexed Echocardiographic Parameters (A)

		TTD (cm)	TRD (cm)	TLD (cm)	TCD (cm)	CTR
iLVIDd	Pearson Correlation	.021	-.074	.261	.172	.188
(mm/m^2)	Sig. (2-tailed)	.922	.725	.207	.412	.367
iLVIDs	Pearson Correlation	.252	.034	.453*	.387	.213
(mm/m^2)	Sig. (2-tailed)	.224	.872	.023	.056	.306
iEF	Pearson Correlation	-.423*	.034	-.599**	-.468*	-.173
($\%/m^2$)	Sig. (2-tailed)	.035	.871	.002	.018	.407
IVSdi	Pearson Correlation	-.272	.317	-.506**	-.237	-.008
(mm/m^2)	Sig. (2-tailed)	.188	.123	.010	.254	.970
PWdi	Pearson Correlation	-.066	.003	-.337	-.272	-.271
(mm/m^2)	Sig. (2-tailed)	.752	.988	.100	.189	.189
LVMi	Pearson Correlation	.012	.086	.015	.060	.076
(g/m^2)	Sig. (2-tailed)	.955	.683	.942	.777	.720
RWTi	Pearson Correlation	-.359	.031	-.535**	-.418*	-.144
	Sig. (2-tailed)	.078	.882	.006	.038	.493

Abbreviations: see 'List of Abbreviations'; *: Correlation is significant at the 0.05 level (2-tailed); **: Correlation is highly significant at the 0.01 level (2-tailed)

Table 4.38: Correlation of Radiological & Indexed Echocardiographic Parameters (B)

		TTD (cm)	TRD (cm)	TLD (cm)	TCD (cm)	CTR
iRAD (mm/m^2)	Pearson Correlation	-.872	-.874	-.845	-.851	.757
	Sig. (2-tailed)	.326	.323	.359	.351	.453
iLAD (mm/m^2)	Pearson Correlation	-.858	-.860	-.830	-.837	.775
	Sig. (2-tailed)	.344	.341	.377	.369	.435
iRVD (mm/m^2)	Pearson Correlation	-.998*	-.997*	-1.000**	-1.000*	.276
	Sig. (2-tailed)	.043	.046	.010	.018	.822
iTAPSE (mm/m^2)	Pearson Correlation	-.932	-.930	-.950	-.946	-.023
	Sig. (2-tailed)	.236	.239	.203	.211	.985
iAorta (mm/m^2)	Pearson Correlation	-.830	-.827	-.858	-.852	-.242
	Sig. (2-tailed)	.376	.380	.343	.351	.845

Abbreviations: see 'List of Abbreviations'; *: Correlation is significant at the 0.05 level (2-tailed); **: Correlation is highly significant at the 0.01 level (2-tailed)

Table 4.39: Correlation of Radiological & Indexed Echocardiographic Parameters (B)

		TTD (cm)	TRD (cm)	TLD (cm)	TCD (cm)	CTR
iLVIDd (mm/m^2)	Pearson Correlation	-.957	-.959	-.941	-.945	.597
	Sig. (2-tailed)	.186	.183	.219	.212	.593
iLVIDs (mm/m^2)	Pearson Correlation	-.833	-.836	-.804	-.811	.803
	Sig. (2-tailed)	.373	.370	.406	.398	.406
iEF ($\%/m^2$)	Pearson Correlation	-.983	-.982	-.991	-.989	.160
	Sig. (2-tailed)	.118	.122	.085	.093	.897
IVSdi (mm/m^2)	Pearson Correlation	-.919	-.921	-.898	-.903	.683
	Sig. (2-tailed)	.257	.254	.290	.283	.522
PWdi (mm/m^2)	Pearson Correlation	-.993	-.994	-.986	-.988	.449
	Sig. (2-tailed)	.075	.072	.108	.101	.704
LVMi (g/m^2)	Pearson Correlation	-.910	-.912	-.888	-.893	.699
	Sig. (2-tailed)	.272	.269	.305	.297	.507
RWTi	Pearson Correlation	-.993	-.993	-.985	-.987	.450
	Sig. (2-tailed)	.076	.073	.109	.101	.703

Abbreviations: see 'List of Abbreviations'; *: Correlation is significant at the 0.05 level (2-tailed); **: Correlation is highly significant at the 0.01 level (2-tailed)

Table 4.40: Correlation of Radiological & Indexed Echocardiographic Parameters (C)

		TTD (cm)	TRD (cm)	TLD (cm)	TCD (cm)	CTR
iRAD (mm/m^2)	Pearson Correlation	-.367	-.199	-.140	-.268	.239
	Sig. (2-tailed)	.102	.387	.545	.240	.297
iLAD (mm/m^2)	Pearson Correlation	-.493*	-.231	-.215	-.352	.390
	Sig. (2-tailed)	.023	.314	.350	.118	.081
iRVD (mm/m^2)	Pearson Correlation	.058	.115	.089	.161	.242
	Sig. (2-tailed)	.803	.621	.702	.487	.291
iTAPSE (mm/m^2)	Pearson Correlation	-.027	.120	-.146	-.016	.006
	Sig. (2-tailed)	.908	.604	.528	.944	.980
iAorta (mm/m^2)	Pearson Correlation	-.054	.105	.122	.179	.543*
	Sig. (2-tailed)	.817	.649	.597	.437	.011

Abbreviations: see 'List of Abbreviations'; *: Correlation is significant at the 0.05 level (2-tailed); **: Correlation is highly significant at the 0.01 level (2-tailed)

Table 4.41: Correlation of Radiological & Indexed Echocardiographic Parameters (C)

		TTD (cm)	TRD (cm)	TLD (cm)	TCD (cm)	CTR
iLVIDd (mm/m^2)	Pearson Correlation	-.186	-.423	.295	-.112	.241
	Sig. (2-tailed)	.419	.056	.195	.629	.293
iLVIDs (mm/m^2)	Pearson Correlation	-.003	-.272	.323	.032	.111
	Sig. (2-tailed)	.990	.233	.153	.892	.631
iEF ($\%/m^2$)	Pearson Correlation	-.302	.167	-.514*	-.263	.118
	Sig. (2-tailed)	.183	.470	.017	.248	.611
IVSdi (mm/m^2)	Pearson Correlation	.242	.168	.092	.206	-.113
	Sig. (2-tailed)	.290	.466	.693	.370	.625
PWdi (mm/m^2)	Pearson Correlation	-.011	-.111	.168	.041	.131
	Sig. (2-tailed)	.962	.633	.467	.861	.572
LVMi (g/m^2)	Pearson Correlation	.217	-.006	.319	.242	.053
	Sig. (2-tailed)	.345	.979	.158	.291	.820
RWTi	Pearson Correlation	-.024	.026	-.029	-.002	.038
	Sig. (2-tailed)	.918	.912	.901	.995	.870

Abbreviations: see 'List of Abbreviations'; *: Correlation is significant at the 0.05 level (2-tailed); **: Correlation is highly significant at the 0.01 level (2-tailed)

Table 4.42: Correlation of Radiological & Indexed Echocardiographic Parameters (D)

		TTD (cm)	TRD (cm)	TLD (cm)	TCD (cm)	CTR
iRAD (mm/m^2)	Pearson Correlation	.120	.085	-.032	.025	-.369*
	Sig. (2-tailed)	.528	.656	.867	.896	.045
iLAD (mm/m^2)	Pearson Correlation	-.073	-.009	-.204	-.137	-.321
	Sig. (2-tailed)	.700	.961	.281	.469	.084
iRVD (mm/m^2)	Pearson Correlation	-.395*	-.430*	-.299	-.426*	-.273
	Sig. (2-tailed)	.031	.018	.109	.019	.145
iTAPSE (mm/m^2)	Pearson Correlation	-.407*	-.194	-.456*	-.401*	-.159
	Sig. (2-tailed)	.026	.305	.011	.028	.402
iAorta (mm/m^2)	Pearson Correlation	-.143	-.133	-.135	-.159	-.122
	Sig. (2-tailed)	.450	.482	.478	.400	.521

Abbreviations: see 'List of Abbreviations'; *: Correlation is significant at the 0.05 level (2-tailed); **: Correlation is highly significant at the 0.01 level (2-tailed)

Table 4.43: Correlation of Radiological & Indexed Echocardiographic Parameters (D)

		TTD (cm)	TRD (cm)	TLD (cm)	TCD (cm)	CTR
iLVIDd (mm/m^2)	Pearson Correlation	-.370*	-.098	-.466**	-.356	-.095
	Sig. (2-tailed)	.044	.607	.009	.054	.618
iLVIDs (mm/m^2)	Pearson Correlation	-.429*	-.290	-.474**	-.464**	-.301
	Sig. (2-tailed)	.018	.121	.008	.010	.105
iEF ($\%/m^2$)	Pearson Correlation	-.193	-.118	-.173	-.176	-.034
	Sig. (2-tailed)	.307	.534	.362	.353	.857
IVSdi (mm/m^2)	Pearson Correlation	-.432*	-.176	-.392*	-.349	.149
	Sig. (2-tailed)	.017	.353	.032	.058	.431
PWdi (mm/m^2)	Pearson Correlation	-.301	.066	-.404*	-.227	.147
	Sig. (2-tailed)	.106	.728	.027	.228	.439
LVMi (g/m^2)	Pearson Correlation	-.175	.138	-.277	-.106	.194
	Sig. (2-tailed)	.354	.468	.139	.577	.305
RWTi	Pearson Correlation	-.276	-.046	-.296	-.217	.101
	Sig. (2-tailed)	.140	.808	.112	.248	.596

Abbreviations: see 'List of Abbreviations'; *: Correlation is significant at the 0.05 level (2-tailed); **: Correlation is highly significant at the 0.01 level (2-tailed)

Table 4.44: Right Ventricular Function in Total Study Participants of Group A, B, C and D							
RV Function		**Total Study Population**				**Total**	**p-value**
		A	**B**	**C**	**D**		
	Depressed	5	0	6	2	13	0.009**
		6.3%	0.0%	7.6%	2.5%	16.5%	
	Dysfunction (Systolic)	6	0	1	0	7	
		7.6%	0.0%	1.3%	0.0%	8.9%	
	Normal	14	3	14	28	59	
		17.7%	3.8%	17.7%	35.4%	74.7%	
Total		25	3	21	30	79	
		31.6%	3.8%	26.6%	38.0%	100.0%	

p-value ≤ 0.05: significant (*); p-value ≤ 0.01: highly significant (**); Test applied: Pearson's Chi-square

Table 4.45: Left Ventricular Function in Total Study Participants of Group A, B, C and D							
LV Function		**Total Study Population**				**Total**	**p-value**
		A	**B**	**C**	**D**		
	Dysfunction (Systolic & Diastolic)	11	0	5	3	19	0.010**
		13.9%	0.0%	6.3%	3.8%	24.1%	
	Dysfunction (Systolic Only)	11	3	9	12	35	
		13.9%	3.8%	11.4%	15.2%	44.3%	
	Normal	3	0	7	15	25	
		3.8%	0.0%	8.9%	19.0%	31.6%	
Total		25	3	21	30	79	
		31.6%	3.8%	26.6%	38.0%	100.0%	

p-value ≤ 0.05: significant (*); p-value ≤ 0.01: highly significant (**); Test applied: Pearson's Chi-square

Table 4.46: Right Ventricular (RV) Function in Males and Females of Group A, B, C and D								
			Groups				Total	p-value
			A	B	C	D		
Male	RV Function	Depressed	4	0	2	1	7	0.075
			9.1%	0.0%	4.5%	2.3%	15.9%	
		Dysfunction (Systolic)	4	0	0	0	4	
			9.1%	0.0%	0.0%	0.0%	9.1%	
		Normal	8	2	8	15	33	
			18.2%	4.5%	18.2%	34.1%	75.0%	
	Total		16	2	10	16	44	
			36.4%	4.5%	22.7%	36.4%	100.0%	
Female	RV Function	Depressed	1	0	4	1	6	0.225
			2.9%	0.0%	11.4%	2.9%	17.1%	
		Dysfunction (Systolic)	2	0	1	0	3	
			5.7%	0.0%	2.9%	0.0%	8.6%	
		Normal	6	1	6	13	26	
			17.1%	2.9%	17.1%	37.1%	74.3%	
	Total		9	1	11	14	35	
			25.7%	2.9%	31.4%	40.0%	100.0%	

p-value ≤ 0.05: significant (*); p-value ≤ 0.01: highly significant (**); Test applied: Pearson's Chi-square

Table 4.47: Left Ventricular (LV) Function in Males and Females of Group A, B, C and D								
			Groups				Total	p-value
			A	B	C	D		
Male	LV Function	Dysfunction (Systolic & Diastolic)	11	0	3	2	16	0.014*
			25.0%	0.0%	6.8%	4.5%	36.4%	
		Dysfunction (Systolic Only)	4	2	4	7	17	
			9.1%	4.5%	9.1%	15.9%	38.6%	
		Normal	1	0	3	7	11	
			2.3%	0.0%	6.8%	15.9%	25.0%	
	Total		16	2	10	16	44	
			36.4%	4.5%	22.7%	36.4%	100.0%	
Female	LV Function	Dysfunction (Systolic & Diastolic)	0	0	2	1	3	0.352
			0.0%	0.0%	5.7%	2.9%	8.6%	
		Dysfunction (Systolic Only)	7	1	5	5	18	
			20.0%	2.9%	14.3%	14.3%	51.4%	
		Normal	2	0	4	8	14	
			5.7%	0.0%	11.4%	22.9%	40.0%	
	Total		9	1	11	14	35	
			25.7%	2.9%	31.4%	40.0%	100.0%	

p-value ≤ 0.05: significant (*); p-value ≤ 0.01: highly significant (**); Test applied: Pearson's Chi-square

Table 4.48: Comparison of LVMi to Cardiothoracic Ratio (CTR)							
				Cardiothoracic Ratio		Total	p-value
				≤ 0.5	> 0.5		
Male	LVMi (g/m²) (Males)	≤ 115	Count	23	12	35	0.078
			% of Total	52.3%	27.3%	79.5%	
		> 115	Count	3	6	9	
			% of Total	6.8%	13.6%	20.5%	
	Total		Count	26	18	44	
			% of Total	59.1%	40.9%	100.0%	
Female	LVMi (g/m²) (Females)	≤ 95	Count	19	5	24	0.134
			% of Total	54.3%	14.3%	68.6%	
		> 95	Count	6	5	11	
			% of Total	17.1%	14.3%	31.4%	
	Total		Count	25	10	35	
			% of Total	71.4%	28.6%	100.0%	

Abbreviations: see 'List of Abbreviations'; p-value ≤ 0.05: significant (*); p-value ≤ 0.01: highly significant (**); Test applied: Pearson's Chi-square

Table 4.49: Comparison of RWT to Cardiothoracic Ratio (CTR)							
				Cardiothoracic Ratio		Total	p-value
				≤ 0.5	> 0.5		
Male	RWT	≤ 0.42	Count	22	18	40	0.081
			% of Total	50.0%	40.9%	90.9%	
		> 0.42	Count	4	0	4	
			% of Total	9.1%	0.0%	9.1%	
	Total		Count	26	18	44	
			% of Total	59.1%	40.9%	100.0%	
Female	RWT	≤ 0.42	Count	19	9	28	0.350
			% of Total	54.3%	25.7%	80.0%	
		> 0.42	Count	6	1	7	
			% of Total	17.1%	2.9%	20.0%	
	Total		Count	25	10	35	
			% of Total	71.4%	28.6%	100.0%	

Abbreviations: see 'List of Abbreviations'; p-value ≤ 0.05: significant (*); p-value ≤ 0.01: highly significant (**); Test applied: Pearson's Chi-square

Table 4.50: Comparison of LVMi to Right Wall Thickness (RWT) in Male Participants						
				LVMi (g/m^2) (Male)		Total
				≤ 115	> 115	
Male	RWT	≤ 0.42	Count	31	9	40
			% of Total	70.5%	20.5%	90.9%
		> 0.42	Count	4	0	4
			% of Total	9.1%	0.0%	9.1%
	Total		Count	35	9	44
			% of Total	79.5%	20.5%	100.0%

Abbreviations: see 'List of Abbreviations'. Data presented as numbers and percentages. Test Applied: Pearson's Chi-square

Table 4.51: LV Hypertrophy in Male Participants (Linear Method)	
	Total Number (%)
Normal	31 (70.5%)
Eccentric Hypertrophy	9 (20.5%)
Concentric Remodeling	4 (9.1%)
Concentric Hypertrophy	0 (0%)

Data presented as numbers and percentages

Table 4.52: Comparison of LVMi to Right Wall Thickness (RWT) in Female Participants						
				LVMi (g/m^2) (Female)		Total
				≤ 95	> 95	
Female	RWT	≤ 0.42	Count	19	9	28
			% of Total	54.3%	25.7%	80.0%
		> 0.42	Count	5	2	7
			% of Total	14.3%	5.7%	20.0%
	Total		Count	24	11	35
			% of Total	68.6%	31.4%	100.0%

Abbreviations: see 'List of Abbreviations'. Data presented as numbers and percentages. Test Applied: Pearson's Chi-square

Table 4.53: LV Hypertrophy in Female Participants (Linear Method)	
	Total Number (%)
Normal	19 (54.3%)
Eccentric Hypertrophy	9 (25.7%)
Concentric Remodeling	5 (14.3%)
Concentric Hypertrophy	2 (5.7%)

Data presented as numbers and percentages

CHAPTER 5

DISCUSSION

The current study investigated heart size on chest X-ray (PA view) and compared it to 2D transthoracic echocardiography, which is the gold standard for measuring heart size. Such a study has not been done before in Pakistan, in which the study participants were categorized into four groups, based on a comparison of the findings obtained from chest X-ray (PA view) and echocardiography. Such categorization was not done in any previous study before the current study. The participants of each group were assessed for the differences which led to them being categorized into their respective groups. The radiographic parameters measured included the transverse right cardiac diameter (TRCD or TRD), the transverse left cardiac diameter (TLCD or TLD), the transverse cardiac diameter (TCD), the transverse thoracic diameter (TTD), and the cardiothoracic ratio (CTR). To assess the accuracy of these measurements, they were compared to the echocardiographic parameters measured in routine clinical practice by echocardiologists. The parameters for the atria were the right atrial diameter (RAD) in apical 4-chamber view and the left atrial diameter (LAD) in PLAX view. The parameters for the right ventricle were the right ventricular diameter (RVD) in PLAX view, and TAPSE measured by M-mode tracing in the apical 4-chamber view. The parameters for the left ventricle included the end-diastolic and end-systolic left ventricular internal diameters (LVIDd and LVIDs, respectively), end-diastolic interventricular septum thickness (IVSd), and end-diastolic posterior wall thickness (PWd), which were all measured in the PLAX view. The LV ejection fraction (EF) was determined by the biplane (Simpson's) method in the apical 4-chamber and apical 2-chamber views. The LV mass (LVM) and relative wall thickness (RWT) were calculated using their respective equations. In contrast to our study, previous studies in this regard focused on ventricular end-diastolic measurements (Monfared et al., 2015) or LV ejection fraction only (Siddiqui et al., 2013), while some included left atrium as well, omitting the right atrium (Sinha et al., 2013). It was rarely seen that all chambers were included in a comparative study comparing chest X-rays (PA view) with echocardiography. Sinha et al (2013) took all the measurements in their study using M-mode echocardiography.

The current study was a prospective cross-sectional study, and most of the studies performed in this regard were also prospective comparative cross-sectional studies. Comparing an imaging modality or any screening test with a gold standard requires a cross-sectional study (Mathes & Pieper, 2019). The sample size of current study was sufficient for statistical analysis, as there have been studies conducted with smaller sample sizes. There was a disparity in gender distribution of the participants in current study, but this was expected of a cross-sectional study, due to the design nature of such studies. The sample size and gender distribution compared favorably to a study by Siddiqui et al (2013). In contrast, Sinha et al (2013) had a small sample size comprising of male subjects only, and Monfared et al (2015) used a larger sample size with equal proportions of each gender. Mckee and Ferrier (2017) used a larger sample size with female subjects half the total number of males. Similarly, in a retrospective study by Gwaba et al (2018), a large sample size was used but with female subjects less than half the total number of males. The age limit of participants set in the current study compared to that of Gwaba et al (2018), but the mean age of participants in current study was comparatively lower. The participants in the study by Monfared et al (2015) had the upper and lower age limits set higher. Similarly, the lower age limit was set higher in the study by Siddiqui et al (2013).

Since most studies that compared heart size on chest X-ray (PA view) with echocardiography involved the same radiological but different echocardiographic parameters, we compared the radiological measurements with those measured in the aforementioned studies and compared the echocardiographic measurements with ASE reference values (Lang et al., 2015). The mean values of radiological parameters in the male and female participants of current study were comparable to a study by Mensah et al (2015), and another study by Gameraddin et al (2014). The mean values for males with normal heart size in current study compared more favorably than females, who had a smaller normal heart size. When the mean values of the total study participants and those of both the genders with normal heart size (on echocardiography) in current study were compared to a study in the Indian population by Mehra et al (2019), there was a considerable difference between the mean values of males in both studies and a much smaller difference between the mean values of females.

When the echocardiographic measurements were compared with the reference values provided by ASE (for the normal heart), the mean RAD in males, and the mean LVIDd and

LVIDs in females with enlarged hearts in current study were within the reference range. The values for the same in normal-sized hearts were much lower than the upper limit of normal reference range. The mean values for LAD and RVD in both genders with enlarged hearts were just marginally above the upper limit of normal reference range defined by ASE. These differences could be due to the heart size of current study population being smaller at baseline, resulting in the values for a normal heart size being much smaller and corresponding to the lower limit of normal ASE reference range. Thus, even when enlarged, the measurements are below or just above the upper limit of normal reference values. The males in the current study with enlarged hearts had a mean value of LVIDd just above the upper limit of normal reference range, and that of LVIDs was considerably higher. The values for the same in normal-sized hearts were much lower than the upper limit of normal. This was also observed for RVD in both genders. Similar differences were observed in an Iranian study by Sadeghpour et al (2013), in which the normal mean values of several echocardiographic parameters obtained were smaller than the reference values in ASE guidelines, even when indexed to BSA. Daimon et al (2008) reported similar findings that the Japanese hearts were smaller than the ASE reference values, but the measurements indexed to BSA were within the reference range. Similar findings were also reported by Bansal et al (2016) and Mukherjee et al (2021), who noted a disparity in the normal mean values of echocardiographic parameters in the Indian population compared to ASE reference values. The similarities observed in our geographic region could be due to a shared common ancestry, which suggests that the values of heart size in this region are smaller and that regional differences do exist.

The mean LV EF in current study population was considerably lower than the reference values in ASE guidelines, and the females had a slightly higher value for EF in both the normal-sized and enlarged hearts. This difference was most probably due to the study population comprising of patients with cardiovascular disease. Similarly, due to the same reason, the mean TAPSE in our study was closer to the lower normal reference limit. A TAPSE value above or below the normal ASE reference range represents an abnormal RV function (Mitchell et al., 2019). The values for IVSd, PWd, and aortic diameter showed little changes and the measured values were within the normal defined range of ASE. The females with normal heart size in current study had smaller echocardiographic values for most

parameters compared to males but the difference was small. Similar findings were also reported by a study in the Chinese population (Yao et al., 2015).

The findings of chest X-ray (PA view), i.e. a normal or enlarged heart size, were compared to the findings of echocardiography for the same. The results obtained were used to determine the sensitivity, specificity, and predictive value of chest X-rays (PA view) in determining an enlarged heart. The sensitivity and specificity of the current study compared better to most other studies (Abd-Hazaa et al., 2007; McKee & Ferrier, 2017; Md Siddiqui et al., 2013; Monfared et al., 2015), this could most probably be attributed to the study population in current study consisting of patients with heart-related complaints or disorders, and a smaller timeframe between echocardiography and chest X-rays (PA view) when they were performed. These differences can also be attributed to the echocardiographic parameters used, as these parameters differed from one study to another. The positive predictive value (PPV) and negative predictive value (NPV) in our study were different from other studies, as they were determined using the same variables that were used to determine the sensitivity and specificity. Moreover, the predictive values are influenced by the prevalence of a condition or disease, which in turn is subjected to regional variations.

The four groups in current study were evaluated individually, and the differences were reported. Although the mean cardiac diameter (TCD) in Group A (true positive) was slightly larger than the mean TCD of Group B (false positive), the CTR in Group A was considerably greater. The three participants who were categorized into Group B in current study, were two males aged 65 and 75 years, and a female aged 73 years. A similar observation was reported by Mensah et al (2015), who attributed such changes to an increased cardiac diameter (TCD) with age. An increase in TCD is due to increased cardiac ventricular muscle thickness resulting from increased vascular resistance or loss of elasticity of the great vessels. Mensah et al also reported a reduction in thoracic diameter (TTD) after the sixth decade of life, which was attributed to reduced ribcage mobility and compliance (Inoue et al., 1999). These differences reflect the smaller thoracic diameter of Group B participants because when CTR was calculated, the cardiac diameter was used as a numerator and the thoracic diameter was used as the denominator. Thus, a smaller TTD and an increased TCD will result in a larger value of CTR. Another factor observed to have contributed to the difference in CTR was the

physical characteristics of the group participants, as the height of one of the males in this group was one of the two tallest heights of all participants in the study.

The mean cardiac diameter in Group D (true negative) was slightly smaller than that of Group C (false negative) and the CTR in both groups was similar, with that of Group C being greater by only a very small measure. This difference was due to the strict criteria set in the current study for identifying an enlarged heart on echocardiography, which was an enlarged value for any one of the echocardiographic parameters that included LVIDd, LVIDs, IVSd, PWd, LAD, RVD, and RAD. As a result, a measurement for any of the mentioned parameters equal to or just over the normal upper reference value was considered as an enlarged heart size on echocardiography.

The total number of participants who truly had an enlarged heart size on echocardiography were represented by Group A and C (true positive and false negative, respectively). Those with a normal heart size on echocardiography were represented by Group B and D (false positive and true negative, respectively). Thus, the echocardiographic values of Group A and C represent the range at which cardiothoracic ratio (CTR) can be expected to appear increased or normal respectively, on a chest X-ray (PA view) of a participant with an enlarged heart size determined on echocardiography. This implies that, for a heart with enlarged size determined on the gold standard (echocardiography), the cardiac silhouette may appear enlarged on a chest X-ray (PA view) and correspond to the mean values of echocardiographic parameters in Group A; or may appear normal and correspond to the mean values of echocardiographic parameters in Group C. Similarly, the echocardiographic values of Group B and D represent the range at which the cardiothoracic ratio (CTR) will appear increased or normal respectively, on a chest X-ray (PA view) of a participant with a normal heart size determined on echocardiography. This implies that, for a heart of normal size determined on the gold standard (echocardiography), the cardiac silhouette may appear enlarged on a chest X-ray (PA view) and correspond to the mean values of echocardiographic parameters in Group B; or may appear normal and correspond to the mean values of echocardiographic parameters in Group D.

These findings can be useful to a clinician, especially in a poor or limited-resource setting. It implies that for a normal CTR on chest X-ray (PA view), the mean values of

echocardiographic parameters will be between the mean values of Group C and D. Similarly, for an increased CTR on chest X-ray (PA view), the mean values of echocardiographic parameters will be between the mean values of Group A and B. By comparison, there was a greater difference between the mean measurements of Group D and A (true negative compared to true positive) than there was between Group D and C (true negative compared to false negative). Similarly, the difference between the measured values of Group A and C (true positive compared to false negative) was smaller but significant compared to that between Group A and B (true positive compared to false positive) which was much greater. Thus, as far as the size of the heart is concerned, a chest X-ray (PA view) and the value of CTR can serve as a very useful tool. This is in agreement with the findings of similar studies (Abd-Hazaa et al., 2007; Jung et al., 1995; Morales et al., 2012). Several studies have determined CTR in different races and geographical regions, e.g. one study mentions the normal CTR in African countries to be higher than what was considered normal for caucasian populations (Nickol & Wade, 1982). The current study has determined the mean CTR for a heart of normal and enlarged size, and also demonstrated that even if the CTR is normal, a functional disorder of the heart may be present. The LV EF was suboptimum in the current study population because they were patients with heart-related disorders or complaints.

The findings of our study focused on the size of the heart, and the findings related to heart function were expected, as it is frequently assessed and reported on echocardiography. Echocardiography can assess structural and functional aspects of the heart, which the chest X-ray (PA view) cannot offer. Yet, how the structural and functional factors affect a heart's size can be investigated on a chest X-ray (PA view), and if supplemented with or investigated together with a more superior or advanced imaging modality, a great wealth of information can be inferred. The discussion here is not to disqualify, discredit or redeem an imaging modality that is over a hundred years old, but to investigate any findings that may be translatable from an advanced imaging technique to a simpler one.

When a correlation was performed between the parameters of chest X-ray (PA view) and echocardiography, the results showed that for each of the four groups, there was a strong statistical correlation (positive and negative) between some parameters and none in others. Current study showed that the participants in Group A had a strong positive correlation between CTR and the right ventricular diameter (RVD), and PASP. This implies that in an

enlarged heart on both chest X-ray (PA view) and echocardiography, the CTR matches more to an increase in RVD. An increase in PASP reflects an increase in pulmonary vascular pressure, which may appear as pulmonary congestion on a radiograph. The cardiac diameter (TCD) had a strong positive correlation with systolic left ventricular internal diameter (LVIDs) and a strong negative correlation with LV EF. This is an important observation, which implies that as the cardiac diameter increases, LV EF decreases. It is established in other studies that LV EF decreases as the LV size increases, as seen in dilated cardiomyopathy (Nabeta et al., 2019). Similar to current study, Morales et al (2012) also found a negative correlation between TCD and LV EF. In contrast, Clarke et al (2000) reported a weak correlation between CTR and LV EF. The current study also found that TLD had a positive correlation with both diastolic and systolic LV internal diameters (LVIDd and LVIDs, respectively), and a negative correlation with LV EF and RWT. The TTD had a strong positive correlation with LVIDs.

In Group B the CTR did not correlate with any of the echocardiographic parameters, but the TCD, TLD, TRD, and TTD had a positive correlation with LVIDd, and a negative correlation with PWd and RWT. There were only three participants categorized in this group, and one of the participant's PASP could not be measured due to turbulent tricuspid blood flow (turbulent TR jet). In Group C, a negative correlation was observed between TLD and LV EF, and no other correlation was present. In Group D the CTR did not correlate with any of the echocardiographic parameters. The TCD, TLD, and TTD had a positive correlation with RAD. The TTD and TLD had a positive correlation with LAD as well, and the TLD showed a positive correlation with the aortic diameter. These correlations are important, as they imply that in a heart of normal size, the cardiac silhouette on chest X-ray (PA view) corresponds more to the diameters of the right and left atria and aorta.

When indexed values were used, there was a slightly improved or worsened correlation between some parameters, elimination or introduction of new but negative correlations in others. These differences most probably resulted from the fact that while the echocardiographic parameters were indexed to BSA (D&D) during analysis, the radiological parameters were not indexed (McKee & Ferrier, 2017). Several studies confirm that echocardiographic measurements are influenced by BSA, while for chest X-ray imaging there is no available data if the BSA has any influence (Bansal et al., 2016).

In the current study, a significant number of participants showed radiological signs of pulmonary congestion. Those with an enlarged heart on echocardiography, pulmonary vascular congestion was observed more frequently compared to those with normal heart size. Most of the participants with normal heart size on chest X-rays (PA view) did not show pulmonary congestion. There was an equal number of participants with normal and enlarged heart size who had congestion present. Pulmonary congestion, which is often a manifestation of cardiogenic pulmonary edema, is associated with pulmonary vascular disease, RV overload and dysfunction, and increased mortality. Data from studies reinforce the need for aggressive decongestion in heart failure to deter progression of the disease and developing a biventricular heart failure (Melenovsky et al., 2015).

The demographic characteristics of the current study are comparable to the findings of most studies conducted in our geographical region. The heights of the male participants were similar to those of males in India and Iran (Ahranjani et al., 2012; Som et al., 2014). The heights of female participants were similar to those observed for females in the Indian population and smaller than those observed for females in the Iranian population. The weights of current study participants were considerably higher, for both males and females, compared to those reported by a study in India, but compared in agreement to the values reported by a study in Iran (Haghdoost et al., 2008). The BMI for both genders in the current study was greater than their counterparts in India but similar to the values observed in the Iranian population. These differences are most probably due to the current study including diseased participants, most of them being obese which is also reflected in the higher number of comorbidities such as diabetes mellitus and hypertension, while the studies in India and Iran included healthy participants. In all these studies, including current study, the females had a higher BMI compared to males. The lower BMI values in males observed in current study also compared favorably to a study by Xiao et al (2019) and Djalalinia et al (2015), who observed a similar difference in BMI between males and females. In current study, this difference can be attributed to the greater mean height of male participants, compared to females. The BSA of the participants in current study was determined using two formulae, which were the Mosteller formula (Mos.) and the Dubois and Dubois (D&D) formula. A separate analysis by averaging the BSA obtained from the two formulae was also done. There was a statistically significant difference observed between males and females for each of the

three BSA formulae used. BSA (D&D) has been more frequently used in research, and the current study also used this formula (Flint & Hall, 2021).

The current study showed that lower education level is associated with an increased incidence of heart disease. This finding compares favorably to a study by Dégano et al (2017), who reported that the incidence of cardiovascular diseases was reduced in those with university education when compared to those with primary or lower education. Occupation plays an important contributing role and it is influenced profoundly by the education level. Most participants in current study were housewives, followed by retired persons, shopkeepers, and farmers. The findings of current study are consistent with those of Warren et al (2010), identifying sedentary behavior to increase the risk of cardiovascular disease. Findings reported by Chung et al (2009) and Xue et al (2019) state that the physical activity level of retired persons influences the outcome for developing cardiovascular disease. Although farmers would be expected to have a healthier lifestyle and diet, and thus protected from cardiovascular disease, it has been reported that they are a vulnerable population for developing heart disease, mainly because of abandoning traditional methods of farming and adopting urban diets (Vardavas et al., 2010).

The guidelines of physical activity for American adults recommend at least 150 minutes of moderate-intensity aerobic activity (e.g. walking) or 75 minutes of vigorous-intensity aerobic activity (e.g. jogging) in a week, or a combination of both. Muscle strength training activities are also recommended on two or more days per week. The physical activity level in current study showed that females had a less physically active lifestyle compared to males. Thus, females as housewives, unique aging physiology with hormonal changes, and infrequent physical activity are more predisposed to develop cardiovascular diseases (Keteepe-Arachi & Sharma, 2017).

More than half of the participants in current study did not have any comorbidity. Among the remaining, a large number of participants had two associated comorbid conditions, i.e. diabetes mellitus and hypertension. Long & Dagogo-Jack (2011) observed a similar finding. The next most frequent comorbid condition observed was hypertension. Since the study population comprised mostly of diseased persons, a very high number of participants did not have any addictions, and those who had an addiction were cigarette smokers and naswar

users. There was a small number of those who took two substances for addiction, e.g. pan and naswar, or pan and cigarette smoking. A small minority of participants had quit their addiction.

The most common diagnosis observed in current study was NSTEMI (Non-ST Elevated MI). The next common diagnoses were STEMI (ST Elevated MI) and valvular heart disease. Our findings are in agreement with international statistics for heart diseases. An estimated 15.9 million people worldwide suffered from MI in 2015, STEMI was observed in more than 3 million people and NSTEMI in more than 4 million people. Men had STEMIs twice as often as women, and in the developed world those who had STEMI had an increased risk of death by about 10% (Singh et al., 2020).

Valvular heart disease encompasses several common cardiovascular disorders that account for 10% to 20% of cardiac surgical procedures in the United States (Maganti et al., 2010). The most common cause in the developed countries for valvular heart disease is degenerative valvular diseases, while in the developing world it is rheumatic fever and a rising incidence of degenerative valvular disease. It has been observed historically, the conditions that were alien to our geographical region and more common in the Western world became permanent residents of this part of the world. While the developed countries have the resources and the infrastructure available to tend to their populations' needs, a developing country with severe financial constraints and facing multiple challenges will not be able to address the issue (Ray, 2010).

In the current study, LV dysfunction was observed to be more common than RV dysfunction. A depressed RV function was more common than RV dysfunction, with a slightly higher number of males affected. In participants with LV dysfunction, more males had both diastolic and systolic dysfunction than females, and the females had a slightly higher number of systolic dysfunction. Females frequently had a normal LV function, which has been reported by several studies including Gerdts et al (2008) who found that the females retained a higher LV EF through the course of a long-term treatment for hypertension. Women are believed to be more commonly affected by heart failure with normal or preserved LV EF (Regitz-Zagrosek et al., 2007).

The LV hypertrophy and LV remodeling, are key compensatory processes that arise over time in response to excessive hemodynamic pressure or volumetric burden. Current study compared favorably to a study by Bornstein et al (2021), in which the prevalence of LV hypertrophy in the general population at high risk or untreated hypertensive persons was high. A relatively higher prevalence of eccentric LV hypertrophy was observed, compared to concentric hypertrophy (Cuspidi et al., 2012).

Based on relative wall thickness (RWT) and the LV mass index (LVMi), the left ventricular hypertrophy can be categorized into two types; concentric hypertrophy when LVMi is > 115 g/m^2 in males or > 95 g/m^2 in females and RWT is > 0.42; or eccentric hypertrophy when LVMi is > 115 g/m^2 in males or > 95 g/m^2 in females and RWT is ≤ 0.42. RWT thus further classifies an increase in LV mass into the subtypes mentioned. Concentric LV hypertrophy is caused by a chronically increased workload on the heart as seen in chronic hypertension or aortic stenosis. Eccentric LV hypertrophy is induced by an increased filling pressure of the left ventricle, otherwise known as diastolic overload, seen in patients with regurgitant valve lesions such as aortic or mitral regurgitation as well as in dilated cardiomyopathy (Bornstein et al., 2021). In current study, there were a considerable number of participants who had hypertension, and most had concurrent diabetes mellitus. The most common pattern of hypertrophy observed after eccentric hypertrophy was concentric remodeling, in which the LVMi was more than the cutoff value for normal and the value for RWT was ≤ 0.42. This finding compares favorably to a study by Ganau et al (1992), who investigated the patterns of LV hypertrophy and geometric remodeling in essential hypertension. They observed that in untreated hypertensive patients, concentric LV remodeling and eccentric LV hypertrophy were more common than concentric LV hypertrophy.

CHAPTER 6

CONCLUSION

6.1 Conclusion of Study

The current study determined heart size on chest X-ray (PA view) and compared it to the most commonly measured routine parameters for estimation of the same on echocardiography. There were strong (positive and negative) correlations observed between several of the radiological and echocardiographic parameters. It can be concluded thus, that the cardiac silhouette on a chest X-ray (PA view) precisely demonstrates the heart size through a simple measurement that has a high specificity and reasonable accuracy.

As a screening test, if an enlarged heart is reported on a chest X-ray (PA) view, the actual chance or probability of having an enlarged heart on echocardiography increases six-folds (represented by the positive likelihood ratio). Similarly, if a chest X-ray (PA view) reports a normal size of the heart, the actual probability of having an enlarged heart on echocardiography is reduced minimally (represented by the negative likelihood ratio).

The prevalence of cardiomegaly observed in current study reflects that heart diseases may not always be accompanied by cardiomegaly, and a normal heart size on chest X-ray (PA view) may not have a normal function. But there are additional findings to consider that may help a clinician make a better judgment regarding the heart size when it appears normal on a chest X-ray (PA view), e.g. pulmonary congestion, which was a frequent radiographic finding in current study.

6.2 Recommendations:

i. A nationwide, multicenter study should be conducted to establish the normal reference radiological and echocardiographic values for the Pakistani population.
ii. Regional studies at the provincial level should be conducted with equal ethnic and gender representation, using different imaging modalities e.g. radiography, 2D transthoracic echocardiography, magnetic resonance imaging (MRI), and computerized tomography scans (CT).

iii. An echocardiography laboratory should be established at the national or provincial level, with the purpose to receive echocardiographic images and data for analysis. It can serve as a national database, which will help future researchers, as well as undergraduate and postgraduate students.

iv. Similar studies should be conducted involving only healthy or diseased populations, or both. Current study can be replicated and conducted in combination with another imaging or investigation modality, e.g. MRI or ECG.

v. Fluoroscopy should be considered for comparison with chest X-ray (PA view), as both share similar working principles, and echocardiography as well. At least three to five cardiac cycles should be recorded fluoroscopically, and an assessment of the heart made to be compared to radiographic and echocardiographic measurements. Several methods are available for recording images and motion during fluoroscopy, e.g. digital fluorography or photofluorography for recording images, and Super-VHS (or S-video) or cine fluorography for recording motion.

vi. A single standard measurement complementing CTR should be defined for echocardiography by ASE or EACVI, to ascertain the overall size of the heart.

6.3 Strengths of Study

i. It is the first time, to the best of our knowledge, that a study comparing heart size on two imaging modalities has been performed in Pakistan, in which parameters measured on both modalities were correlated.

ii. The participants were divided into four groups based on the findings and each group was investigated for the differences in study parameters. Earlier studies did not group the participants.

iii. The radiographic measurements were obtained using computer software (Fiji ImageJ) specially designed for research purposes.

iv. The echocardiographic parameters used in defining an enlarged heart were those that are used in routine practice by cardiologists.

v. In contrast to most other studies, the current study included measurements related to all the chambers of the heart. The function of both the ventricles (EF of LV and TAPSE of RV) was also assessed in current study.

vi. The part of our population most susceptible to developing heart diseases was identified, e.g. due to a sedentary lifestyle or occupation. Awareness programs for lifestyle modification and prevention of developing heart diseases should be tailored according to the education level and occupation of the target population.

vii. The findings of current study can help clinicians working in a limited resource setting to extract valuable information from a chest X-ray (PA view), and make better therapeutic decisions.

viii. A single view of chest X-ray was used in the study, i.e. PA view only, for minimum radiation exposure. It can serve as a cost-effective means for those patients who cannot afford it.

6.4 Limitations of Study

i. The imaging modalities used, i.e. radiography and echocardiography, use two very different working principles, the former uses ionizing radiation and the latter uses sound waves.

ii. Chest X-ray (PA view) images were obtained using a digital camera.

iii. The sample size was small due to the limited time of the study, and it was conducted in a single city.

iv. Ethnic representation was not equal in the study, and there was a slight disparity in the gender distribution.

v. The comorbidities considered did not include hyperlipidemia.

CHAPTER 7

REFERENCES

Abd-Hazaa, M., Sharif, S., & Kadhum, A. A.-H. (2007). Validity of chest x-ray in estimation of cardiac size in comparison to echocardiography. *The Medical Journal of Basrah University*, *25*(2), 48–51.

Abu-Issa, R., Waldo, K., & Kirby, M. L. (2004). Heart fields: One, two or more? *Developmental Biology*, *272*(2), 281–285. https://doi.org/10.1016/j.ydbio.2004.05.016

Adhikary, K., Jha, S., Ghimire, R., & Pradhan, S. (2003). Comparison of Plain X-ray finding of Ventricular Enlargement with Echocardiography. *Nepalese Heart Journal*, *2*, 26–38. https://doi.org/10.3126/njh.v2i2.26035

Agrawal, S., Kumar, S., gabhane, V., Acharya, S., & Wanjari, A. (2019). Electrocardiography and Echocardiography Correlation in Patients of Left Ventricular Hypertrophy. *Journal Of Clinical And Diagnostic Research*, *13*. https://doi.org/10.7860/JCDR/2019/42697.13329

Ahranjani, S. A., Kashani, H., Forouzanfar, M., Meybodi, H. A., Larijani, B., Aalaa, M., & Mohajeri-Tehrani, M. (2012). Waist Circumference, Weight, and Body Mass Index of Iranians based on National Non-Communicable Disease Risk Factors Surveillance. *Iranian Journal of Public Health*, *41*(4), 35–45.

Ajmone Marsan, N., Michalski, B., Cameli, M., Podlesnikar, T., Manka, R., Sitges, M., Dweck, M. R., & Haugaa, K. H. (2020). EACVI survey on standardization of cardiac chambers quantification by transthoracic echocardiography. *European Heart Journal. Cardiovascular Imaging*, *21*(2), 119–123. https://doi.org/10.1093/ehjci/jez297

Akhter, S. A. (2011). The heart and pericardium. *Thoracic Surgery Clinics*, *21*(2), 205–217. https://doi.org/10.1016/j.thorsurg.2011.01.007

Alam, M., Rosenhamer, G., & Höglund, C. (1989). Comparability of echocardiography and chest X-ray following myocardial infarction. *Journal of Internal Medicine*, *226*(3), 171–175. https://doi.org/10.1111/j.1365-2796.1989.tb01375.x

Alberg, A. J., Park, J. W., Hager, B. W., Brock, M. V., & Diener-West, M. (2004). The use of "overall accuracy" to evaluate the validity of screening or diagnostic tests. *Journal of General Internal Medicine*, *19*(5), 460–465. https://doi.org/10.1111/j.1525-1497.2004.30091.x

Alghamdi, S., Abdelaziz Hassan, I., Albadri, M., Alyanbaawi, S., Aljondi, R., & Tajaldeen, A. (2020). Study of cardiomegaly using chest x-ray. *Journal of Radiation Research and Applied Sciences*, *13*(1). https://doi.org/10.1080/16878507.2020.1756187

Alhaji Saganuwan, S. (2015). Standardization and Scoring of the Body Surface Area (BSA) Formulas for Calculation of the Doses of Anticancer Agents for Cancer Patients from the North-Western Nigeria. *Journal of Cancer Science & Therapy*, *07*. https://doi.org /10.4172/1948-5956.1000319

Alì, M., Monti, C. B., Secchi, F., Spairani, R., Speciani, M., Di Leo, G., & Sardanelli, F. (2020). Fast thoracic MRI as an alternative to chest x-ray: A retrospective evaluation of 287 patients. *Clinical Imaging*, *60*(2), 244–248. https://doi.org/10.1016/j.clinimag.2019.12.016

Amin, H., & Siddiqui, W. J. (2020). Cardiomegaly. In *StatPearls*. StatPearls Publishing.

Ampanozi, G., Krinke, E., Laberke, P., Schweitzer, W., Thali, M. J., & Ebert, L. C. (2018). Comparing fist size to heart size is not a viable technique to assess cardiomegaly. *Cardiovascular Pathology : The Official Journal of the Society for Cardiovascular Pathology*, *36*, 1–5. https://doi.org/10.1016/j.carpath.2018.04.009

Anderson, R., Brown, N., & Webb, S. (2002). Development and structure of the atrial septum. *Heart: British Cardiac Society*, *88*, 104–110.

Arts, T., Lumens, J., Kroon, W., & Delhaas, T. (2012). Control of whole heart geometry by intramyocardial mechano-feedback: A model study. *PLoS Computational Biology*, *8*(2), e1002369. https://doi.org/10.1371/journal.pcbi.1002369

Ashley, E. A., & Niebauer, J. (2004). *Cardiology Explained*. Remedica.

Aziz, F., Tk, L. A., Enweluzo, C., Dutta, S., & Zaeem, M. (2013). Diastolic heart failure: A concise review. *Journal of Clinical Medicine Research*, *5*(5), 327–334. https://doi.org/10.4021/jocmr1532w

Baker, B. J., Scovil, J. A., Kane, J. J., & Murphy, M. L. (1983). Echocardiographic detection of right ventricular hypertrophy. *American Heart Journal*, *105*(4), 611–614. https://doi.org/10.1016/0002-8703(83)90485-4

Bansal, M., Mohan, J. C., & Sengupta, S. P. (2016). Normal echocardiographic measurements in Indian adults: How different are we from the western populations? A pilot study. *Indian Heart Journal*, *68*(6), 772–775. https://doi.org/10.1016/j.ihj.2016.02.018

Blauwet, L. A., & Cooper, L. T. (2010). Myocarditis. *Progress in Cardiovascular Diseases*, *52*(4), 274–288. https://doi.org/10.1016/j.pcad.2009.11.006

Bornstein, A. B., Rao, S. S., & Marwaha, K. (2021). Left Ventricular Hypertrophy. In *StatPearls*. StatPearls Publishing.

Buijtendijk, M. F. J., Barnett, P., & van den Hoff, M. J. B. (2020). Development of the human heart. *American Journal of Medical Genetics. Part C, Seminars in Medical Genetics*, *184*(1), 7–22. https://doi.org/10.1002/ajmg.c.31778

Caraballo, C., Desai, N. R., Mulder, H., Alhanti, B., Wilson, F. P., Fiuzat, M., Felker, G. M., Piña, I. L., O'Connor, C. M., Lindenfeld, J., Januzzi, J. L., Cohen, L. S., & Ahmad, T. (2019). Clinical Implications of the New York Heart Association Classification. *Journal of the American Heart Association*, *8*(23), e014240. https://doi.org/10.1161/JAHA.119.014240

Cativo Calderon, E. H., Mene-Afejuku, T. O., Valvani, R., Cativo, D. P., Tripathi, D., Reyes, H. A., & Mushiyev, S. (2017). D-Shaped Left Ventricle, Anatomic, and Physiologic Implications. *Case Reports in Cardiology*, *2017*, 4309165. https://doi.org/10.1155/2017/4309165

Cervantes, K., Salgado, R., Choi, M., & Hd, K. (2003). *Rapid assessment of referral care systems: A guide for program managers.*

Chana, H. S., Martin, C. A., Cakebread, H. E., Adjei, F. D., & Gajendragadkar, P. R. (2015). Diagnostic accuracy of cardiothoracic ratio on admission chest radiography to detect left or right ventricular systolic dysfunction: A retrospective study. *Journal of the Royal Society of Medicine*, *108*(8), 317–324. https://doi.org/10.1177/0141076815588314

Chang, E., Varghese, M., & Singer, K. (2018). Gender and Sex Differences in Adipose Tissue. *Current Diabetes Reports*, *18*(9), 69. https://doi.org/10.1007/s11892-018-1031-3

Charalampidis, C., Youroukou, A., Lazaridis, G., Baka, S., Mpoukovinas, I., Karavasilis, V., Kioumis, I., Pitsiou, G., Papaiwannou, A., Karavergou, A., Tsakiridis, K., Katsikogiannis, N., Sarika, E., Kapanidis, K., Sakkas, L., Korantzis, I., Lampaki, S., Zarogoulidis, K., & Zarogoulidis, P. (2015). Pleura space anatomy. *Journal of Thoracic Disease*, *7* (Suppl 1), S27-32. https://doi.org/10.3978/j.issn.2072-1439.2015.01.48

Choi, J. O., Shin, M. S., Kim, M. J., Jung, H. O., Park, J. R., Sohn, I. S., Kim, H., Park, S. M., Yoo, N. J., Choi, J. H., Kim, H. K., Cho, G. Y., Lee, M. R., Park, J. S., Shim, C. Y., Kim, D. H., Shin, D. H., Shin, G. J., Shin, S. H., Park, S. W. (2015). Normal Echocardiographic Measurements in a Korean Population Study: Part I. Cardiac Chamber and Great Artery Evaluation. *Journal of Cardiovascular Ultrasound*, *23*(3), 158–172. https://doi.org/10.4250/jcu.2015.23.3.158

Chung, E., & Leinwand, L. A. (2014). Pregnancy as a cardiac stress model. *Cardiovascular Research*, *101*(4), 561–570. https://doi.org/10.1093/cvr/cvu013

Chung, S., Domino, M. E., & Stearns, S. C. (2009). The Effect of Retirement on Weight. *The Journals of Gerontology: Series B*, *64B*(5), 656–665. https://doi.org/10.1093/geronb/gbn044

Clark, A. L., & Coats, A. J. (2000). Unreliability of cardiothoracic ratio as a marker of left ventricular impairment: Comparison with radionuclide ventriculography and echocardiography. *Postgraduate Medical Journal*, *76*(895), 289–291. https://doi.org/10.1136/pmj.76.895.289

Clarke, G. M., Conti, S., Wolters, A. T., & Steventon, A. (2019). Evaluating the impact of healthcare interventions using routine data. *BMJ*, *365*. https://doi.org/10.1136/bmj.l2239

Correale, M., Ieva, R., Manuppelli, V., Rinaldi, A., & Di Biase, M. (2009). Controversies in echocardiography: 2D vs 3D vs 4D. *Minerva Cardioangiologica*, *57*(4), 443–455.

Cosyns, B., & Lancellotti, P. (2016). Normal reference values for echocardiography: A call for comparison between ethnicities. *European Heart Journal - Cardiovascular Imaging*, *17*(5), 523–524. https://doi.org/10.1093/ehjci/jev353

Cuspidi, C., Sala, C., Negri, F., Mancia, G., & Morganti, A. (2012). Prevalence of left-ventricular hypertrophy in hypertension: An updated review of echocardiographic studies. *Journal of Human Hypertension*, *26*(6), 343–349. https://doi.org/10.1038/jhh.2011.104

Daimon, M., Watanabe, H., Abe, Y., Hirata, K., Hozumi, T., Ishii, K., Ito, H., Iwakura, K., Izumi, C., Matsuzaki, M., Minagoe, S., Abe, H., Murata, K., Nakatani, S., Negishi, K., Yoshida, K., Tanabe, K., Tanaka, N., Tokai, K., & Yoshikawa, J. (2008). Normal Values of Echocardiographic Parameters in Relation to Age in a Healthy Japanese Population - The JAMP Study. *Circulation Journal : Official Journal of the Japanese Circulation Society*, *72*, 1859–1866. https://doi.org/10.1253/circj.CJ-08-0171

de Lange, F. J., Moorman, A. F. M., Anderson, R. H., Männer, J., Soufan, A. T., de Gier-de Vries, C., Schneider, M. D., Webb, S., van den Hoff, M. J. B., & Christoffels, V. M. (2004). Lineage and morphogenetic analysis of the cardiac valves. *Circulation Research*, *95*(6), 645–654. https://doi.org/10.1161/01.RES.0000141429.13560.cb

Dégano, I. R., Marrugat, J., Grau, M., Salvador-González, B., Ramos, R., Zamora, A., Martí, R., & Elosua, R. (2017). The association between education and cardiovascular disease incidence is mediated by hypertension, diabetes, and body mass index. *Scientific Reports*, *7*(1), 12370–12370. PubMed. https://doi.org/10.1038/s41598-017-10775-3

Dewey, F., Rosenthal, D., Murphy, D., Froelicher, V., & Ashley, E. (2008). Does Size Matter? Clinical Applications of Scaling Cardiac Size and Function for Body Size. *Circulation*, *117*, 2279–2287. https://doi.org/10.1161/CIRCULATIONAHA.107.736785

Djalalinia, S., Moghaddam, S., Peykari, N., Kasaeian, A., Sheidaei, A., Mansouri, A., Mohammadi, Y., Parsaeian, M., Mehdipour, P., Larijani, B., & Farzadfar, F. (2015). Mortality attributable to excess body mass Index in Iran: Implementation of the comparative risk assessment methodology. *International Journal of Preventive Medicine*, *6*(1), 107–107. https://doi.org/10.4103/2008-7802.169075

Douglas, P. S., Carabello, B. A., Lang, R. M., Lopez, L., Pellikka, P. A., Picard, M. H., Thomas, J. D., Varghese, P., Wang, T. Y., Weissman, N. J., & Wilgus, R. (2019). 2019 ACC/AHA/ASE Key Data Elements and Definitions for Transthoracic Echocardiography: A Report of the American College of Cardiology/American Heart Association Task Force on Clinical Data Standards (Writing Committee to Develop Clinical Data Standards for Transthoracic Echocardiography) and the American Society of Echocardiography. *Circulation: Cardiovascular Imaging*, *12*(7), e000027. https://doi.org/10.1161/HCI.0000000000000027

Dressler, G. (2009). Advances in early kidney specification, development and patterning. *Development (Cambridge, England)*, *136*, 3863–3874. https://doi.org/10.1242/dev.034876

Dyer, L. A., & Kirby, M. L. (2009). The role of secondary heart field in cardiac development. *Developmental Biology*, *336*(2), 137–144. https://doi.org/10.1016/j.ydbio.2009.10.009

Ellis, J., Martin, R., Wilde, P., Tometzki, A., Senkungu, J., & Nansera, D. (2007). Echocardiographic, chest X-ray and electrocardiogram findings in children presenting with heart failure to a Ugandan paediatric ward. *Tropical Doctor*, *37*(3), 149–150. https://doi.org/10.1258/004947507781524665

Ellis, S., & Aziz, Z. (2016). Radiology as an aid to diagnosis in lung disease. *Postgraduate Medical Journal*, *92*(1092), 620–623. https://doi.org/10.1136/postgradmedj-2015-133825

Elmissiri, A., Meniawy, K., Sakr, S., & Mohamed, A. (2016). Normal reference values of echocardiographic measurements in young Egyptian adults. *The Egyptian Heart Journal*. https://doi.org/10.1016/j.ehj.2016.01.002

Fakoya, A. O. J., Otohinoyi, D. A., Marcelle, T., & Yusuf, J. (2017). The Palm-Heart Diameter: A Prospective Simple Screening Tool for Identifying Heart Enlargement. *Open Access Macedonian Journal of Medical Sciences*, *5*(7), 818–824. https://doi.org/10.3889/oamjms.2017.181

Flint, B., & Hall, C. A. (2021). Body Surface Area. In *StatPearls*. StatPearls Publishing.

Fonseca, C., Mota, T., Morais, H., Matias, F., Costa, C., Oliveira, A. G., & Ceia, F. (2004). The value of the electrocardiogram and chest X-ray for confirming or refuting a suspected diagnosis of heart failure in the community. *European Journal of Heart Failure*, *6*(6), 807–812, 821–822. https://doi.org/10.1016/j.ejheart.2004.09.004

François, C. J., & Schiebler, M. L. (2016). Imaging of Pulmonary Hypertension. *Radiologic Clinics of North America*, *54*(6), 1133–1149. https://doi.org/10.1016/j.rcl.2016.05.011

Fujiu, K., & Nagai, R. (2014). Fibroblast-mediated pathways in cardiac hypertrophy. *Journal of Molecular and Cellular Cardiology*, *70*, 64–73. https://doi.org/10.1016/j.yjmcc.2014.01.013

Fukuta, H., & Little, W. C. (2008). The cardiac cycle and the physiologic basis of left ventricular contraction, ejection, relaxation, and filling. *Heart Failure Clinics*, *4*(1), 1–11. https://doi.org/10.1016/j.hfc.2007.10.004

Gameraddin, M., Al-Raddadi, M., Yousef, M., Nashashqi, W., Ali, A., Salih, S., & Ahmed, B. (2014). Evaluation of Cardiothoracic Ratio of Normal Subjects in Al madinah Al Munawwara Using Chest Radiographs. *La Pensée*.

Ganau, A., Devereux, R. B., Roman, M. J., de Simone, G., Pickering, T. G., Saba, P. S., Vargiu, P., Simongini, I., & Laragh, J. H. (1992). Patterns of left ventricular hypertrophy and geometric remodeling in essential hypertension. *Journal of the American College of Cardiology*, *19*(7), 1550–1558. https://doi.org/10.1016/0735-1097(92)90617-v

Garijo, J. M., Wijeysundera, D. N., Munro, J. C., & Meineri, M. (2017). Correlation Between Transhepatic and Subcostal Inferior Vena Cava Views to Assess Inferior Vena Cava Variation: A Pilot Study. *Journal of Cardiothoracic and Vascular Anesthesia*, *31*(3), 973–979. https://doi.org/10.1053/j.jvca.2017.02.003

George, R. M., & Firulli, A. B. (2019). Hand Factors in Cardiac Development. *Anatomical Record (Hoboken, N.J. : 2007)*, *302*(1), 101–107. https://doi.org/10.1002/ar.23910

Gerdts, E., Okin, P. M., de Simone, G., Cramariuc, D., Wachtell, K., Boman, K., & Devereux, R. B. (2008). Gender differences in left ventricular structure and function during antihypertensive treatment: The Losartan Intervention for Endpoint Reduction in Hypertension Study. *Hypertension* , *51*(4), 1109–1114. https://doi.org/10.1161/HYPERTENSIONAHA.107.107474

Gersh, B. J., Sliwa, K., Mayosi, B. M., & Yusuf, S. (2010). Novel therapeutic conceptsThe epidemic of cardiovascular disease in the developing world: Global implications. *European Heart Journal*, *31*(6), 642–648. https://doi.org/10.1093/eurheartj/ehq030

Gewitz, M. H., Baltimore, R. S., Tani, L. Y., Sable, C. A., Shulman, S. T., Carapetis, J., Remenyi, B., Taubert, K. A., Bolger, A. F., Beerman, L., Mayosi, B. M., Beaton, A., Pandian, N. G., & Kaplan, E. L. (2015). Revision of the Jones Criteria for the diagnosis of acute rheumatic fever in the era of Doppler echocardiography: A scientific statement from the American Heart Association. *Circulation*, *131*(20), 1806–1818. https://doi.org/10.1161/CIR.0000000000000205

Gollub, M. J., Panu, N., Delaney, H., Sohn, M., Zheng, J., Moskowitz, C. S., Rademaker, J., & Liu, J. (2012). Shall we report cardiomegaly at routine computed tomography of the chest? *Journal of Computer Assisted Tomography*, *36*(1), 67–71. https://doi.org/10.1097/RCT.0b013e318241e585

Gottdiener, J. S., Bednarz, J., Devereux, R., Gardin, J., Klein, A., Manning, W. J., Morehead, A., Kitzman, D., Oh, J., Quinones, M., Schiller, N. B., Stein, J. H., & Weissman, N. J. (2004). American Society of Echocardiography recommendations for use of echocardiography in clinical trials. *Journal of the American Society of Echocardiography : Official Publication of the American Society of Echocardiography*, *17*(10), 1086–1119. https://doi.org/10.1016/j.echo.2004.07.013

Gray, H. (2015). *Gray's Anatomy, The Anatomical Basis of Clinical Practice* (41st ed.). Elsevier.

Gupta, C., Palimar, V., Saxena, A., & D'Souza, A. (2014). A morphometric study of measurements of heart in adults and its relation with age and height of the individual: A post-mortem study. *CHRISMED Journal of Health and Research*, *1*(4), 263.

Gwaba, N., Isaacs, F., & Harneck, M. (2018). Echocardiography in patients with chest x-ray diagnosis of cardiomegaly at an academic hospital in Zambia. *Medical Journal of Zambia, 45*(4), 196 - 202.

Haghdoost, A., Mirzazadeh, A., & Alikhani, s. (2008). Secular Trend of Height Variations in Iranian Population Born between 1940 and 1984. *Iranian Journal of Public Health*, *37*.

Hajouli, S., & Ludhwani, D. (2021). Heart Failure And Ejection Fraction. In *StatPearls*. StatPearls Publishing.

Harkness, A., Ring, L., Augustine, D. X., Oxborough, D., Robinson, S., & Sharma, V. (2020). Normal reference intervals for cardiac dimensions and function for use in echocardiographic practice: A guideline from the British Society of Echocardiography. *Echo Research and Practice*, *7*(1), G1–G18. https://doi.org/10.1530/ERP-19-0050

Harris, I. S., & Black, B. L. (2010). Development of the Endocardium. *Pediatric Cardiology*, *31*(3), 391–399. https://doi.org/10.1007/s00246-010-9642-8

Hudsmith, L., Petersen, S., Francis, J., Robson, M., & Neubauer, S. (2005). Normal Human Left and Right Ventricular and Left Atrial Dimensions Using Steady State Free Precession Magnetic Resonance Imaging. *Journal of Cardiovascular Magnetic Resonance : Official Journal of the Society for Cardiovascular Magnetic Resonance*, *7*, 775–782. https://doi.org/10.1080/10976640500295516

Ilercil, A., O'Grady, M. J., Roman, M. J., Paranicas, M., Lee, E. T., Welty, T. K., Fabsitz, R. R., Howard, B. V., & Devereux, R. B. (2001). Reference values for echocardiographic measurements in urban and rural populations of differing ethnicity: The Strong Heart Study. *Journal of the American Society of Echocardiography : Official Publication of the American Society of Echocardiography*, *14*(6), 601–611. https://doi.org/10.1067/mje.2001.113258

Inoue, K., Yoshii, K., & Ito, H. (1999). Effect of aging on cardiothoracic ratio in women: A longitudinal study. *Gerontology*, *45*(1), 53–58. https://doi.org/10.1159/000022056

Joseph, S. M., Cedars, A. M., Ewald, G. A., Geltman, E. M., & Mann, D. L. (2009). Acute decompensated heart failure: Contemporary medical management. *Texas Heart Institute Journal*, *36*(6), 510–520.

Joshi, S. D., Joshi, S. S., & Athavale, S. A. (2010). Origins of the coronary arteries and their significance. *Clinics (Sao Paulo, Brazil)*, *65*(1), 79–84. https://doi.org/10.1590/S1807-59322010000100012

Jung, G., Landwehr, P., Schanzenbächer, G., Faeber, B., & Lackner, K. (1995). [Value of thoracic radiography in the assessment of cardiac size. A comparison with left ventricular cardiography]. *RoFo : Fortschritte Auf Dem Gebiete Der Rontgenstrahlen Und Der Nuklearmedizin*, *162*(5), 368—372. https://doi.org/10.1055/s-2007-1015902

Kassirer, J. (2014). Imperatives, expediency, and the new diagnosis. *Diagnosis*, *1*(1). https://doi.org/10.1515/dx-2013-0004

Kassirer, J. P. (2010). Teaching clinical reasoning: Case-based and coached. *Academic Medicine : Journal of the Association of American Medical Colleges*, *85*(7), 1118–1124. https://doi.org/10.1097/acm.0b013e3181d5dd0d

Kassirer, J. P., & Kopelman, R. I. (1989). Cognitive errors in diagnosis: Instantiation, classification, and consequences. *The American Journal of Medicine*, *86*(4), 433–441. https://doi.org/10.1016/0002-9343(89)90342-2

Kau, T., Sinzig, M., Gasser, J., Lesnik, G., Rabitsch, E., Celedin, S., Eicher, W., Illiasch, H., & Hausegger, K. A. (2007). Aortic development and anomalies. *Seminars in Interventional Radiology*, *24*(2), 141–152. https://doi.org/10.1055/s-2007-980040

Kelly, A. M., & Frauenfelder, T. (2019). Diseases of the Chest Wall, Pleura, and Diaphragm. In J. Hodler, R. A. Kubik-Huch, & G. K. von Schulthess (Eds.), *Diseases of the Chest, Breast, Heart and Vessels 2019-2022: Diagnostic and Interventional Imaging* (pp. 95–106). Springer International Publishing. https://doi.org/10.1007/978-3-030-11149-6_9

Kelly, R. G., Buckingham, M. E., & Moorman, A. F. (2014). Heart fields and cardiac morphogenesis. *Cold Spring Harbor Perspectives in Medicine*, *4*(10). https://doi.org/10.1101/cshperspect.a015750

Keteepe-Arachi, T., & Sharma, S. (2017). Cardiovascular Disease in Women: Understanding Symptoms and Risk Factors. *European Cardiology*, *12*(1), 10–13. https://doi.org/10.15420/ecr.2016:32:1

Kinova, E., & Goudev, A. (2012). *Early Detection and Prediction of Cardiotoxicity - Biomarker and Echocardiographic Evaluation*. https://doi.org/10.5772/33561

Kugler, J., & Verghese, A. (2010). The physical exam and other forms of fiction. *Journal of General Internal Medicine*, *25*(8), 756–757. PubMed. https://doi.org/10.1007/s11606-010-1400-3

Kumar, A., & Cannon, C. P. (2009). Acute coronary syndromes: Diagnosis and management, part I. *Mayo Clinic Proceedings*, *84*(10), 917–938. https://doi.org/10.1016/S0025-6196(11)60509-0

Kumar, V., K. Abbas, A., & C. Aster, J. (2015). *Robbins and Cotran Pathologic Basis of Disease* (9th ed.). Elsevier Saunders.

La Gerche, A., Baggish, A. L., Knuuti, J., Prior, D. L., Sharma, S., Heidbuchel, H., & Thompson, P. D. (2013). Cardiac imaging and stress testing asymptomatic athletes to identify those at risk of sudden cardiac death. *JACC. Cardiovascular Imaging*, *6*(9), 993–1007. https://doi.org/10.1016/j.jcmg.2013.06.003

Lang, R. M., Badano, L. P., Mor-Avi, V., Afilalo, J., Armstrong, A., Ernande, L., Flachskampf, F. A., Foster, E., Goldstein, S. A., Kuznetsova, T., Lancellotti, P., Muraru, D., Picard, M. H., Rietzschel, E. R., Rudski, L., Spencer, K. T., Tsang, W., & Voigt, J. U. (2015). Recommendations for cardiac chamber quantification by echocardiography in adults: An update from the American Society of Echocardiography and the European Association of Cardiovascular Imaging. *Journal of the American Society of Echocardiography : Official Publication of the American Society of Echocardiography*, *28*(1), 1-39.e14. https://doi.org/10.1016/j.echo.2014.10.003

Lang, R. M., Bierig, M., Devereux, R. B., Flachskampf, F. A., Foster, E., Pellikka, P. A., Picard, M. H., Roman, M. J., Seward, J., Shanewise, J. S., Solomon, S. D., Spencer, K. T., Sutton, M. S. J., & Stewart, W. J. (2005). Recommendations for chamber quantification: A report from the American Society of Echocardiography's Guidelines and Standards Committee and the Chamber Quantification Writing Group, developed in conjunction with the European Association of Echocardiography, a branch of the European Society of Cardiology. *Journal of the American Society of Echocardiography : Official Publication of the American Society of Echocardiography*, *18*(12), 1440–1463. https://doi.org/10.1016/j.echo.2005.10.005

Lee, K. F., & Olak, J. (1994). Anatomy and physiology of the pleural space. *Chest Surgery Clinics of North America*, *4*(3), 391–403.

Lin, C. J., Lin, C. Y., Chen, C. H., Zhou, B., & Chang, C. P. (2012). Partitioning the heart: Mechanisms of cardiac septation and valve development. *Development (Cambridge, England)*, *139*(18), 3277–3299. https://doi.org/10.1242/dev.063495

Lindsey, S., Butcher, J., & Yalcin, H. (2014). Mechanical Regulation of Cardiac Development. *Frontiers in Physiology*, *5*, 318. https://doi.org/10.3389/fphys.2014.00318

Long, A. N., & Dagogo-Jack, S. (2011). Comorbidities of diabetes and hypertension: Mechanisms and approach to target organ protection. *Journal of Clinical Hypertension (Greenwich, Conn.)*, *13*(4), 244–251. PubMed. https://doi.org/10.1111/j.17517176.2011.00434.x

Longbak, S., Mangset, W., & Sirisena, U. (June 2017). Determination of cardiothoracic ratio (CTR) of normal fresh undergraduate students of University of JOS using plain chest radiographs. *International Research Journal of Pure and Applied Physics, 5*(2), 29-36.

Maganti, K., Rigolin, V. H., Sarano, M. E., & Bonow, R. O. (2010). Valvular heart disease: Diagnosis and management. *Mayo Clinic Proceedings*, *85*(5), 483–500. PubMed. https://doi.org/10.4065/mcp.2009.0706

Majonga, E. D., Norrish, G., Rehman, A. M., Kranzer, K., Mujuru, H. A., Nathoo, K., Odland, J. O., Kaski, J. P., & Ferrand, R. A. (2018). Racial Variation in Echocardiographic Reference Ranges for Left Chamber Dimensions in Children and

Adolescents: A Systematic Review. *Pediatric Cardiology*, *39*(5), 859–868. https://doi.org/10.1007/s00246-018-1873-0

Malik, A., Brito, D., & Chhabra, L. (2021). Congestive Heart Failure. In *StatPearls*. StatPearls Publishing.

Mannan, S., Khalil, M., Rahman, M., & Ahmed, M. S. (2009). Measurement of different external dimensions of the heart in adult Bangladeshi cadaver. *Mymensingh Medical Journal : MMJ*, *18*(2), 175–178.

Mathes, T., & Pieper, D. (2019). An algorithm for the classification of study designs to assess diagnostic, prognostic and predictive test accuracy in systematic reviews. *Systematic Reviews*, *8*(1), 226. https://doi.org/10.1186/s13643-019-1131-4

Mc Namara, K., Alzubaidi, H., & Jackson, J. K. (2019). Cardiovascular disease as a leading cause of death: How are pharmacists getting involved? *Integrated Pharmacy Research & Practice*, *8*, 1–11. https://doi.org/10.2147/IPRP.S133088

McKee, J. L., & Ferrier, K. (2017). Is cardiomegaly on chest radiograph representative of true cardiomegaly: A cross-sectional observational study comparing cardiac size on chest radiograph to that on echocardiography. *The New Zealand Medical Journal*, *130*(1464), 57–63.

Melenovsky, V., Andersen, M. J., Andress, K., Reddy, Y. N., & Borlaug, B. A. (2015). Lung congestion in chronic heart failure: Haemodynamic, clinical, and prognostic implications. *European Journal of Heart Failure*, *17*(11), 1161–1171. https://doi.org/10.1002/ejhf.417

Mehra, S., & Kumar, S. (2019). Study of Interrelationship between Heart Diameter and Cardio-Thoracic Ratio with Body Habitus: A Hospital Based Study to Evaluate Cardiac Enlargement. *Pravara Medical Review, 11*, 4-8.

Mensah, Y. B., Mensah, K., Asiamah, S., Gbadamosi, H., Idun, E. A., Brakohiapa, W., & Oddoye, A. (2015). Establishing the Cardiothoracic Ratio Using Chest Radiographs in an Indigenous Ghanaian Population: A Simple Tool for Cardiomegaly Screening. *Ghana Medical Journal*, *49*(3), 159–164. https://doi.org/10.4314/gmj.v49i3.6

Misfeld, M., & Sievers, H.-H. (2007). Heart valve macro- and microstructure. *Philosophical Transactions of the Royal Society of London. Series B, Biological Sciences*, *362*(1484), 1421–1436. https://doi.org/10.1098/rstb.2007.2125

Mitchell, C., Rahko, P. S., Blauwet, L. A., Canaday, B., Finstuen, J. A., Foster, M. C., Horton, K., Ogunyankin, K. O., Palma, R. A., & Velazquez, E. J. (2019). Guidelines for Performing a Comprehensive Transthoracic Echocardiographic Examination in Adults: Recommendations from the American Society of Echocardiography. *Journal of the American Society of Echocardiography : Official Publication of the American Society of Echocardiography*, *32*(1), 1–64. https://doi.org/10.1016/j.echo.2018.06.004

Miwa, K., & Fujita, M. (2008). Small heart syndrome in patients with chronic fatigue syndrome. *Clinical Cardiology*, *31*(7), 328–333. https://doi.org/10.1002/clc.20227

Molina, D. K., & DiMaio, V. J. M. (2012). Normal organ weights in men: Part I-the heart. *The American Journal of Forensic Medicine and Pathology*, *33*(4), 362–367. https://doi.org/10.1097/PAF.0b013e31823d298b

Molina, D. K., & DiMaio, V. J. M. (2015). Normal Organ Weights in Women: Part I-The Heart. *The American Journal of Forensic Medicine and Pathology*, *36*(3), 176–181. https://doi.org/10.1097/PAF.0000000000000174

Monfared, A., Agha Farajollah, S., Sabour, F., Farzanegan, R., & Taghdisi, S. (2015). Comparison of radiological findings of chest x-ray with echocardiography in determination of the heart size. *Iranian Red Crescent Medical Journal*, *17*(1), e18242. https://doi.org/10.5812/ircmj.18242

Moore, K. L., Persaud, T. V. N., & Torchia, M. G. (2020). *The developing human: Clinically oriented embryology*. Saunders/ Elsevier.

Moorman, A. F. M., & Christoffels, V. M. (2003). Development of the cardiac conduction system: A matter of chamber development. *Novartis Foundation Symposium*, *250*, 25–34; discussion 34-43, 276–279.

Moorman, A., Webb, S., Brown, N. A., Lamers, W., & Anderson, R. H. (2003). Development of the heart: (1) formation of the cardiac chambers and arterial trunks. *Heart: British Cardiac Society*, *89*(7), 806–814. https://doi.org/10.1136/heart.89.7.806

Moorthy, R. S. (2002). Doppler Ultrasound. *Medical Journal, Armed Forces India*, *58*(1), 1–2. https://doi.org/10.1016/S0377-1237(02)80001-6

Morales, M. A., Prediletto, R., Rossi, G., Catapano, G., Lombardi, M., & Rovai, D. (2012). Routine Chest X-ray: Still Valuable for the Assessment of Left Ventricular Size and Function in the Era of Super Machines? *Journal of Clinical Imaging Science*, *2*, 25. https://doi.org/10.4103/2156-7514.96540

Mukherjee, A., Halder, S. K., Nandi, S., Mandal, M., Khanra, D., & Biswas, K. (2021a). A study on normal reference values of echocardiographic chamber dimensions in young eastern Indian adults. *Indian Heart Journal*, *73*(1), 77–84. https://doi.org/10.1016/j.ihj.2020.12.010

Nabeta, T., Inomata, T., Ishii, S., Yazaki, M., Fujita, T., Iida, Y., Ikeda, Y., Maekawa, E., Naruke, T., Koitabashi, T., & Ako, J. (2019). Dilated cardiomyopathy with re-worsening left ventricular ejection fraction. *Heart and Vessels*, *34*(1), 95–103. https://doi.org/10.1007/s00380-018-1214-5

Nadar, S. K., & Shaikh, M. M. (2019). Biomarkers in Routine Heart Failure Clinical Care. *Cardiac Failure Review*, *5*(1), 50–56. https://doi.org/10.15420/cfr.2018.27.2

Naqvi, N., McCarthy, K., & Ho, S. (2018). Anatomy of the atrial septum and interatrial communications. *Journal of Thoracic Disease*, *10*, S2837–S2847. https://doi.org/10.21037/jtd.2018.02.18

Nauta, J. F., Hummel, Y. M., Tromp, J., Ouwerkerk, W., van der Meer, P., Jin, X., Lam, C. S. P., Bax, J. J., Metra, M., Samani, N. J., Ponikowski, P., Dickstein, K., Anker, S. D., Lang, C. C., Ng, L. L., Zannad, F., Filippatos, G. S., van Veldhuisen, D. J., van Melle, J. P., & Voors, A. A. (2020). Concentric vs. Eccentric remodelling in heart failure with reduced ejection fraction: Clinical characteristics, pathophysiology and response to treatment. *European Journal of Heart Failure*, *22*(7), 1147–1155. https://doi.org/10.1002/ejhf.1632

Nickol, K., & Wade, A. J. (1982). Radiographic heart size and cardiothoracic ratio in three ethnic groups: A basis for a simple screening test for cardiac enlargement in men. *The British Journal of Radiology*, *55*(654), 399–403. https://doi.org/10.1259/0007-1285-55-654-399

Nwoye, L. O., & Al-Shehri, M. A. (2003). A formula for the estimation of the body surface area of Saudi male adults. *Saudi Medical Journal*, *24*(12), 1341–1346.

Patel, D. A., Lavie, C. J., Milani, R. V., & Ventura, H. O. (2011). Left atrial volume index predictive of mortality independent of left ventricular geometry in a large clinical cohort with preserved ejection fraction. *Mayo Clinic Proceedings*, *86*(8), 730–737. https://doi.org/10.4065/mcp.2010.0682

Pfaffenberger, S., Bartko, P., Graf, A., Pernicka, E., Babayev, J., Lolic, E., Bonderman, D., Baumgartner, H., Maurer, G., & Mascherbauer, J. (2013). Size matters! Impact of age, sex, height, and weight on the normal heart size. *Circulation. Cardiovascular Imaging*, *6*(6), 1073–1079. https://doi.org/10.1161/CIRCIMAGING.113.000690

Pfeffer, M. A., Shah, A. M., & Borlaug, B. A. (2019). Heart Failure With Preserved Ejection Fraction In Perspective. *Circulation Research*, *124*(11), 1598–1617. https://doi.org/10.1161/CIRCRESAHA.119.313572

Pollock, J. D., & Makaryus, A. N. (2021). Physiology, Cardiac Cycle. In *StatPearls*. StatPearls Publishing.

Poppe, K. K., Doughty, R. N., Gardin, J. M., Hobbs, F. D. R., McMurray, J. J. V., Nagueh, S. F., Senior, R., Thomas, L., Whalley, G. A., Aune, E., Brown, A., Badano, L. P., Cameron, V., Chadha, D. S., Chahal, N., Chien, K. L., Daimon, M., Dalen, H., Detrano, R., Salvetti, M. (2015). Ethnic-Specific Normative Reference Values for Echocardiographic LA and LV Size, LV Mass, and Systolic Function: The 'EchoNoRMAL' Study. *JACC: Cardiovascular Imaging*, *8*(6), 656–665. https://doi.org/10.1016/j.jcmg.2015.02.014

Proschek, P., & Vogl, T. J. (2015). Chest and Mediastinum. *Diagnostic and Interventional Radiology*, 479–587. PMC. https://doi.org/10.1007/978-3-662-44037-7_19

Prummel, K. D., Nieuwenhuize, S., & Mosimann, C. (2020). The lateral plate mesoderm. *Development (Cambridge, England)*, *147*(12). https://doi.org/10.1242/dev.175059

Qureshi, W. T., Leigh, J. A., Swett, K., Dharod, A., Allison, M. A., Cai, J., Gonzalez, F. 2nd, Hurwitz, B. E., Shah, S. J., Desai, A. A., Spevack, D. M., & Rodriguez, C. J. (2016). Comparison of Echocardiographic Measures in a Hispanic/Latino Population With the 2005 and 2015 American Society of Echocardiography Reference Limits (The Echocardiographic Study of Latinos). *Circulation. Cardiovascular Imaging*, *9*(1). https://doi.org/10.1161/CIRCIMAGING.115.003597

Rana, M. S., Sizarov, A., Christoffels, V., & Moorman, A. (2014). Development of the Human Aortic Arch System Captured in an Interactive Three-Dimensional Reference Model. *American Journal of Medical Genetics. Part A*, *164*. https://doi.org/10.1002/ajmg.a.35881

Ray, S. (2010). Changing epidemiology and natural history of valvular heart disease. *Clinical Medicine*, *10*(2), 168. https://doi.org/10.7861/clinmedicine.10-2-168

Redlarski, G., Palkowski, A., & Krawczuk, M. (2016). Body surface area formulae: an alarming ambiguity. *Scientific reports*, *6*, 27966. https://doi.org/10.1038/srep27966

Regitz-Zagrosek, V., Brokat, S., & Tschope, C. (2007). Role of gender in heart failure with normal left ventricular ejection fraction. *Progress in Cardiovascular Diseases*, *49*(4), 241–251. https://doi.org/10.1016/j.pcad.2006.08.011

Roberts, K., & Weinhaus, A. (2005). *Anatomy of the Thoracic Wall, Pulmonary Cavities, and Mediastinum* (pp. 25–50). https://doi.org/10.1007/978-1-59259-835-9_3

Ruddox, V., Mathisen, M., Bækkevar, M., Aune, E., Edvardsen, T., & Otterstad, J. E. (2013). Is 3D echocardiography superior to 2D echocardiography in general practice? A systematic review of studies published between 2007 and 2012. *International Journal of Cardiology*, *168*(2), 1306–1315. https://doi.org/10.1016/j.ijcard.2012.12.002

Ruwhof, C., & van der Laarse, A. (2000). Mechanical stress-induced cardiac hypertrophy: Mechanisms and signal transduction pathways. *Cardiovascular Research*, *47*(1), 23–37. https://doi.org/10.1016/S0008-6363(00)00076-6

Ryu, D. R. (2016). Normal Reference Values for Doppler Echocardiography: Influences of Ageing, Gender and Ethnicity. *Journal of Cardiovascular Ultrasound*, *24*(2), 112–114. https://doi.org/10.4250/jcu.2016.24.2.112

Sadeghpour, A., Shahrabi, M., Bakhshandeh, H., & Naderi, N. (2013). Normal Echocardiographic Values of 368 Iranian Healthy Subjects. *Archives of Cardiovascular Imaging*, *1*, 72–79. https://doi.org/10.5812/acvi.15662

Sadler, T. W. (2019). *Langman's medical embryology*. Lippincott Williams & Wilkins.

Salerno, M., Sharif, B., Arheden, H., Kumar, A., Axel, L., Li, D., & Neubauer, S. (2017). Recent Advances in Cardiovascular Magnetic Resonance: Techniques and Applications. *Circulation. Cardiovascular Imaging*, *10*(6). https://doi.org/10.1161/CIRCIMAGING.116.003951

Samuelsson, O., Hartford, M., Wilhelmsen, L., Berglund, G., & Wikstrand, J. (1989). Radiological heart enlargement in treated hypertensive men: A comparative study of chest X-ray examination and M-mode echocardiography. *Journal of Internal Medicine*, *225*(2), 77–83. https://doi.org/10.1111/j.1365-2796.1989.tb00043.x

Sant, S. (2008). *Chapter-13 Respiratory System, Body Cavities and Diaphragm* (pp. 216–232). https://doi.org/10.5005/jp/books/10252_13

Saremi, F., Sánchez-Quintana, D., Mori, S., Muresian, H., Spicer, D. E., Hassani, C., & Anderson, R. H. (2017). Fibrous Skeleton of the Heart: Anatomic Overview and Evaluation of Pathologic Conditions with CT and MR Imaging. *Radiographics : A Review Publication of the Radiological Society of North America, Inc*, *37*(5), 1330–1351. https://doi.org/10.1148/rg.2017170004

Sarullo, F., Franco, A., Ohmes, L., Gaudino, M., Rong, L., Girardi, L., Salerno, Y., Sarullo, S., Weinsaft, J., & Kim, J. (2017). Serendipity and innovation: history and evolution of transthoracic echocardiography. *Journal Of Thoracic Disease, 9*(4), S257-S263. doi:10.21037/jtd.2017.03.9

Sathananthan, G., Zahid, S., Aggarwal, G., Chik, W., Friedman, D., & Thiagalingam, A. (2015). Cardiac orientation: Is there a correlation between the anatomical and the

electrical axis of the heart? *British Journal of Cardiology*, *22*. https://doi.org/10.5837/bjc.2015.016

Shahjehan, R. D., & Bhutta, B. S. (2021). Coronary Artery Disease. In *StatPearls*. StatPearls Publishing.

Siddiqui, Md., Shahnaj Sultana, Abul Hossain, & Muhammad Siddiqui. (2013). Electrocardiography and Chest X-ray in Prediction of Left Ventricular Systolic Dysfunction. *KYAMC Journal*, *2*(1). https://doi.org/10.3329/kyamcj.v2i1.13515

Siddiqui, W. (2019). *Cardiomegaly*. In *StatPearls*. StatPearls Publishing.

Singh, A., Museedi, A. S., & Grossman, S. A. (2020). *Acute Coronary Syndrome* (29083796). StatPearls Publishing, Treasure Island (FL); PubMed. http://europepmc.org/abstract/MED/29083796

Sinha, U., Sahay, U., Athavale, S., Deopujari, R., & Kumar, S. (2013). Comparative study of cardiac size by chest X-ray and echocardiography. *Journal of the Anatomical Society of India*, *62*, 28–32. https://doi.org/10.1016/S0003-2778(13)80008-1

Smith, H. L. (1928). The relation of the weight of the heart to the weight of the body and of the weight of the heart to age. *American Heart Journal*, *4*(1), 79–93. https://doi.org/10.1016/S0002-8703(29)90099-5

Som, S., Ulijaszek, S., Pal, M., Bharati, S., & Bharati, P. (2014). Variation in height and BMI of adult Indians. *Journal of Biosocial Science*, *46*(1), 47–65. https://doi.org/10.1017/S002193201300014X

Srivastava, D., & Olson, E. N. (2000). A genetic blueprint for cardiac development. *Nature*, *407*(6801), 221–226. https://doi.org/10.1038/35025190

Steeds, R. P., Wheeler, R., Bhattacharyya, S., Reiken, J., Nihoyannopoulos, P., Senior, R., Monaghan, M. J., & Sharma, V. (2019). Stress echocardiography in coronary artery disease: A practical guideline from the British Society of Echocardiography. *Echo Research and Practice*, *6*(2), G17–G33. https://doi.org/10.1530/ERP-18-0068

Stroumpoulis, K. I., Pantazopoulos, I. N., & Xanthos, T. T. (2010). Hypertrophic cardiomyopathy and sudden cardiac death. *World Journal of Cardiology*, *2*(9), 289–298. https://doi.org/10.4330/wjc.v2.i9.289

Tam, P. P. L., & Trainor, P. A. (1994). Specification and segmentation of the paraxial mesoderm. *Anatomy and Embryology*, *189*(4), 275–305. https://doi.org/10.1007 /BF00190586

Tong, C., Nair, N., Doersch, K., Liu, Y., & Rosas, P. (2014). Cardiac myosin-binding protein-C is a critical mediator of diastolic function. *Pflugers Archiv : European Journal of Physiology*, *466*. https://doi.org/10.1007/s00424-014-1442-1

Trivedi, S. K., Gupta, O. P., Jain, A. P., Jajoo, U. N., Kamble, A. N., & Bharambe, M. S. (1993). Left ventricular M-mode echocardiographic measurements of Indian population. *The Journal of the Association of Physicians of India*, *41*(1), 14–16.

Tsakok, M., & Gleeson, F. V. (2018). The chest radiograph in heart disease. *Medicine*, *46*. https://doi.org/10.1016/j.mpmed.2018.05.007

Tsiviltidou, P., Chatzifotiou, E., Nikolaou, A., Dimitriadis, I., Tagarakis, G., & Anestakis, D. (2017). *Histopathological differences between hypertrophic and dilated cardiomyopathy*.

Tzahor, E., & Evans, S. M. (2011). Pharyngeal mesoderm development during embryogenesis: Implications for both heart and head myogenesis. *Cardiovascular Research*, *91*(2), 196–202. https://doi.org/10.1093/cvr/cvr116

Utomi, V., Oxborough, D., Whyte, G. P., Somauroo, J., Sharma, S., Shave, R., Atkinson, G., & George, K. (2013). Systematic review and meta-analysis of training mode, imaging modality and body size influences on the morphology and function of the male athlete's heart. *Heart: British Cardiac Society*, *99*(23), 1727–1733. https://doi.org/10.1136 /heartjnl- 2012-303465

van Gils, F. A. (1981). The fibrous skeleton in the human heart: Embryological and pathogenetic considerations. *Virchows Archiv. A, Pathological Anatomy and Histology*, *393*(1), 61–73. https://doi.org/10.1007/BF00430871

Vardavas, C. I., Linardakis, M. K., Hatzis, C. M., Saris, W. H. M., & Kafatos, A. G. (2010). Cardiovascular disease risk factors and dietary habits of farmers from Crete 45 years after the first description of the Mediterranean diet. *European Journal of Cardiovascular Prevention and Rehabilitation : Official Journal of the European Society of Cardiology, Working Groups on Epidemiology & Prevention and Cardiac Rehabilitation and Exercise Physiology*, *17*(4), 440–446. https://doi.org/10.1097/HJR.0b013e32833692ea

Viragh, S., & Challice, C. E. (1981). The origin of the epicardium and the embryonic myocardial circulation in the mouse. *The Anatomical Record*, *201*(1), 157–168. https://doi.org/10.1002/ar.1092010117

Virani, S. S., Alonso, A., Aparicio, H. J., Benjamin, E. J., Bittencourt, M. S., Callaway, C. W., Carson, A. P., Chamberlain, A. M., Cheng, S., Delling, F. N., Elkind, M. S. V., Evenson, K. R., Ferguson, J. F., Gupta, D. K., Khan, S. S., Kissela, B. M., Knutson, K. L., Lee, C. D., Lewis, T. T. (2021). Heart Disease and Stroke Statistics - 2021 Update. *Circulation*, *143*(8), e254–e743. https://doi.org/10.1161/CIR.0000000000000950

Walker, H. K., Hall, W. D., & Hurst, J. W. (Eds.). (1990). *Clinical Methods: The History, Physical, and Laboratory Examinations* (3rd ed.). Butterworths.

Warren, T. Y., Barry, V., Hooker, S. P., Sui, X., Church, T. S., & Blair, S. N. (2010). Sedentary behaviors increase risk of cardiovascular disease mortality in men. *Medicine and Science in Sports and Exercise*, *42*(5), 879–885. PubMed. https://doi.org/10.1249/MSS.0b013e3181c3aa7e

Webb, J., Fovargue, L., Tøndel, K., Porter, B., Sieniewicz, B., Gould, J., Rinaldi, C. A., Ismail, T., Chiribiri, A., & Carr-White, G. (2018). The Emerging Role of Cardiac Magnetic Resonance Imaging in the Evaluation of Patients with HFpEF. *Current Heart Failure Reports*, *15*(1), 1–9. https://doi.org/10.1007/s11897-018-0372-1

Webb, S., Qayyum, S. R., Anderson, R. H., Lamers, W. H., & Richardson, M. K. (2003). Septation and separation within the outflow tract of the developing heart. *Journal of Anatomy*, *202*(4), 327–342. https://doi.org/10.1046/j.1469-7580.2003.00168.x

Wexler, R. K., Elton, T., Pleister, A., & Feldman, D. (2009). Cardiomyopathy: An overview. *American Family Physician*, *79*(9), 778–784.

Winters, N., & Bader, D. (2013). Development of the Serosal Mesothelium. *Journal of Developmental Biology*, *1*, 64–81. https://doi.org/10.3390/jdb1020064

Xiao, X., Wang, W., Sa, R., Qiu, L., & Liu, F. (2019). The Investigation of Sex Differences in the Effect of Body Mass Index. *International Journal of Hypertension*, *2019*, 1–5. https://doi.org/10.1155/2019/1360328

Xue, B., Head, J., & McMunn, A. (2019). The Impact of Retirement on Cardiovascular Disease and Its Risk Factors: A Systematic Review of Longitudinal Studies. *The Gerontologist*, *60*(5), e367–e377. https://doi.org/10.1093/geront/gnz062

Yagel, S., Kivilevitch, Z., Cohen, S., Valsky, D., Messing, B., Shen, O., & Achiron, R. (2010). The fetal venous system, Part I: normal embryology, anatomy, hemodynamics, ultrasound evaluation and Doppler investigation. *Ultrasound in Obstetrics & Gynecology : The Official Journal of the International Society of Ultrasound in Obstetrics and Gynecology*, *35*, 741–750. https://doi.org/10.1002/uog.7618

Yao, G. H., Zhang, M., Yin, L. X., Zhang, C., Xu, M. J., Deng, Y., Liu, Y., Deng, Y. B., Ren, W. D., Li, Z. A., Tang, H., Zhang, Q. B., Mu, Y. M., Fang, L. G., Zhang, Y., Investigators, on behalf of the E. M. in N. C. A. (EMINCA) S., Yang, J., Wei, Y., Zhou, Q., Yang, on behalf of the E. M. in N. C. A. (EMINCA) S. I., Ya. (2015). Doppler Echocardiographic Measurements in Normal Chinese Adults (EMINCA): A prospective, nationwide, and multicentre study. *European Heart Journal - Cardiovascular Imaging*, *17*(5), 512–522. https://doi.org/10.1093/ehjci/jev330

Yoshida, J., Kawai, M., Minai, K., Ogawa, K., Ogawa, T., & Yoshimura, M. (2017). Associations between Left Ventricular Cavity Size and Cardiac Function and Overload Determined by Natriuretic Peptide Levels and a Covariance Structure Analysis. *Scientific Reports*, *7*(1), 2037. https://doi.org/10.1038/s41598-017-02247-5

Zaffran, S., Kelly, R. G., Meilhac, S. M., Buckingham, M. E., & Brown, N. A. (2004). Right ventricular myocardium derives from the anterior heart field. *Circulation Research*, *95*(3), 261–268. https://doi.org/10.1161/01.RES.0000136815.73623.BE

Zubair, F., Nawaz, S., Nawaz, A., Nangyal, H., Amjad, N., & Khan, M. (2018). Prevalence of cardiovascular diseases in Punjab, Pakistan: A cross-sectional study. *Journal of Public Health*, *26*. https://doi.org/10.1007/s10389-018-0898-4

CHAPTER 8

APPENDICES

A. BUMDC-FRC Approval Letter

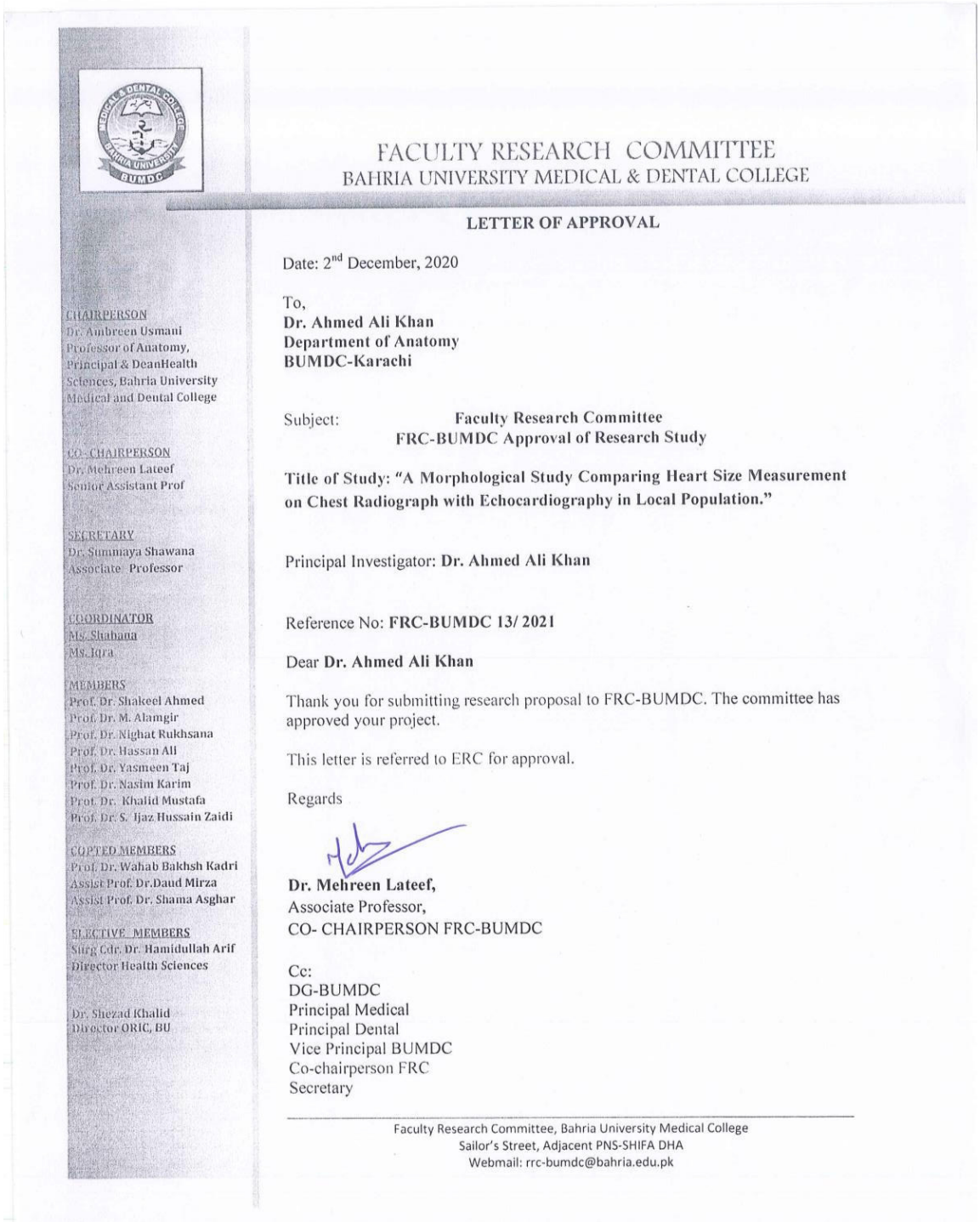

FACULTY RESEARCH COMMITTEE
BAHRIA UNIVERSITY MEDICAL & DENTAL COLLEGE

LETTER OF APPROVAL

Date: 2nd December, 2020

To,
Dr. Ahmed Ali Khan
Department of Anatomy
BUMDC-Karachi

Subject: **Faculty Research Committee**
FRC-BUMDC Approval of Research Study

Title of Study: "A Morphological Study Comparing Heart Size Measurement on Chest Radiograph with Echocardiography in Local Population."

Principal Investigator: **Dr. Ahmed Ali Khan**

Reference No: **FRC-BUMDC 13/ 2021**

Dear **Dr. Ahmed Ali Khan**

Thank you for submitting research proposal to FRC-BUMDC. The committee has approved your project.

This letter is referred to ERC for approval.

Regards

Dr. Mehreen Lateef,
Associate Professor,
CO- CHAIRPERSON FRC-BUMDC

Cc:
DG-BUMDC
Principal Medical
Principal Dental
Vice Principal BUMDC
Co-chairperson FRC
Secretary

CHAIRPERSON
Dr. Ambreen Usmani
Professor of Anatomy,
Principal & DeanHealth Sciences, Bahria University Medical and Dental College

CO- CHAIRPERSON
Dr. Mehreen Lateef
Senior Assistant Prof

SECRETARY
Dr. Sumnaya Shawana
Associate Professor

COORDINATOR
Ms. Shahana
Ms. Iqra

MEMBERS
Prof. Dr. Shakeel Ahmed
Prof. Dr. M. Alamgir
Prof. Dr. Nighat Rukhsana
Prof. Dr. Hassan Ali
Prof. Dr. Yasmeen Taj
Prof. Dr. Nasim Karim
Prof. Dr. Khalid Mustafa
Prof. Dr. S. Ijaz Hussain Zaidi

COPTED MEMBERS
Prof. Dr. Wahab Bakhsh Kadri
Assist Prof. Dr.Daud Mirza
Assist Prof. Dr. Shama Asghar

ELECTIVE MEMBERS
Surg Cdr. Dr. Hamidullah Arif
Director Health Sciences

Dr. Shezad Khalid
Director ORIC, BU

Faculty Research Committee, Bahria University Medical College
Sailor's Street, Adjacent PNS-SHIFA DHA
Webmail: rrc-bumdc@bahria.edu.pk

B. BUMDC-ERC Approval Letter

BAHRIA UNIVERSITY MEDICAL AND DENTAL COLLEGE

Defence phase II, Sailor Street, adjacent to PNS Shifa, Karachi. Tel: 021-35319491-9

ETHICAL REVIEW COMMITTEE

LETTER OF APPROVAL

Date: 15-Jan-21

FRC Reference:
FRC/BUMDC -13/2020-Ana-111

PATRON
Prof. Ambreen Usmani
Principal & Dean
Health Sciences(BU)

CHAIRPERSON
Dr. Quratulain Javaid

SECRETARY
Dr. Ambreen Surti

MEMBERS
Prof M Alamgir
Prof Anis Jafarey
Ms Nighat Huda
Surg Cdre Amir Ejaz
Prof Reza H Syed
Ms Shabina Arif
Mr M Amir Sultan
Surg Lt Cdr Farah
Surg Lt Cdr Sadia

Dr. Ahmed Ali Khan,

Subject: Institutional Approval of research study

Title of Study: "A Morphological Study Comparing Heart Size Measurement on Chest Radiograph with Echocardiography in Local Population"

Principal Investigator: Dr. Ahmed Ali Khan

Reference No: ERC 67/2021

Dear Dr. Ahmed Ali Khan,

Thank you for submitting the above mentioned study proposal. ERC Bahria University Medical and Dental College has reviewed this project in the meeting held on 14-Jan-2021 and gives approval. Kindly notify us when the research is complete.

Regards,

15/1/2021

DR. QURATULAIN JAVAID
Chairperson, ERC
BUMDC

Cc:
DG-BUMDC
Principal BUMDC
Chairperson ERC

C. Consent Form (English)

WRITTEN INFORMED CONSENT FORM OF PARTICIPANT

I am giving my consent to participate voluntarily and at my own will in the research project that aims for determination of heart size with chest X-ray and echocardiography. The project will evaluate parameters for estimation of the variations in heart size attributed to different types of underlying pathology, using the aforementioned imaging modalities.

I have been explained in detail the nature and significance of participating in the project and I understand the provided explanation.

I have been told that findings of my disease and my data will be kept strictly confidential and will be used only for the benefit of community, publications and paper presentations.

I have been explained that these investigations will be conducted to evaluate my health status and to diagnose and monitor my disease process. For this purpose I fully agree to give the chest X-ray film and echocardiography report to the researcher.

I have been fully informed about the risks involved in this study. Chest X-ray is a routine investigation that involves ionising radiation, but a single chest x-ray exposes the patient to a safe amount of radiation which will not cause any harm. Echocardiography involves use of sound waves, and it is known to be a very safe imaging modality.

I have been fully informed about the benefits of this study, which will compare the ability of a basic low cost tool (i.e. chest X-ray) to a more advanced investigation (i.e. echocardiography) in precisely measuring the heart size, to identify disease progression for early treatment & rehabilitation.

I also agree to give all relevant information needed, in full and to the best of my knowledge to the researcher. It is clarified to me that no incentive, financial assistance or reimbursement will be provided to me for participating in the study whereas I do have the right to withdraw from the study at any time.

I am advised to contact **Dr. Ahmed Ali Khan** on mobile number **03178797943**, or visit **PNS Shifa/ NICVD**, **Karachi** in case of query/ emergency related to my disease.

Name of Participant:	**S/o, D/o, W/o:**	**Signature of Participant:**
Name of Researcher:	**Signature of Researcher:** **Date:**	

NBC Secretariat: Pakistan Medical Research Council, Shahrah-e- Jamhuriat, Off Constitution Avenue, Sector G-5/2, Islamabad. www.pmrc.org.pk, email: pmrc@isb.comsats.net.pk, Tel: +92-51-9207386, 9216793, 9205480,
Fax: 051-9216774, 9204559

D. Consent Form (Urdu)

شرکاء رضامندی فارم (اقرارنامہ)

۱۔ میں اپنی رضامندی سے تحقیق میں حصہ لے رہا ہوں/ لے رہی ہوں۔ اس تحقیق میں کہ جس کا مقصد دل کا حجم ناپنا ہے بذریعہ ایکسرے (سینہ) اور ایکوکارڈیوگرافی (دل کا الٹراساؤنڈ)۔ اس تحقیق میں متعین مقدار (عوامل/ پیرامیٹرز) کی قدر پیمائی کر کے مختلف بیماریوں کے اثر سے دل کے حجم میں تبدیلیاں معلوم کرنا ہے۔

۲۔ مجھے اس تحقیق کی فطرت کے حوالے سے اور اس میں حصہ لینے کی اہمیت کے حوالے سے مکمل تفصیل سے آگاہ کیا گیا ہے میں فراہم شدہ معلومات کو سمجھتے ہوئے اس میں حصہ لے رہا ہوں/ لے رہی ہوں۔

۳۔ میری ذاتی اور بیماری سے متعلق معلومات کو مکمل پوشیدہ رکھا جائے گا اور صرف پیپر پبلیکیشن کی غرض سے استعمال ہوگا۔

۴ مجھے بتایا گیا ہے کہ میرے ٹیسٹ کیے جائیں گے جس سے میری صحت کا اندازہ لگایا جائے گا اور میری بیماری کی نگرانی کی جائے گی۔ اس مقصد کے لیے میں مکمل راضی ہوں کہ میری ایکسرے فلم اور رپورٹ اور ایکوکارڈیوگرافی رپورٹ میں محقق کو مہیّا کروں گا/ کرونگی۔

۵۔ مجھے اس تحقیق سے منسلک کسی بھی قسم کے خطرے سے مکمل تفصیل سے آگاہ کر دیا گیا ہے۔ ایکسرے (سینہ) ایک معمول کا ٹیسٹ ہے، جس میں بے ضرر مقدار میں تابکار شعائیں استعمال ہوتی ہیں، جس سے کوئی نقصان نہیں ہوتا۔ ایکوکارڈیوگرافی میں صوتی لہریں استعمال ہوتی ہیں جسے بہت محفوظ جانا جاتا ہے۔

۶۔ مجھے اس تحقیق کے فوائد کے متعلق مکمل آگاہ کر دیا گیا ہے، جس میں دل کا حجم درست ناپنے کیلئے بنیادی کم خرچ ایکسرے (سینہ) کا جدید ایکوکارڈیوگرافی سے موازنہ کیا جائے گا۔ اس سے بیماری کا بروقت تشخیص ممکن ہوگا تا کہ علاج بروقت شروع کیا جا سکے۔

۷۔ مجھے واضح کر دیا گیا ہے کہ مجھے اس تحقیق میں شرکت کی عوض کوئی مالی فائدہ، بازآدائیگی یا رقم فراہم نہیں کی جائے گی۔

۸۔ میں اس بات سے راضی ہوں کہ تمام متعلقہ ضروری معلومات جو اس مقصد کے لیے درکار ہوں گی، میں اپنے علم کے مطابق مہیّا کروں گا / کروں گی۔

۹۔ مجھے کسی بھی وقت اس تحقیق سے اپنی مرضی سے نکلنے کا حق حاصل ہے یا محقق کو مجھے تحقیق سے نکالنے کا حق حاصل ہے۔

۱۰۔ مجھے آگاہ کر دیا گیا ہے کہ میں اس تحقیق سے متعلق اپنی بیماری کے بارے میں ڈاکٹر احمد علی خان سے رابطہ رکھوں (0317-8797943) یا ایمرجنسی کی صورت میں پی۔ این۔ ایس شفاء یا این۔ آئی۔ سی۔ وی۔ ڈی، کراچی میں تشریف لے آؤں۔

شرکت کرنے والے کا نام ---------- دستخط: ----------

والد یا شوہر کا نام ---------- تاریخ: ----------

محقق کا نام ---------- دستخط: ----------

تاریخ: ----------

E. Subject Evaluation Proforma

Subject Evaluation Form

Case No./ Patient I.D. _____**Date:**_____**Contact No.:**_____

Name:_____**S/o, D/o, W/o** _____**Gender**: □ *Male* □ *Female*

Age:_____**Ethnicity**:_____ **Marital Status**: □ *Unmarried* □ *Married* □ *Divorced* □ *Widowed*

Address:_____**City**:_____**Province**:_____**Special Needs/ Impairment**: □*No* □*Yes, specify*_____

Education: □*None* □ *Primary* □*Metric* □*Inter.* □*Graduate.* □ *Post-Graduate* □ *Other, Specify (Madrasah, etc)*_____

Occupation: □ *Unemployed* □ *Homemaker* □ *Laborer* □ *Private Job* □ *Government Job* □ *Armed Forces* □ *Other:*_____

Weight *(Kg)*:_____**Height** *(m)*:_____**BMI:** _____**BSA:** _____

Purpose of Chest X-ray & Echocardiography: □ *Doctor's advice* □ *Medical Fitness Checkup* □*Follow up*_____

□*Please fill the following items if you are/ patient is presenting with Heart related complaints:*

Onset of Symptoms: □*Acute* □*Chronic* **Previous diagnosis** (*if applicable, specify*):_____

Symptoms Experienced: □*Chest Pain* □*Palpitations* □*Breathlessness* □*Paroxysmal nocturnal dyspnea*
□*Orthopnea* □ *Exertional Dyspnea* □*Peripheral Edema (*□*unilateral* □*bilateral;* □*pitting* □*non-pitting)*
□*Other:*_____

Duration of Symptoms: min/ h/ d/ mo/ yr _____**Relieved by**: _____**Aggravated by**:_____

□*To be filled by all the subjects:*

Current Illness Details (if applicable): _____

Any Past Medical Conditions: □No □Yes, Specify_____(e.g. Diabetes Mellitus, Hypertension, Covid-19, Pulmonary TB, etc);

Taking Any Medications: □No □Yes, Specify _____

Family History: □ **Diabetes Mellitus** □ **Heart Diseases** □ **Hypertension** □ **Other:** _____

Addictions: □*Smoking – Cig. / Bheedi / Huqa* (Pack Year :_____) □*Pan/Gutka/ Bettle Nut* □*Other:*_____

Level of Physical Activity: □*None* □*Infrequent* □*Walk ≤ 30 min daily* □*Walk ≥ 30 min daily*
□*Running/ Jogging* □*Others (gym, cycling, swimming)*_____

Physical Examination Findings:_____**Blood Pressure** (*mmHg*) **:** _____ **Pulse** (*bpm*) **:**_____

Chest X-ray (PA View) Case/ ID: _____

MEASUREMENTS		LUNG FIELDS
TCD :	**TTD :**	**Pulmonary Vasculature**: □Normal □Congestion □Oligemia
TRD :	**TLD :**	**Associated Pulmonary Disease**: □No □Yes
CTR :	**Additional Findings:**	

Echocardiography (echo) - Comment on Heart Size: **Normal/ Enlarged** Case/ ID: _____

Left Ventricle	LVIDd:	EF%:
	LVIDs:	Post. Wall Thick:
	IVSd:	Aorta:
Left Atrium	Diameter:	
Right Ventricle	Diameter:	TAPSE:
Right Atrium	Diameter:	

F. Hospital/ Institute Card (Echocardiography)

NICVD
NATIONAL INSTITUTE OF CARDIOVASCULAR DISEASES

ECHOCARDIOGRAPHIC REPORT

Study Requested:
Doppler/Imaging

Loacation: _____ Date : _____

Name: _____ M.R. No. _____ Echo No. _____ Tape No. _____

Weight: _____ Height: _____ Age: _____ Gender: _____

Clinical diagnosis: _____

M-Mode/2 D

Measurements in mm Figures in bracket indicate normal values in mm

Left Ventricle	Systolic	EPSS (<7)
	Diastolic (<55)	E.f. (>55%)
	Septal Thickness (11)	Post. Wall Thickness (<11)
Left Atrium (<40		Aorta (<40)
Mitral Valve		Aortic Valve
Right Ventricle (<25)		Pulmonarty Artery

Structural Interpretaion:

DOPPLER:
Flow Abnormality (Colour Flow Mapping)

Pressure Gradinet (mm Hg)

Estimated RV/MPA Pressure (mm Hg)

Final Echo Dx:

G. Hospital/ Institute Card (Radiology)

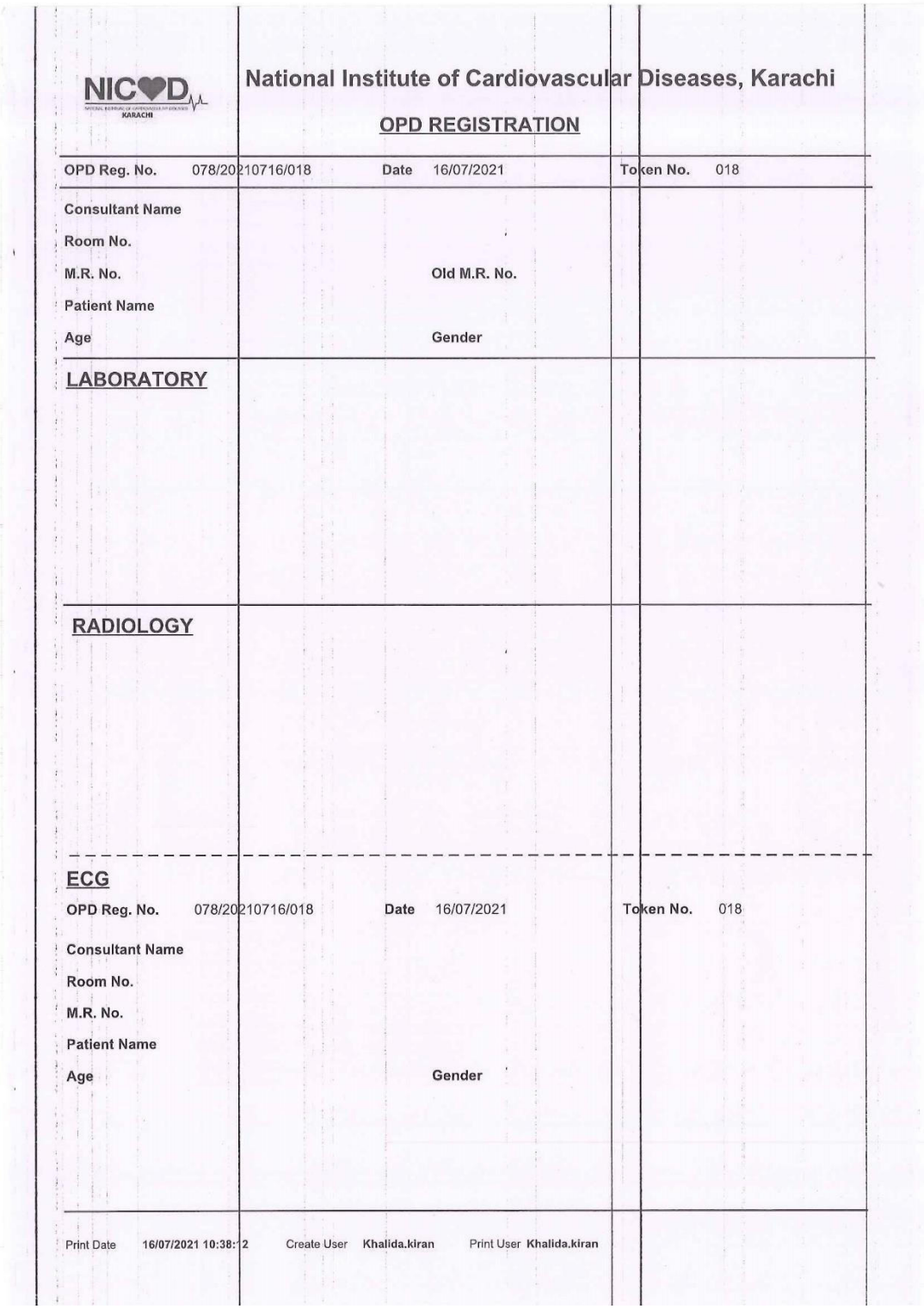

NICVD KARACHI

National Institute of Cardiovascular Diseases, Karachi

OPD REGISTRATION

OPD Reg. No. 078/20210716/018 Date 16/07/2021 Token No. 018

Consultant Name

Room No.

M.R. No. Old M.R. No.

Patient Name

Age Gender

LABORATORY

RADIOLOGY

ECG

OPD Reg. No. 078/20210716/018 Date 16/07/2021 Token No. 018

Consultant Name

Room No.

M.R. No.

Patient Name

Age Gender

Print Date 16/07/2021 10:38:12 Create User Khalida.kiran Print User Khalida.kiran

H. Plagiarism Report

DR. AHMED ALI KHAN

ORIGINALITY REPORT

11%	7%	9%	2%
SIMILARITY INDEX	INTERNET SOURCES	PUBLICATIONS	STUDENT PAPERS

PRIMARY SOURCES

1	www.ncbi.nlm.nih.gov Internet Source	1%
2	"Abstracts", European Journal of Heart Failure, 2016. Publication	1%
3	tehj.springeropen.com Internet Source	1%
4	Submitted to South Florida State College (formerly South Florida Community College) Student Paper	<1%
5	www.ajol.info Internet Source	<1%
6	Mark C. Petrie, John J. V. McMurray. "It cannot be cardiac failure because the heart is not enlarged on the chest X-ray", European Journal of Heart Failure, 2003 Publication	<1%
7	www.thaiheart.org Internet Source	<1%